FACULTY
OF MATHEMATICS
AND PHYSICS
Charles University

**MASTER THESIS**

Bc. Jan Pekař

# Quantum graphs with circulant vertex couplings

Institute of Theoretical Physics

Supervisor of the master thesis: prof. RNDr. Pavel Exner, Dr.Sc.
Study programme: Physics
Study branch: Theoretical Physics

Prague 2023

I declare that I carried out this master thesis independently, and only with the cited sources, literature and other professional sources. It has not been used to obtain another or the same degree.

I understand that my work relates to the rights and obligations under the Act No. 121/2000 Sb., the Copyright Act, as amended, in particular the fact that the Charles University has the right to conclude a license agreement on the use of this work as a school work pursuant to Section 60 subsection 1 of the Copyright Act.

In ............. date .............  ..................................

Author's signature

My deepest gratitude goes to my supervisor prof. RNDr. Pavel Exner, Dr.Sc. for his invaluable advice, shared experience, patience and overall help during the writing of this thesis.

Title: Quantum graphs with circulant vertex couplings

Author: Bc. Jan Pekař

Institute: Institute of Theoretical Physics

Supervisor: prof. RNDr. Pavel Exner, Dr.Sc., Institute of Theoretical Physics

Abstract: Motivated by recent investigation of several particular situations, we study various quantum graphs equipped with circulant vertex couplings and characterize their spectral properties. The case of a star graph is analyzed in full generality, and the same applies to the condition determining the spectrum of periodic rectangular lattices. Special attention is paid to permutation-invariant vertex conditions on a rectangular lattice, as well as to a coupling interpolating between the $\delta$ and 'rotational' coupling on a quantum chain, with the focus on low- and high-energy bands and the discrete spectrum. We describe not only their dependence on the topology and the vertex condition, but also provide detail of their behaviour with respect to the parameters involved.

Keywords: Quantum graphs, self-adjoint vertex coupling, time-reversal invariance, PT-symmetry, spectral properties, scattering properties, periodic systems

# Contents

# Introduction

Quantum graphs, not always necessarily known under this name, have been used since the 1930s as models in various fields of physics, mathematics, chemistry and engineering. Only since the end of the 1980s, however, the concept has been gradually transformed into a coherent, and more widely studied, subject - we can account this growth to the relevance of quantum graphs as simplified models in mentioned scientific areas anytime one considers wave propagation through systems at a wide range of scales, from macroscopic to nanostructures. Those include for example quantum wires, photonic crystals or carbon nanostructures. Beyond their use as models of specific systems, quantum graphs provide a testing ground to study fundamental properties of quantum dynamics, for instance, manifestations of quantum chaos. Altogether, this is a field full of exciting challenges inviting multidisciplinary approaches; for its broad survey we refer to the monograph [BK13].

In the article [SK15] (see also [SV23]), techniques of quantum graphs were used to model the anomalous Hall effect. Their results prompted further research into time-reversal non-invariant graphs, because in order to derive an expression for Hall voltage, their model involves only atomic orbitals with a specific orientation. This is hardly justifiable from the first principles. The needed violation of the time-reversal invariance can be, however, achieved by an appropriate choice of the vertex coupling conditions. The first example of that type was presented in the paper [ET18], where they have shown how spectral properties of quantum graphs heavily depend on their topology, in particular, on the vertex-degree parity. The same effect was also observed in spectra of other periodic system investigated in [BET21].

The matrices describing such vertex coupling belong to the circulant class, together with many others like those characterizing the well-known $\delta$ or $\delta'$ couplings. In contrast to the 'rotational coupling', those are invariant with respect to the time reversal. Despite this difference, such couplings have a common property: in planar graphs they exhibit a PT-symmetry. This concept is usually associated with non-selfadjointness of the Hamiltonian [ET21], but here one has an unitary evolution invariant with respect to the combined transformations, as demonstrated in the paper [ET21].

The aim of this thesis is to examine graphs with circulant vertex couplings from a broader point of view. In the examples to be analyzed, we will pay particular attention to the dependence on the parameters of the models. Examples can be found in previous works: in [BET22], the effects of graph edge lengths modifications were considered, and in [ETT18], an interpolation between different vertex couplings was considered. We intend to perform an analogous analysis in combination and greater detail.

Let us briefly describe the structure of this thesis. The first chapter introduces the concept of quantum graph in a mathematically rigorous way, as a preliminary to the presentation of the results in the following chapters. Here we will also introduce circulant matrices and derive some of their properties which will be needed further. At the end of the chapter, we recall how one describes symmetries in the context of quantum graphs.

The second chapter is devoted to the simplest situation when the graph has a single vertex being of the star form. We determine here the number and the functional form of graph Hamiltonian eigenvalues in dependence on the vertex condition, introduce the associated scattering matrix and compute its general form, and finally, we inspect its behaviour for low and high energies.

The third chapter deals with spectral properties of a periodic quantum graph in the form of a rectangular lattice. After deriving the corresponding spectral condition for the general circulant matrix, we focus on the case of lattices with coupling belonging to the class of permutation-invariant ones and describe completely their spectral structure.

Finally, the fourth chapter is concerned with another periodic quantum graph, this time a one-dimensional quantum chain. This model was previously studied for different length configurations and vertex conditions, for example, in [BET22] or [DET08]. Here we combine it with the interpolating coupling proposed in [ETT18], and by means of the techniques used in the previous chapter, we examine the spectrum as a function of the parameters in full generality.

# 1. Preliminaries

## 1.1 Quantum graphs

A quantum graph, as a mathematical object, consists of three components - a *metric graph* $\Gamma$; a *differential operator* $H$; and *vertex conditions.* The following definitions of those components are taken or paraphrased from [BK13], and because this thesis is not necessarily about the most general aspects of the graph theory, it will only feature the concepts required to understand our reasoning and results; a detailed exposition of the theory the reader can find in the aforementioned book.

### 1.1.1 Metric graphs

**Definition 1.1** (Graph). *A graph* $\Gamma$ *consists of*

- *a set of vertices* $\{v_i\} = \mathcal{v}$*; the number of its elements finite or countably infinite;*
- *and a set of edges* $\{e_j\}$ *connecting (some or all of) them.*

As we can see, the basic notion of a graph does not have additional structures, for example, it is not equipped with a metric, which is important for quantum graphs.

The symbol $v_i \in e_j$ means that the vertex $v_i$ is an endpoint of the edge $e_j$. Vertices $u$ and $v$ are *adjacent*, denoted $u\sim v$, if there is an edge connecting them. The topology of a graph is specified by $|\mathcal{v}| \times |\mathcal{v}|$ *adjacency matrix* $A_{\Gamma,uv}$, generally defined as

$$A_{\Gamma,uv} = \begin{cases} 1 & \text{if } u\sim v, \\ 0 & \text{otherwise.} \end{cases}$$

The *degree* $d_u$ of a vertex $u$ is the number of edges emanating from given $u$, and it holds that

$$d_u = \sum_{v\in\mathcal{v}} A_{\Gamma,uv}.$$

The edges can be undirected (without specified direction), or directed (each edge has assigned one origin and one terminal vertex). Directed edges are called *bonds*, and if all edges of a graph are bonds, the graph is then called *directed graph* or *digraph.* With respect to vertices, bonds can be either *incoming* or *outgoing*. One can convert a non-oriented graph to a digraph by exchanging each edge for a pair of bonds $b$ and $\bar{b}$ with opposite directions - bond $b$ is then called *reversal* to $\bar{b}$ (and vice versa). Analogously, a directed graph can be made undirected - through natural projection that maps mutually reversal bonds into a single edge - but only if it is possible for all connections between vertices.

Graphs, where one treats edges only as relations between vertices, are also called *discrete* or *combinatorial.* On the other hand, if we consider edges as individual one-dimensional objects on their own, then we call those graphs *complexes.* Metric graphs are complexes, and as such we require more from their edges - namely we want to describe their character in greater detail.

**Definition 1.2** (Metric graph)**.** *A graph $\Gamma$ is a metric graph if it satisfies Definition* (1.1) *with these additional conditions:*

1. *a length $L_b \in (0,\infty\rangle$ is assigned to each bond $b$. If an edge has infinite length, it will have only one vertex (at its beginning) and will be called* lead*;*

2. *the lengths of the bonds that are mutually reversal are assumed to be equal, $L_b = L_{\bar{b}}$. Therefore, length of an edge $e$ is also defined, $L_e = L_b$;*

3. *a coordinate $x_b \in \langle 0, L_b\rangle$ is assigned to each bond, increasing in the direction of the bond;*

4. *the relation $x_{\bar{b}} = L_b - x_b$ holds for coordinates on mutually reversed bonds.*

*If all edges are of equal length, the metric graph $\Gamma$ is then called* equilateral*.*

The suggestiveness of the name tells us that each metric graph can be equipped with a natural metric - a sequence of edges $\{e_j\}_{j=1}^{M}$ between vertices $v$ and $w$ (also called *path*) has length $\sum_{j=1}^{M} L_j$, and distance $\rho(v,w)$ between said vertices is then the minimal length of the path connecting them. Here we implicitly assume that loops (single edge with both ends connected to one vertex) or multiple edges between any two vertices are not present, as they can be broken into individual pieces through the introduction of new, so-called "dummy", vertices with $d_v = 2$. And since there is the coordinate $x$ on each edge, it is not problematic to define the distance between two arbitrary points belonging to the graph.

It should be noted that for quantum graphs (or any metric graph for that matter) it is usually assumed that the degree of each vertex is finite and positive (this, for example, means that vertices not connected to any edge are prohibited).

**Definition 1.3.** *A connected metric graph $\Gamma$ is called* infinite *if it has infinitely many vertices, otherwise it is called* finite*. A finite graph with all edges of finite length is called* compact*.*

While here we will deal with both finite and infinite graphs, they will always be undirected.

One last note regarding metric graphs - vertices are obviously their points, but the same is true for all points $x$ on the edge $e$. So when we speak about functions on metric graph $\Gamma$, we are able to define them also along the edges. Moreover, the coordinates living on them then enable the definition of the Lebesgue measure $dx$ on the graph. This in turn enables the definition of some standard function spaces on $\Gamma$. Let us recall the notation typically used for Sobolev spaces, in a scope sufficient for our research (in particular, we define it only in one dimension).

**Definition 1.4** (Weak derivative, Sobolev space)**.** *Suppose that $\Omega$ is an open subinterval of $\mathbb{R}$. Let $f$ be a function locally integrable on $\Omega$, $f \in L^1_{loc}(\Omega)$. The function $f$ has a weak derivative of order $k \in \mathbb{N}_0$ if there exist a function $g \in L^1_{loc}(\Omega)$ satisfying*

$$\int_\Omega f(x)\partial^k\psi(x)dx = (-1)^k \int_\Omega g(x)\psi(x)dx$$

*for all $\psi \in C_c^\infty(\Omega)$, i.e. infinitely differentiable functions with compact support.*

*Suppose $k \in \mathbb{N}_0$, $1 \le p \le \infty$. Then the Sobolev space $W^{k,p}(\Omega)$ consists of equivalence classes of functions $f$ satisfying*

$$W^{k,p}(\Omega) = \{f \in L^p(\Omega) : \forall\, n \in \mathbb{N}_0, n \le k, \partial^n f \in L^p(\Omega)\},$$

*where the derivative is taken in a weak sense. The standard norm on these spaces is defined as*

$$\|f\|_{W^{k,p}(\Omega)} = \left(\sum_{n=0}^{k} \int_\Omega |\partial^n f|^p\right)^{\frac{1}{p}} \quad \text{for } 1 \le p < \infty,$$
$$\|f\|_{W^{k,\infty}(\Omega)} = \max_{n \le k} \sup_\Omega |\partial^n f| \qquad \text{for } p = \infty.$$

*We usually denote $H^k(\Omega) := W^{k,2}$.*

In particular, $H^0(\Omega) = L^2(\Omega)$. Extending these to quantum graphs is then quite straightforward.

**Definition 1.5.** *1. The space $L^2(\Gamma)$ on $\Gamma$ consists of equivalence classes of measurable and square-integrable functions on each edge $e$ in a way that*

$$\|f\|^2_{L^2(\Gamma)} := \sum_{e \in \{e\}} \|f\|^2_{L^2(e)} < \infty.$$

*2. The Sobolev space $H^1(\Gamma)$ on $\Gamma$ consist of equivalence classes of continuous functions belonging to $H^1(e)$ on each edge $e$ in a way that*

$$\|f\|^2_{H^1(\Gamma)} := \sum_{e \in \{e\}} \|f\|^2_{H^1(e)} < \infty.$$

The requirement of continuity is a natural condition for $f$ from $H^1(\Gamma)$, because then $f$ assumes the same value on all edges adjacent to a particular $v$, and $f(v)$ is uniquely defined for all vertices. There is then a clear similarity to traditional one-dimensional setting, in which $H^1$ functions are continuous.

In contrast, there is no such condition, and therefore no natural definition of $H^k(\Gamma)$, for $k > 1$, because we do not necessarily know what should functions satisfy at the graph vertices. This freedom of choice largely influences how our studied system behaves, as will be seen later. Until specified, we require at least smoothness of functions along the edges, and for our later examples, it is preferable to consider this weaker condition even for $H^1$.

**Definition 1.6.** *By $\tilde{H}^k(\Gamma)$, $k \in \mathbb{N}$, we denote space*

$$\tilde{H}^k(\Gamma) := \bigoplus_{e \in \{e\}} H^k(e),$$

*in which all functions $f$ living on $\Gamma$ belong to the Sobolev space $H^k(e)$ on each edge and*

$$\|f\|^2_{\tilde{H}^k(\Gamma)} := \sum_{e \in \{e\}} \|f\|^2_{H^k(e)} < \infty.$$

### 1.1.2 Differential operator

The leap from a metric to a quantum graph is made by assigning a differential (or even more general) operator on $\Gamma$. In our setting, but also commonly in physical applications, we will call this operator the *Hamiltonian*, as we consider a quantum particle "living" on the graph - the graph acts as a configuration space for said particle. Hamiltonian can be interpreted as an operator of the total energy of the system and is usually required to be self-adjoint. The most studied operator assigns to function $f(x_e)$ its negative second derivative on each edge:

$$f(x_e) \mapsto -\frac{d^2 f}{dx_e^2}(x_e). \tag{1.1}$$

More generally, the Schrödinger operator might be used; its action is described as

$$f(x_e) \mapsto -\frac{d^2 f}{dx_e^2}(x_e) + V(x_e) f(x_e),$$

where $V(x)$ is called an *electric potential.*

*Remark.* We understand the term 'electric potential' as a potential related to all non-magnetic forces. It usually stems from the interaction of charge with an external field, but can correspond to any other force, for example gravitational.

Both of these two operators do not contain first-order derivatives or terms proportional to them, therefore they might be used on undirected metric graphs (their edges respectively). This is not the case of a magnetic Schrödinger operator

$$f(x_b) \mapsto \left(\frac{1}{i}\frac{d}{dx_b} - A(x_b)\right)^2 f(x_b) + V(x_b) f(x_b),$$

with a *magnetic potential* $A(x)$, which is (one-dimensional) vector field. Here we need to specify individual bonds and their direction - but it can be shown that these problems can be solved, or rather circumvented, by slight change to the structure of the graph [BK13, Section 2.6]. Overall, in this thesis we will restrict ourselves only to (1.1).

An operator cannot be properly defined without a description of its domain, which should also include information about the smoothness of functions on the edges and conditions at the vertices. Additional conditions are imposed if we also require it to be self-adjoint - Hamiltonian then represents an observable quantity. When we consider operator (1.1) (or more general one with "nice" enough potentials), it is satisfactory for functions $f$ to be in Sobolev space $H^2(e)$ on each edge $e$. Then we must "just" find the self-adjoint extensions through boundary conditions; this procedure is explained in detail in [BK13, Section 1.4.1].

### 1.1.3 Vertex conditions

Once we assume that the domain of the operator is in Sobolev space $H^2(e)$ on each edge $e$, we can use Sobolev trace theorem to show that functions $f$ and their first derivatives are correctly defined at the endpoints (vertices) of edges in question as the appropriate one-sided limits. Thus, the vertex boundary condition may only contain data from boundary values of $f$ and $df/dx$. In this work we assume that studied graphs only have *local vertex conditions* - for a fixed vertex $v$, its condition takes values only from functions and their derivatives at the vertex $v$ - as these are the simplest and physically natural vertex conditions. It can be shown that non-local conditions can be transformed into a local one living inside a single vertex by modifying the topology of the graph [BK13, Section 1.4.6], even though this might not preserve their type.

Our operator (1.1) acts as a second-order operator, therefore the ODE theory tells us we need to establish two conditions for each edge to acquire the solution. The number of conditions at every vertex then must be equal to its degree $d_v$. The most general (homogeneous) condition can be written as

$$A_v F(v) + B_v F'(v) = 0,$$

where $F(v)$ is a $d_v$ dimensional vector of functions, each living on its own edge incident to vertex $v$, evaluated at the said $v$; similarly with $F'(v)$ as a vector of first derivatives; and $A_v$ and $B_v$ are $d_v \times d_v$ matrices. To have the correct number of independent conditions means that rank of $d_v \times 2d_v$ matrix $(A_v, B_v)$ must be full, i.e. $d_v$.

As the proof of the following theorem takes several pages and an additional lemma to complete, it will not be shown here and we will rather focus on its results - how should we choose vertex condition in order to achieve self-adjoint Hamiltonian; the interested reader can find it in [BK13, Section 1.4.1].

**Theorem 1.1.** *Let $\Gamma$ be a metric graph with finitely many edges. Consider the operator acting as $-\frac{d^2 f}{dx_e^2}$ on each edge $e$ with the domain consisting of functions that belong to $\tilde{H}^2(\Gamma)$ and satisfying some local vertex conditions involving vertex values of functions and their derivatives. The operator is self-adjoint if and only if the vertex conditions can be written in one of the following ways:*

1. *For every vertex $v$ of degree $d_v$ there exist $d_v \times d_v$ matrices $A_v$ and $B_v$ such that the $d_v \times 2d_v$ matrix $(A_v, B_v)$ has the maximal rank, the matrix $A_v B_v^*$ (where $B_v^*$ denotes Hermitian adjoint of $B_v$) is self-adjoint and the boundary values of $f$ satisfy*

$$A_v F(v) + B_v F'(v) = 0$$

2. *For every vertex $v$ of degree $d_v$ there exist a unitary $d_v \times d_v$ matrix $U_v$ such that the boundary values of $f$ satisfy*

$$i(U_v - I)F(v) + (U_v + I)F'(v) = 0,$$

*where $I$ is a $d_v \times d_v$ identity matrix.*

3. *For every vertex $v$ of degree $d_v$, there are three mutually orthogonal projectors $P_{D,v}$, $P_{N,v}$ and $P_{R,v} = I - P_{D,v} - P_{N,v}$, acting in $\mathbb{C}^{d_v}$, and an invertible self-adjoint operator $\Lambda_v$, acting in the subspace $P_{R,v}\mathbb{C}^{d_v}$, such that the boundary values of $f$ satisfy*

$$\begin{aligned} P_{D,v} F(v) &= 0 \\ P_{N,v} F'(v) &= 0 \\ P_{R,v} F'(v) &= \Lambda_v P_{R,v} F(v) \end{aligned}$$

As it is obvious from the assumptions, Theorem 1.1 is valid for finite graphs only. Similar results, whose proofs are present in [BK13, Section 1.4.4], can be obtained for (countably) infinite graphs if we assume lengths of all edges uniformly bounded from below ($0 < L_0 \leq L_e \leq \infty$), with additional specifics on the domain of the Hamiltonian - mainly we require that $\sum_e \|f\|^2_{H^2(e)} < \infty$ and the third type of condition from Theorem 1.1 is satisfied for all $v$. While it is possible to consider quantum graphs without restrictions on the lengths of their edges, i.e. $\inf L_e = L_0 > 0$ is not satisfied, the problem of self-adjointness becomes much more complicated, see [EKMN18].

Here we list some examples of common vertex conditions (compare with standard terminology used with regards to differential equations), and their representations as unitary matrices $U_v$ - here we denote $d_v \times d_v$ unit matrix as $I$ and $d_v \times d_v$ matrix with 1 in all entries as $J$:
Dirichlet vertex condition

$$\begin{cases} f(x) \text{ is continuous at } v, \\ f(v) = 0, \\ U_v = -I. \end{cases}$$

Kirchhoff vertex condition (also called Neumann, standard or free)

$$\begin{cases} f(x) \text{ is continuous at } v, \\ \sum_e \frac{df}{dx_e}(v) = 0, \\ U_v = I. \end{cases}$$

$\delta$-type vertex condition

$$\begin{cases} f(x) \text{ is continuous at } v, \\ \sum_e \frac{df}{dx_e}(v) = \alpha_v f(v),\, \alpha_v \in \mathbb{R}, \\ U_v = \frac{2}{d_v + i\alpha_v} J - I. \end{cases} \tag{1.2}$$

And while written explicitly above, they can be summarized into

$$\begin{cases} f(x) \text{ is continuous at } v, \\ \cos(\gamma_v) \sum_e \frac{df}{dx_e}(v) = \sin(\gamma_v) f(v), \\ U_v = \frac{2}{d_v + i\tan(\gamma_v)} J - I,\, \gamma_v \neq \pi/2 \end{cases}$$

where $\gamma_v = 0$ corresponds to Kirchhoff, $\gamma_v = \pi/2$ to Dirichlet, and all other values between to $\delta$-type condition (and only for this type is the $U_v$ matrix formula present usable).

Similar to $\delta$-type condition is $\delta'$-type condition, with roles of functions and their derivatives switched:

$$\begin{cases} \text{values of } \frac{df}{dx_e}(v) \text{ are independent of } e \text{ adjacent to the } v, \\ \sum_e f_e(v) = \alpha_v \frac{df}{dx_e}(v), \alpha_v \in \mathbb{R}, \\ U_v = \frac{-2}{d_v - i\alpha_v} J + I. \end{cases} \tag{1.3}$$

These are all examples of permutation-invariant vertex conditions. Their name comes from the fact that the vertex condition stays the same after any permutation of edges adjacent to the vertex, and they can be generally written as

$$U = rJ + sI, \tag{1.4}$$

where $\{r, s\} \in \mathbb{C}$. We will closely examine the spectral properties of a rectangular lattice equipped with this condition in Section 3.2.

### 1.1.4 Periodic graphs

A larger part of this thesis regards infinite graphs, but all of them will be periodic. As was shown in [BK13], this allows us to solve relevant equations inside the elementary cell, also called *fundamental domain*, and then extend the solution on the whole graph.

**Definition 1.7** (Periodic graph)**.** *An infinite combinatorial, metric, or quantum graph* $\Gamma$ *is said to be* periodic *(or* $\mathbb{Z}^n$*-periodic) if there is a free abelian group* $G = \mathbb{Z}^n$ *and mapping* $(g, x) \in G \times \Gamma \mapsto gx \in \Gamma$ *with following properties:*

1. ***Group action****:*
   - *For any* $g \in G$*, the mapping* $x \mapsto gx$ *is a bijection of* $\Gamma$*.*
   - $0x = x$ *for every* $x \in \Gamma$*, with* $0 \in G$ *being the neutral element.*
   - $(g_i g_j)x = g_i(g_j x)$ *for any* $g_i, g_j \in G, x \in \Gamma$*.*
2. ***Continuity****: For any* $g \in G$*, the mapping* $x \mapsto gx$ *is continuous.*
3. ***Faithfulness****: If* $gx = x$ *for some* $x \in \Gamma$*, then* $g = 0$*.*
4. ***Discreteness****: For any* $x \in \Gamma$*, there is a neighbourhood* $U$ *of* $x$ *such that* $gx \notin U$ *for* $g \neq 0$*.*
5. ***Co-compactness****: The space of orbits* $\Gamma/G$ *is compact, i. e. the* $\Gamma$ *can be obtained by* $G$*-shifts of a compact subset.*
6. ***Structure preservation****:*
   - $gu \sim gv$ *if and only if* $u \sim v$*. Specifically,* $G$ *acts bijectively on edges.*
   - *In the case of a metric or quantum graph, the action preserves lengths of edges:* $L_{ge} = L_e$*.*
   - *For quantum graphs, the action commutes with the Hamiltonian* $H$ *and preserves the vertex conditions.*

**Definition 1.8** (Fundamental domain)**.** *If there exist a compact part* $Q$ *of* $\Gamma$ *satisfying:*

- *the union of all* $G$*-shifts of* $Q$ *covers the* $\Gamma$
$$\bigcup_{g \in G} gQ = \Gamma;$$
- *differently shifted copies of* $Q$ *have only finitely many common parts, none of which are vertices;*

*then the* $Q$ *is called* fundamental domain *of* $\Gamma$*. This* $Q$ *is not uniquely defined.*

### 1.1.5 Floquet-Bloch theory

**Definition 1.9** (Character). Character *of the group* $G$ *is a homomorphism* $\varsigma : G \mapsto \mathbb{C} \setminus \{0\}$, *with* $\mathbb{C} \setminus \{0\}$ *being considered as a group with respect to multiplication. Therefore*

$$\varsigma(e) = 1, \textit{ where } e \textit{ is the unit of } G,$$
$$\varsigma(g_i g_j) = \varsigma(g_i)\varsigma(g_j) \textit{ for any } g_i, g_j \in G.$$

**Lemma 1.1.** *Every character of* $G = \mathbb{Z}^n$ *can be represented by a vector* $\theta \in \mathbb{C}^n$*:*

$$\varsigma(g) = e^{i\theta \cdot g}, g \in G.$$

*This character is unitary (maps* $G$ *into the unit circle) if and only if* $\theta \in \mathbb{R}^n$*.*

Vectors $\theta$ are in physics known as *quasi-momenta*. Characters represented as such are $2\pi$-periodic with respect to (individual components of) $\theta$. If we consider only real quasi-momenta, we can restrict their values to any fundamental domain $B$ of the action of $2\pi\mathbb{Z}^n$. $B$ is usually chosen as the cube

$$B = \langle -\pi, \pi\rangle^n,$$

which is in quantum theory called *Brillouin zone*.

If we factor out group action and $2\pi$-periodicity, we get a complex vector with non-zero components

$$z := e^{i\theta} = (e^{i\theta_1}, \dots, e^{i\theta_n})$$

called *Floquet multipliers*.

**Definition 1.10** (Floquet transform). *Floquet transform of the function* $f$ *is defined as*

$$f(v) \mapsto \hat{f}(v,z) = \sum_{g \in \mathbb{Z}^n} f(gv) z^{-g},$$

*where* $g$ *acts on vertex* $v$ *and* $z$ *is a Floquet multiplier.*

The Floquet transform on a quantum graph reduces the Hamiltonian $H$ to a set of differential operators $H(z)$ on fundamental domain $Q$ [BK13]. We choose this domain conveniently in a way that there are no original vertices on the domain boundary. Additional vertices of degree one then automatically appear on the edges in the points crossing our chosen boundary, with their respective vertex condition (continuation of the function on the edge). Concrete examples of this technique will be shown in the following chapters.

### 1.1.6 Spectral properties

The spectrum $\sigma(H)$ of the operator $H$ in $L^2(\Gamma)$ is the union of the closed finite intervals of eigenvalue ranges,

$$I_j = \{h_j(z) : z \in B\}$$

called *spectral bands*. *Band-gap structure* is then the name for the representation

$$\sigma(H) = \bigcup_j I_j;$$

some of the intervals in question might be only points.

With a periodic self-adjoint Hamiltonian $H$, its spectrum can contain only absolutely continuous or pure point parts [BK13, Section 4.3.2]. Additionally, bound states and compactly supported eigenfunctions may appear due to the failure of the uniqueness of continuation principle for relevant equations [BK13, Section 3.4] - corresponding eigenvalues are infinitely degenerated and in physics they are called *flat bands*.

## 1.2 Circulant matrices

We have seen that vertex conditions are specified by $d_v \times d_v$ matrices. Our attention will now be focused on a special class of the said matrices.

**Definition 1.11** (Circulant matrix). *Let $\boldsymbol{c}$ be general vector (*generating vector*) in the form $\boldsymbol{c} = (c_1, c_2, c_3, \ldots, c_n)^\top$, where $c_l \in \mathbb{C}$ for all $l = 1, \ldots, n$. Then the $n \times n$ circulant matrix $C$ is given as follows:*

$$C = \begin{pmatrix} c_1 & c_2 & c_3 & \cdots & c_n \\ c_n & c_1 & c_2 & \cdots & c_{n-1} \\ \vdots & c_n & c_1 & \ddots & \vdots \\ c_3 & \cdots & \ddots & \ddots & c_2 \\ c_2 & c_3 & \cdots & c_n & c_1 \end{pmatrix}.$$

*In other words, element $C_{ij}$ is given as $C_{ij} = c_{j-i+1 \pmod{n}}$.*

We shall make and prove (or at least give the general idea of the proof) several claims about properties of circulant matrices, which will be useful later on.

**Proposition 1.1** (Eigenvectors and eigenvalues). *The normalized eigenvectors of circulant matrices are independent of the choice of the vector $\boldsymbol{c}$. They have the form $\phi_l = \frac{1}{\sqrt{n}}(1, \omega^l, \omega^{2l}, \ldots, \omega^{(n-1)l})^\top$, where $\omega := e^{2\pi i/n}$. Furthermore, eigenvalues $\lambda_l$ can be written in the form $\lambda_l = \sum_{a=1}^{n} c_a \omega^{l(a-1)}$.*

*Proof.* When we multiply the supposed eigenvector $\phi_l$ by circulant matrix from the left, the first entry of the resulting vector is

$$\frac{1}{\sqrt{n}} \sum_{a=1}^{n} c_a \omega^{l(a-1)} = \frac{1}{\sqrt{n}} \cdot \sum_{a=1}^{n} c_a \omega^{l(a-1)}.$$

The second entry is then

$$\frac{1}{\sqrt{n}} \sum_{a=1}^{n} c_{a-1} \omega^{l(a-1)} = \frac{\omega^l}{\sqrt{n}} \cdot \sum_{a=1}^{n} c_{a-1} \omega^{l(a-2)} = \frac{\omega^l}{\sqrt{n}} \cdot \sum_{a=1}^{n} c_a \omega^{l(a-1)},$$

where we used the same $a$ as the summation index after the second equality, for the values, over which we sum, are same due to mod $n$ nature of $c_a$ and $\omega$. The $m$-th entry is

$$\frac{1}{\sqrt{n}} \sum_{a=1}^{n} c_{a-m+1} \omega^{l(a-1)} = \frac{\omega^{l(m-1)}}{\sqrt{n}} \cdot \sum_{a=1}^{n} c_a \omega^{l(a-1)}.$$

From that we can conclude that $\phi_l$ is the sought eigenvector, and the eigenvalues are indeed in the form $\lambda_l = \sum_{a=1}^{n} c_a \omega^{l(a-1)}$; there cannot be more than $n$ eigenvalues (excluding multiplicity).

□

**Proposition 1.2** (Commutativity)**.** *Any two given circulant matrices commute, i.e.* $C\widetilde{C} = \widetilde{C}C$.

*Proof.* The demanded property follows from the set of equations, whose relevance we will comment on later. First, let us denote $W = C\widetilde{C}$. Then (in all calculations we work in mod $n$ arithmetic, if needed):

$$
\begin{aligned}
W_{ij} &= \sum_{a=1}^{n} C_{ia}\widetilde{C}_{aj} = \sum_{a=1}^{n} c_{a-i+1}\widetilde{c}_{j-a+1} \\
&= \sum_{a=1}^{n} c_{a+1}\widetilde{c}_{j-i-a+1} = \sum_{a=1}^{n} c_{a+j+1}\widetilde{c}_{-i-a+1} \\
&= \sum_{a=1}^{n} c_{j-(n-a)+1+n}\widetilde{c}_{n-i-a+1} = \sum_{a=1}^{n} c_{j-(n-a)+1}\widetilde{c}_{(n-a)-i+1} \\
&= \sum_{a=1}^{n} c_{j-a+1}\widetilde{c}_{a-i+1} = \sum_{a=1}^{n} \widetilde{C}_{ia}C_{aj}
\end{aligned}
$$

The first equality is expression of a general element of $W$ from matrix multiplication, the second then uses the property of circulant matrices from Definition 1.11. The third and fourth use different forms of values from the sum - specifically, we use shifted summation indices throughout those steps, but we can rename them back to $a$, similarly to Proposition 1.1. The fifth one then uses modular property of defining vector $\mathbf{c}$, $c_{-j} = c_{n-j}$. The sixth just regroups index $a$, the seventh uses renaming, and finally the eighth one is just expression of matrix multiplication $\widetilde{C}C$.

□

**Proposition 1.3** (Diagonalization, expression of $c_l$)**.** *Circulant matrices are diagonalizable by the discrete Fourier transform, i.e.* $D = VCV^*$*, where* $C$ *is a circulant matrix,* $D$ *is a diagonal matrix with circulant matrix's eigenvalues on its diagonal and* $V$ *is an unitary DFT matrix, where*

$$
V = \frac{1}{\sqrt{n}} \begin{pmatrix}
1 & 1 & 1 & 1 & \dots & 1 \\
1 & \omega^{-1} & \omega^{-2} & \omega^{-3} & \dots & \omega^{-(n-1)} \\
1 & \omega^{-2} & \omega^{-4} & \omega^{-6} & \dots & \omega^{-2(n-1)} \\
\vdots & \vdots & \vdots & \vdots & & \vdots \\
1 & \omega^{-(n-1)} & \omega^{-2(n-1)} & \omega^{-3(n-1)} & \dots & \omega^{-(n-1)^2}
\end{pmatrix}.
$$

*The coefficients* $c_l$ *can be cast as* $c_l = \frac{1}{n}\sum_{a=1}^{n} \lambda_a \omega^{-a(l-1)}$.

*Sketch of proof.* Because of Proposition 1.2, any circulant matrix is also a normal matrix, i.e. $[C, C^*] = 0$, because the Hermitian adjoint of a circulant matrix is also circulant. Thus is $C$ unitary diagonalizable from the spectral theorem, which tells us that an operator on a finite-dimensional vector space is normal if and only if it is unitarily diagonalizable. The fact that $V$ is indeed the sought unitary transformation matrix can be verified by direct computation, same as the form of numbers on the diagonal. Expression of the coefficients $c_l$ follows from inverse discrete Fourier transformation, i.e. $C = V^* D V$, where it should be noted that $D_{ii} = \lambda_{i-1 \pmod n}$ with $\lambda_l$ defined in Proposition 1.1.

□

As will be seen later on, the form of vertex condition we will be using is a variant of the second one from Theorem 1.1, so circulant matrices used in them also need to be unitary.

**Proposition 1.4** (Unitarity). *For any circulant matrix $C$ to be unitary requires following conditions to be met:*

$$\begin{cases} \sum_{a=1}^{n} |c_a|^2 = 1 \\ \sum_{a=1}^{n} c_a \overline{c_{a+b}} = 0 \quad \textit{for} \quad b = 1, \dots, n-1 \end{cases}$$

*Proof.* Because Proposition 1.2 holds, we need to check only that $CC^* = I$. Direct calculation and matching of respective matrix entries then gives us the first condition from calculating diagonal terms and the second from calculating off-diagonal ones.

□

*Remark.* There are alternative ways how one can approach these problems - for example Proposition 1.3 can be proven without the help of Proposition 1.2, and Proposition 1.2 would then be immediately obvious, because any pair of circulant matrices is simultaneously diagonalizable.

## 1.3 Symmetries

In quantum mechanics, any transformation of the system can be described by an unitary or an antiunitary operator $\Theta_{\mathbb{T}} : \mathbb{H} \to \mathbb{H}$, where $\mathbb{H}$ is associated Hilbert space of quantum states; under this transformation, quantum states and operators behave as

$$\tilde{\Psi} = \Theta_{\mathbb{T}} \Psi \quad \text{and} \quad \tilde{O} = \Theta_{\mathbb{T}}^* O \Theta_{\mathbb{T}}.$$

An operator is then said to be symmetric, or invariant, under this transformation if $\tilde{O} = O$, which means that

$$\begin{cases} [\Theta_{\mathbb{T}}, O] = 0 \quad \text{for discrete symmetries, or} \\ [G, O] = 0 \quad \text{for continuous symmetries,} \end{cases}$$

where $G$ is a generator of said symmetry.

In our case we are interested in Hamiltonian $H$ of the system described by (1.1) and its (non-)invariance with respect to time-reversal and parity transformations, and how can these transformations be represented as unitary (or antiunitary) operators. In particular, because the action of (1.1) is real and not dependent on the edge orientation, self-adjointness of $H$, which we need, is determined by a boundary condition. We employ the second part of Theorem 1.1, and require the condition to be satisfied for all $\Theta_{\mathbb{T}} F(v)$; symmetry of such Hamiltonian can then be checked by requiring

$$\Theta_{\mathbb{T}}^* U_v \Theta_{\mathbb{T}} = \Theta_{\mathbb{T}}^{-1} U_v \Theta_{\mathbb{T}} = U_v.$$

The first transformation of those listed above is easier to obtain: time inversion must be antilinear, because

$$\Theta_t^* [X,P] \Theta_t = \Theta_t^* i\hbar \Theta_t = -i\hbar,$$

where $X$ and $P$ are operators of position and momentum, respectively. Note that this relation holds only if the operators are applied to sufficiently regular functions; otherwise we have to resort to the Weyl form of the canonical commutation relation. When we are working in our quantum graph setting, we do not consider the internal degrees of freedom of the particles involved, and use $x$ representation; therefore $\Theta_t$ must be just the complex conjugation operator. When acting as an operator transformation, it behaves as

$$\Theta_t^{-1} U_v \Theta_t = \Theta_t U_v \Theta_t = U_v^T, \tag{1.5}$$

because

$$\begin{aligned}
0 &= i(U_v - I)\Theta_t F(v) + (U_v + I)\Theta_t F'(v),\\
0 &= -i\Theta_t (U_v - I)\overline{F(v)} + \Theta_t (U_v + I)\overline{F'(v)},\\
0 &= -i(\overline{U_v} - I)F(v) + (\overline{U_v} + I)F'(v),\\
0 &= -i(I - U_v^T)F(v) + (I + U_v^T)F'(v),\\
0 &= i(U_v^T - I)F(v) + (U_v^T + I)F'(v),
\end{aligned}$$

where we used unitarity relations $U_v^T \overline{U_v} = I$. Therefore $H$ is time-reversal symmetric if and only if its coupling matrix is transpose-symmetric.

A quantum graph is PT-symmetric if it is symmetric under joint parity and time-reversal transformation. Our knowledge of the form of the latter then implies

$$\Theta_p^{-1} U_v \Theta_p = \Theta_p U_v \Theta_p = U_v^T,$$

just imagine both sides of the equation transformed under time-reversal transformation as in (1.5). To gain additional insight we remember that a diagonal matrix is already equal to its transpose and that $U_v$ is a circulant matrix - we know how $D = V U_v V^*$ from Proposition 1.3, and substituting leads us to

$$\Theta_p V^* D V \Theta_p = V^T D \overline{V}$$

resulting in condition

$$\Theta_p = V^T V,$$

and thus

$$\Theta_p = \begin{pmatrix} 1 & 0 & 0 & \dots & 0 & 0 & 0 \\ 0 & 0 & 0 & \dots & 0 & 0 & 1 \\ 0 & 0 & 0 & \dots & 0 & 1 & 0 \\ \vdots & \vdots & \vdots & \iddots & \vdots & \vdots & \vdots \\ 0 & 0 & 1 & \dots & 0 & 0 & 0 \\ 0 & 1 & 0 & \dots & 0 & 0 & 0 \end{pmatrix}.$$

A priori there is no need to have a quantum graph embedded in any ambient space, even though this embedding naturally exists in some applications (for example quantum wire circuits) [BK13, Section 1.3], but parity transformations are intrinsically linked with mirroring in the Euclidean space. Considering quantum graph as planar, we see that $\Theta_p$ has sought properties, because, under given transformation, it preserves edge $e_1$ (or possibly $e_{k+1}$ as well, if $n = 2k$) and switches edge $e_j$ with $e_{n+2-j}$ [ET21].

# 2. Star graph

## 2.1 Basic properties

Let us consider the so-called quantum star graph - one central vertex connecting $n$ semi-infinite edges. The associated Hilbert space of states is $\bigoplus_{l=1}^{n} L^2(\mathbb{R}_+)$ with elements $\Psi = \{\psi_l\}$, while the Hamiltonian of the system is the aforementioned negative Laplacian provided we employ the atomic units, $\hbar = 2m = 1$, which we always do in this thesis: $H\{\psi_l\} = \{-\psi_l^{''}\}$. The vertex boundary conditions making the Laplacian a self-adjoint operator on the graph are given by Theorem 1.1. We will write them in the form

$$(U - I)\Psi + i(U + I)\Psi^{'} = 0, \tag{2.1}$$

where $U$ is an unitary $n \times n$ circulant matrix and $I$ is an unit $n \times n$ matrix; it is obtained from the second one presented by replacing $U_v$ with $U_v^*$. Needless to say, $U_v$ and $U_v^*$ are unitary circulant simultaneously. Even at this stage we can draw

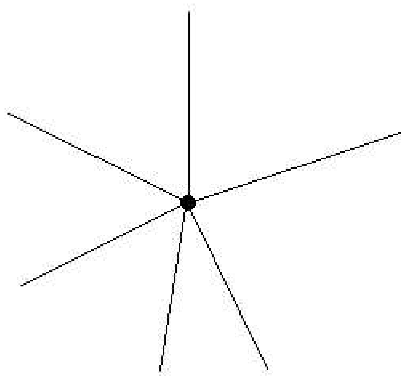

Figure 2.1: An example of a star graph with $n = 6$.

some conclusions about the bound states of a given Hamiltonian. The essential spectrum of any such operator is $\langle 0,\infty)$, as it follows from [Wei12, Theorem 8.19], because any pair referring to different matrices $U$ has a common symmetric restriction of deficiency indices at most $(n, n)$, including the case on $n$ disconnected half-lines, where the property is obvious. The question about the number of bound states, that is, the negative eigenvalues, was addressed in [BET22, Theorem 2.6]; we will prove this claim in a slightly different way.

**Proposition 2.1** (Bound states of a star graph)**.** *For a star graph equipped with the Hamiltonian $H\{\psi_l\} = \{-\psi_l^{''}\}$, the number of its bound states (eigenvalues of the Hamiltonian) is equal to the number of eigenvalues of the unitary matrix $U$, which specifies the boundary condition* (2.1)*, in the upper complex plane.*

*Proof.* When looking for eigenvalues of the Hamiltonian, one solves the following equation

$$H\psi_l = -\kappa^2\psi_l$$

for all $l$. With $H$ specified above, its solution can be written as

$$\psi_l = d_l e^{-\kappa x},$$

where we, without the loss of generality, assume $\kappa > 0$ (as we require $\psi_l \in L^2(\mathbb{R}_+)$). Solutions must also satisfy the indicated boundary condition. That, after the substitution, means

$$(U - I)\mathbf{d} - i\kappa(U + I)\mathbf{d} = 0,$$

which can then be recast as

$$U\mathbf{d} = \frac{1 + i\kappa}{1 - i\kappa}\mathbf{d}.$$

We can clearly see that $\frac{1+i\kappa}{1-i\kappa}$ is an eigenvalue of $U$, and after explicitly retrieving its real and imaginary part,

$$\frac{1 + i\kappa}{1 - i\kappa} = \frac{1 - \kappa^2}{1 + \kappa^2} + \frac{2i\kappa}{1 + \kappa^2},$$

we have one-to-one correspondence between $\kappa$ (consequently $\kappa^2$) and eigenvalues of $U$ in the upper complex plane, because the imaginary part of the eigenvalues is greater than 0.

$\square$

Simple algebraic manipulations then give

$$\kappa_l = -i\frac{\lambda_l - 1}{\lambda_l + 1},$$

where $\lambda_l$ are eigenvalues of $U$ in the upper complex plane, and after recalling Proposition 1.1, we can rewrite values of eigenenergies (in atomic units) in terms of circulant coefficients $c_a$ as

$$\begin{aligned} -\kappa_l^2 &= -\frac{(\lambda_l - 1)(\overline{\lambda_l} - 1)}{(\lambda_l + 1)(\overline{\lambda_l} + 1)} \\ &= -\frac{2 - 2\Re(\lambda_l)}{2 + 2\Re(\lambda_l)} \\ &= -\frac{1 - \Re(\sum_{a=1}^{n} c_a \omega^{l(a-1)})}{1 + \Re(\sum_{a=1}^{n} c_a \omega^{l(a-1)})}, \end{aligned}$$

where $\Re$ denotes the real part of a complex number.

## 2.2 Scattering properties

In general, the scattering vertex matrix can be expressed as [BK13, Lemma 2.1.3.]

$$S(k) = \frac{(k - 1)I + (k + 1)U}{(k + 1)I + (k - 1)U}, \tag{2.2}$$

where $k$ is the momentum of a plane wave in the used units. While this notation may not be necessarily clear from the point of the order of multiplication, as both the numerator and the denominator contain matrices, we should note that all matrices present are circulant, thus their sum with respective coefficients is also circulant, and, recalling Proposition 1.2, we can write the expression in this way interpreting the right-hand side as a function of a single unitary operator in the sense of the functional calculus. If $U$ is circulant, $S(k)$ is circulant as well.

If we define a new variable $\eta := \frac{k-1}{k+1}$, we can rewrite (2.2) as

$$S(k) = \frac{\eta I + U}{I + \eta U}. \tag{2.3}$$

Let us denote $\widetilde{U} := I + \eta U$. This circulant matrix is defined by vector

$$\widetilde{\boldsymbol{c}} = (\widetilde{c_1}, \widetilde{c_2}, \widetilde{c_3}, \ldots, \widetilde{c_n})^\top = (1 + \eta c_1, \eta c_2, \eta c_3, \ldots, \eta c_n)^\top,$$

and its eigenvalues, after we recall Proposition 1.1, are

$$\widetilde{\lambda_l} = \sum_{a=1}^{n} \widetilde{c_a} \omega^{l(a-1)}. \tag{2.4}$$

Its inverse $\widetilde{U}^{-1}$ then has eigenvalues inverse to those in Equation (2.4), and, consequently due to Proposition 1.3, is defined by vector with entries

$$c_l^{'} = \frac{1}{n} \sum_{a=1}^{n} \widetilde{\lambda}_a^{-1} \omega^{-a(l-1)}. \tag{2.5}$$

Equation (2.3) can be rewritten as

$$S(k) = \eta \widetilde{U}^{-1} + \widetilde{U}^{-1} U,$$

so, taking information from (2.5), its general element is given as

$$\begin{aligned} S_{ij} &= \eta c_{j-i+1}^{'} + \sum_{d=1}^{n} c_{d-i+1}^{'} c_{j-d+1} \\ &= \eta \frac{1}{n} \sum_{l=1}^{n} \widetilde{\lambda}_l^{-1} \omega^{-l(j-i)} + \frac{1}{n} \sum_{d=1}^{n} \sum_{l=1}^{n} \widetilde{\lambda}_l^{-1} \omega^{-l(d-i)} c_{j-d+1}. \end{aligned} \tag{2.6}$$

If we do the summation over $d$ first, Equation (2.6) can be substantially simplified. That is because

$$\sum_{d=1}^{n} c_{j-d+1} \omega^{-l(d-i)} = \sum_{d=1}^{n} c_{-d} \omega^{-l(d-i+j+1)} = \omega^{l(i-j)} \sum_{d=1}^{n} c_{-d} \omega^{l(-d-1)} = \lambda_l \omega^{l(i-j)},$$

where we used modular properties of $c_d$ and $\omega$, and the expression of eigenvalues $\lambda_l$. Substituting into Equation (2.6), we have the final expression

$$S_{ij} = \frac{1}{n} \sum_{l=1}^{n} \omega^{l(i-j)} (\eta + \lambda_l) \widetilde{\lambda}_l^{-1}, \tag{2.7}$$

or, equivalently, in terms of coefficients of circulant matrices,

$$S_{ij} = \frac{1}{n} \sum_{l=1}^{n} \omega^{l(i-j)} \frac{\eta + \sum_{a=1}^{n} c_a \omega^{l(a-1)}}{\sum_{b=1}^{n} \widetilde{c}_b \omega^{l(b-1)}}. \tag{2.8}$$

## 2.3 High and low energy limit

Now we take a look into the properties of $S$ matrix in high energy limit $k \to \infty$ and low energy limit $k \to 0$, which is equivalent to $\eta \to 1$ and $\eta \to -1$, respectively. But to do so, we will need the following lemma:

**Lemma 2.1.** $\sum_{a=1}^{n} \omega^{l(a-1)} = 0$ *for all* $l = 1, \dots, n-1$.

*Proof.* By Proposition 1.1, the given sum is equivalent to the expression of eigenvalues of circulant matrix defined by a vector consisting of ones in all its positions. But this matrix has trivially rank one, so all but one eigenvalues are equal to zero, and the only non-zero one corresponds to $d = n$ and is equal to $n$.

□

For the high energy limit, we need to distinguish between two cases - when matrix $U$ has $-1$ in its spectrum, and when it has not. When $-1 \notin \sigma(U)$, we have from Equation (2.7)

$$\lim_{k\to\infty} S_{ij} = \frac{1}{n}\sum_{l=1}^{n} \omega^{l(i-j)} \left(1 + c_1 + \sum_{a=2}^{n} c_a \omega^{l(a-1)}\right)\left(1 + c_1 + \sum_{a=2}^{n} c_a \omega^{l(a-1)}\right)^{-1}, \quad (2.9)$$

where we used specific values of $\lambda_l$ and $\widetilde{\lambda}_l^{-1}$ in given limit. From that, using Lemma 2.1, we can clearly see how

$$\lim_{k\to\infty} S(k) = I, \quad (2.10)$$

as diagonal values will sum to 1 and off-diagonal values will be 0 due to the fact that $i - j$ can be maximally equal to $n - 1 \pmod n$. Note that there is an alternative way to get this result: under our assumption regarding the spectrum of $U$, the operator $I + U$ is invertible and claim (2.10) follows from (2.3) by functional calculus.

When $-1 \in \sigma(U)$, part of the term, corresponding to this eigenvalue, from the sum (2.7), denoted by specific $l$, will be

$$\frac{\eta + \sum_{a=1}^{n} c_a \omega^{l(a-1)}}{1 + \eta \sum_{a=1}^{n} c_a \omega^{l(a-1)}} = \frac{\eta - 1}{1 - \eta} = -1.$$

The previously observed behaviour in the limit $k \to \infty$ is disturbed, as $I + U$ is no longer invertible. Specific values of $S_{ij}$ must be calculated directly and depend on the defining vector $\mathbf{c}$ of circulant matrix $U$, respectively on position of $-1$ in $\sigma(U)$ given by index number $l$ - after substituting into Equation (2.8) we have

$$\lim_{k\to\infty} S_{ij} = \frac{-\omega^{l(i-j)}}{n} + \frac{1}{n}\sum_{d\neq l} \omega^{d(i-j)} \frac{1 + \sum_{a=1}^{n} c_a \omega^{d(a-1)}}{\sum_{b=1}^{n} \widetilde{c}_b \omega^{d(b-1)}},$$

which can be in the limit, now similarly to Equation (2.9), rewritten as

$$\lim_{k\to\infty} S_{ij} = -\frac{\omega^{l(i-j)}}{n} + \frac{1}{n}\sum_{d\neq l} \omega^{d(i-j)}.$$

Finally, we distinguish between diagonal and off-diagonal terms:

$$\begin{aligned}\lim_{k\to\infty} S_{ii} &= -\frac{1}{n} + \frac{n-1}{n} = \frac{n-2}{n},\\ \lim_{k\to\infty} S_{ij} &= -\frac{\omega^{l(i-j)}}{n} + \frac{1}{n}\sum_{d=1}^{n}\omega^{d(i-j)} - \frac{\omega^{l(i-j)}}{n}\\ &= -\frac{2\omega^{l(i-j)}}{n},\end{aligned} \tag{2.11}$$

where we employed Lemma 2.1 for off-diagonal terms. We implicitly assumed that algebraic multiplicity of eigenvalue $-1$ is one - generalization to a case where $-1$ has multiplicity $\mu_A$ is straightforward, as

$$\begin{aligned}\lim_{k\to\infty} S_{ii} &= -\frac{\mu_A}{n} + \frac{n-\mu_A}{n} = \frac{n-2\mu_A}{n},\\ \lim_{k\to\infty} S_{ij} &= -\sum_{l\in M}\frac{\omega^{l(i-j)}}{n} + \frac{1}{n}\sum_{d=1}^{n}\omega^{d(i-j)} - \sum_{l\in M}\frac{\omega^{l(i-j)}}{n}\\ &= -2\sum_{l\in M}\frac{\omega^{l(i-j)}}{n},\end{aligned} \tag{2.12}$$

where $M$ is a set of all $l$ corresponding to $-1$ in $\sigma(U)$ with cardinality of $\mu_A$.

On the other hand, in the low energy limit, we need to be cautious about the presence of 1 in $\sigma(U)$. If 1 is not in the spectrum of $U$, analogical calculation leads to

$$\lim_{k\to 0} S(k) = -I, \tag{2.13}$$

while the other case gives

$$\begin{aligned}\lim_{k\to 0} S_{ii} &= \frac{\mu_A}{n} - \frac{n-\mu_A}{n} = \frac{2\mu_A-n}{n},\\ \lim_{k\to 0} S_{ij} &= \sum_{l\in M}\frac{\omega^{l(i-j)}}{n} - \frac{1}{n}\sum_{d=1}^{n}\omega^{d(i-j)} + \sum_{l\in M}\frac{\omega^{l(i-j)}}{n}\\ &= 2\sum_{l\in M}\frac{\omega^{l(i-j)}}{n},\end{aligned} \tag{2.14}$$

where $M$ and $\mu_A$ now regards 1.

Let us test these formulae in specific examples. Consider defining vector $\mathbf{c}$ with $c_2 = 1$ and other coefficients equal to 0 in dimension $n = 4$. Spectrum of respective $U$, given by Proposition 1.1, is (remembering that in this case $\omega = e^{2\pi i/4} = e^{\pi i/2}$)

$$\begin{aligned}\lambda_1 &= c_2\omega^{1(2-1)} = \omega = i,\\ \lambda_2 &= \omega^2 = -1,\\ \lambda_3 &= \omega^3 = -i,\\ \lambda_4 &= \omega^4 = 1.\end{aligned}$$

Here we have $-1$ with $l = 2$ and 1 with $l = 4$ in $\sigma(U)$, both with multiplicity $\mu_A = 1$. In the high energy limit, individual terms, as by Equation (2.11), are

$$\begin{aligned}\lim_{k\to\infty} S_{ii} &= \frac{1}{2},\\ \lim_{k\to\infty} S_{ij} &= -\frac{\omega^{2(i-j)}}{2} = -\frac{(-1)^{(i-j)}}{2}.\end{aligned}$$

We can see that if $(i-j)$ is even, the corresponding term is equal to $-1/2$, while if $(i-j)$ is odd, matrix entries will be $1/2$. Because $S$ is a circulant matrix regardless of the limit used, we need to compute (for example) the first row only, and finally, we get

$$\lim_{k\to\infty} S = \tfrac{1}{2}\begin{pmatrix} 1 & 1 & -1 & 1 \\ 1 & 1 & 1 & -1 \\ -1 & 1 & 1 & 1 \\ 1 & -1 & 1 & 1 \end{pmatrix}.$$

For the low energy limit, we have

$$\begin{aligned} \lim_{k\to 0} S_{ii} &= -\frac{1}{2}, \\ \lim_{k\to 0} S_{ij} &= \frac{\omega^{4(i-j)}}{2} = \frac{1^{(i-j)}}{2}, \end{aligned}$$

and thus

$$\lim_{k\to 0} S = \tfrac{1}{2}\begin{pmatrix} -1 & 1 & 1 & 1 \\ 1 & -1 & 1 & 1 \\ 1 & 1 & -1 & 1 \\ 1 & 1 & 1 & -1 \end{pmatrix}.$$

Both of these are the same as the results obtained in [ET18] for this particular choice of $U$.

If we choose $\mathbf{c}$ with $c_2 = -1$ and other coefficients 0 again, with dimension $n = 3$, spectrum of $U$, with $\omega = e^{2\pi i/3}$, will be

$$\begin{aligned} \lambda_1 &= -\omega, \\ \lambda_2 &= -\omega^2, \\ \lambda_3 &= -1. \end{aligned}$$

The low energy limit then trivially goes to $-I$ because $1 \notin \sigma(U)$, and the high energy limit can be written as

$$\lim_{k\to\infty} S = \tfrac{1}{3}\begin{pmatrix} 1 & -2 & -2 \\ -2 & 1 & -2 \\ -2 & -2 & 1 \end{pmatrix},$$

which are again results obtained in [ET21].

Let us sum up what we have obtained so far - we proved that the number of star graph's bound states is equal to the number of matrix $U$'s eigenvalues in the upper complex plane, and numerical values of eigenenergies are given by

$$-\kappa_l^2 = -\frac{1-\Re(\lambda_l)}{1+\Re(\lambda_l)}.$$

We calculated the general form of scattering vertex matrix, given by Equation (2.8), and found its limit for $k \to \infty$ and $k \to 0$ in dependence on the spectrum of $U$, given by Equations (2.12) and (2.14) respectively.

# 3. Rectangular graph

## 3.1 Basic properties

Following the results obtained for a star graph, we now consider the first example of a graph with a periodic lattice structure, specifically in the form of a rectangular lattice, whose edges have lengths $l_1$ and $l_2$. The Hamiltonian acting on each edge is still the same as was in the case of a star graph, $H\{\psi_l\} = \{-\psi_l''\}$. The periodicity assumption means that the (general) circulant vertex conditions (2.1) are the same at every vertex, where present matrices now have dimensions 4×4. According to Section 1.1.4, the spectral analysis can be reduced to the investigation of the operator on the fundamental domain sketched in Figure 3.1, which contains a single vertex with the coordinate $x = 0$, and we assume the edge coordinates increase in the upward and right directions.

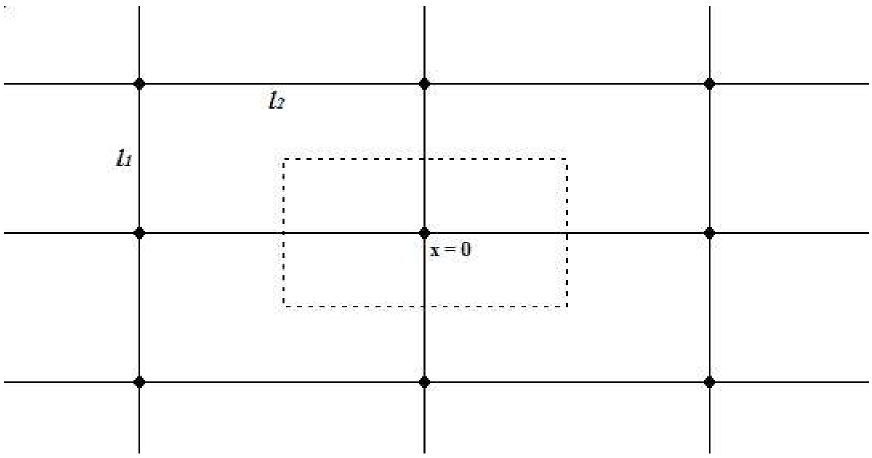


Figure 3.1: A periodic rectangular graph with its elementary cell (fundamental domain) highlighted.

The system is solvable by writing the Ansatz for wave functions on edges as

$$
\begin{aligned}
\psi_1(x) &= a_1 e^{ikx} + b_1 e^{-ikx}, & x \in \langle 0, \frac{l_1}{2} \rangle \\
\psi_2(x) &= a_2 e^{ikx} + b_2 e^{-ikx}, & x \in \langle 0, \frac{l_2}{2} \rangle \\
\psi_3(x) &= \omega_1 (a_1 e^{ik(x+l_1)} + b_1 e^{-ik(x+l_1)}), & x \in \langle -\frac{l_1}{2}, 0 \rangle \\
\psi_4(x) &= \omega_2 (a_2 e^{ik(x+l_2)} + b_2 e^{-ik(x+l_2)}), & x \in \langle -\frac{l_2}{2}, 0 \rangle
\end{aligned}
\tag{3.1}
$$

where the Floquet multipliers, or Bloch phase factors, $e^{i\theta_j}$, $j = 1, 2$ are denoted as $\omega_j$. The fact that

$$
a_3 = a_1 e^{ikl_1},\ b_3 = b_1 e^{-ikl_1},
$$
$$
a_4 = a_2 e^{ikl_2},\ b_4 = b_2 e^{-ikl_2},
$$

comes from the conditions we impose at the elementary cell boundary,

$$\psi_3(-\frac{l_1}{2}) = \psi_1(\frac{l_1}{2}),$$
$$\psi_4(-\frac{l_2}{2}) = \psi_2(\frac{l_2}{2}).$$

Plugging values $\Psi(0)$ and $\Psi'(0)$, where (in contrast to the star graph of the previous chapter) we choose to take the first derivative in the direction of the edge coordinate, into (2.1) leads to a homogeneous linear system of equations for coefficients $a_j$, $b_j$. Its solvability is equivalent to the following determinant being zero

$$\begin{vmatrix} -c_1\eta + c_3\omega_1\mu - 1 & c_1 - c_3\eta\omega_1\overline{\mu} + \eta & -c_2\eta + c_4\omega_2\nu & c_2 - c_4\eta\omega_2\overline{\nu} \\ -c_4\eta + c_2\omega_1\mu & c_4 - c_2\eta\omega_1\overline{\mu} & -c_1\eta + c_3\omega_2\nu - 1 & c_1 - c_3\eta\omega_2\overline{\nu} + \eta \\ -c_3\eta + c_1\omega_1\mu + \eta\omega_1\mu & c_3 - c_1\eta\omega_1\overline{\mu} - \omega_1\overline{\mu} & -c_4\eta + c_2\omega_2\nu & c_4 - c_2\eta\omega_2\overline{\nu} \\ -c_2\eta + c_4\omega_1\mu & c_2 - c_4\eta\omega_1\overline{\mu} & -c_3\eta + c_1\omega_2\nu + \eta\omega_2\nu & c_3 - c_1\eta\omega_2\overline{\nu} - \omega_2\overline{\nu} \end{vmatrix},$$

where we use $\mu = e^{ikl_1}$, $\nu = e^{ikl_2}$ and $\eta = \frac{k-1}{k+1}$ for the sake of brevity. Evaluating the determinant in terms of the original momentum variable $k$ instead of $\eta$, we arrive at the spectral condition

$$\frac{4e^{i(\theta_1+\theta_2)}}{(k+1)^4}\sum_i K_i F_i = 0. \tag{3.2}$$

It is rather long, if written fully, as both coefficients $K_i$ and functions $F_i$ differ in their nature, as polynomials of different order in coefficients $c$ from circulant matrix and variable $k$, or parametric dependence, as functions of $l_1$ and $l_2$; they can be found explicitly in Appendix A.1.

Nevertheless, it becomes particularly simple for the 'extremal' rotationally symmetric coupling,

$$R = \begin{pmatrix} 0 & 1 & 0 & 0 \\ 0 & 0 & 1 & 0 \\ 0 & 0 & 0 & 1 \\ 1 & 0 & 0 & 0 \end{pmatrix}, \tag{3.3}$$

on the square lattice, $l_1 = l_2$; the final spectral condition will be identical to that explicitly derived earlier in [ET18].

## 3.2 Permutation-invariant vertex condition

Permutation-invariant vertex condition (1.4) is a natural class of vertex couplings that directly generalises both the $\delta$ and $\delta'$ condition. In comparison with the general circulant matrix from Definition 1.11, it is much simpler being characterized by only two parameters; in particular, the spectral condition (3.2) simplifies significantly. As we mentioned before, the matrix $U$ specifying vertex condition must be unitary, with the following implication for the parameters:

**Lemma 3.1.** *Matrix $U = rJ + sI$, where $I$ is a $n \times n$ identity matrix and $J$ is a matrix of the same dimensions with 1 in all of its entries, is unitary if and only if $|s| = 1 \wedge |s + nr| = 1$.*

*Proof.* For the implication from the left to the right, the sufficient condition is obtained by substituting the given form of $U$ into Proposition 1.1 in conjunction with Lemma 2.1. From these the matrix $U$ has $n-1$ times degenerated eigenvalue $s$ and one eigenvalue $s+nr$. Both conditions regarding $r$ and $s$ then follow from evaluating unitarity condition $UU^* = U^*U = I$ in the basis set where $U$ is diagonal.

The implication from the right to the left follows from (after a simple manipulation) expressing the unitarity conditions stated in Proposition 1.4.

□

If we use this type of condition for our rectangular lattice, i.e. $c_1 = r + s$, $c_2 = c_3 = c_4 = r$, spectral condition (3.2) is reduced to

$$
\begin{aligned}
-e^{i(\theta_1+\theta_2)}\frac{4}{(k+1)^4}\{ & 4rik[(s-1)^2 + k^2(s+1)^2](\cos\theta_2 \sin kl_1 + \cos\theta_1 \sin kl_2) \\
& +2ik[(s-1)^2(4rs+2r+s^2-1) \\
& +k^2(s+1)^2(4rs-2r+s^2-1)]\sin k(l_1+l_2) \\
& +8rk^2(s-1)(s+1)(\cos\theta_2 \cos kl_1 + \cos\theta_1 \cos kl_2) \\
& +4k^2(s-1)(s+1)(4rs+s^2-1)\cos kl_1 \cos kl_2 \\
& -[2k^2(s-1)(s+1)(4rs+s^2-1) \\
& +k^4(s+1)^3(4r+s+1) \\
& +(s-1)^3(4r+s-1)]\sin kl_1 \sin kl_2\} = 0.
\end{aligned} \tag{3.4}
$$

Let us look into some specific examples. One of the most common permutation-invariant vertex conditions is $\delta$-condition (1.2) - substituting

$$r = \frac{2}{4+i\alpha}, \quad \alpha \in \mathbb{R}, \quad s = -1 \tag{3.5}$$

gives us the left-hand side of Equation (3.4) as

$$2k(\sin k(l_1+l_2) - \cos\theta_2 \sin kl_1 - \cos\theta_1 \sin kl_2) + \alpha \sin kl_1 \sin kl_2.$$

Here we omitted the numerical prefactor $\frac{64ie^{i(\theta_1+\theta_2)}}{(k+1)^4(4+i\alpha)}$, and for convenience, we will continue to do so in other examples as well (with generally different prefactors) - in other words, we display only the part relevant to vanishing of the determinant. Similarly, we have $\delta'$-condition (1.3) with values

$$r = \frac{-2}{4-i\alpha}, \quad \alpha \in \mathbb{R}, \quad s = 1, \tag{3.6}$$

which leads to the left-hand side being

$$2(\sin k(l_1+l_2) + \cos\theta_2 \sin kl_1 + \cos\theta_1 \sin kl_2) - k\alpha \sin kl_1 \sin kl_2.$$

Both of these results are the same as the ones obtained in [EG96] and [Exn96].

## 3.3 Spectral properties

Let us examine spectral condition (3.4) in more detail. It is useful to parametrize coefficients $s$ and $r$ such that

$$
\begin{aligned}
s &= e^{i\vartheta} = \cos\vartheta + i\sin\vartheta \quad \text{and} \\
r &= |r|e^{i\gamma} = |r|(\cos\gamma + i\sin\gamma).
\end{aligned}
$$

As for $s$, we see that unitarity condition regarding $U$ from Lemma 3.1 is satisfied automatically; the second condition then gives

$$|\cos\vartheta + n|r|\cos\gamma + i(\sin\vartheta + n|r|\sin\gamma)| = 1.$$

It can be simplified, using $|s| = 1$, to

$$2n|r|(\cos\vartheta\cos\gamma + \sin\vartheta\sin\gamma) + n^2|r|^2 = 0,$$

leading to either the trivial case of $|r| = r = 0$, or the condition

$$-\frac{2}{n}\cos(\gamma - \vartheta) = |r|,$$

which for $n = 4$ in a rectangular lattice case reads

$$-\frac{1}{2}\cos(\gamma - \vartheta) = |r|.$$

This, in particular, means that $\vartheta$ can be treated as a free parameter chosen from interval $\langle 0, 2\pi)$, while $\gamma$ is without loss of generality restricted to subinterval $\langle \frac{\pi}{2}, \frac{3\pi}{2}\rangle$, including $r = 0$ case. It does not mean that other values of $\gamma$ from $\langle 0, 2\pi)$ are prohibited per se, they just give the same results - if we choose some $\gamma'$ from $\langle -\frac{\pi}{2}, \frac{\pi}{2}\rangle$, we can treat it in the same way as $\gamma - \pi$ with $\gamma \in \langle \frac{\pi}{2}, \frac{3\pi}{2}\rangle$, and

$$\begin{aligned} r' = |r'|e^{i\gamma'} &= -\frac{2}{n}(\cos\gamma' + i\sin\gamma')\cos(\gamma' - \vartheta) \\ &= -\frac{2}{n}[\cos(\gamma - \pi) + i\sin(\gamma - \pi)]\cos(\gamma - \vartheta - \pi) \\ &= -\frac{2}{n}(\cos\gamma + i\sin\gamma)\cos(\gamma - \vartheta) = r. \end{aligned}$$

Substituting our parametrized coefficients into Equation (3.4) gives, discarding irrelevant prefactors, the spectral condition

$$\begin{aligned} &k\cos(\gamma - \vartheta)\,[(\cos\vartheta - 1) + k^2(\cos\vartheta + 1)](\cos\theta_2\sin kl_1 + \cos\theta_1\sin kl_2) \\ &+k\{[-2\cos\gamma + \cos\vartheta\,\cos(\gamma - \vartheta) + \cos(\gamma + \vartheta)] \\ &\quad + k^2[2\cos\gamma - \cos\vartheta\,\cos(\gamma - \vartheta) + \cos(\gamma + \vartheta)]\}\sin k(l_1 + l_2) \\ &+2k^2\,\sin\vartheta\,\cos(\gamma - \vartheta)\,(\cos\theta_2\cos kl_1 + \cos\theta_1\cos kl_2) \\ &+4k^2\,\sin\vartheta\,\cos\gamma\cos kl_1\cos kl_2 \\ &-\{2k^2\sin\vartheta\,\cos\gamma \\ &+k^4[2\sin\gamma\,(\cos\vartheta + 1) - \sin\vartheta\,(\cos\gamma + \cos(\gamma - \vartheta))] \\ &+[2\sin\gamma\,(\cos\vartheta - 1) - \sin\vartheta\,(\cos\gamma - \cos(\gamma - \vartheta))]\}\sin kl_1\sin kl_2 = 0, \end{aligned} \tag{3.7}$$

or, in a form simplified for further purposes,

$$\begin{aligned} &k(A_1 + k^2A_2)(\cos\theta_2\sin kl_1 + \cos\theta_1\sin kl_2) \\ &+k(A_3 + k^2A_4)\sin k(l_1 + l_2) \\ &+k^2A_5(\cos\theta_2\cos kl_1 + \cos\theta_1\cos kl_2) \\ &+k^2A_6\cos kl_1\cos kl_2 \\ &+(k^2A_7 + k^4A_8 + A_9)\sin kl_1\sin kl_2 = 0 \end{aligned} \tag{3.8}$$

(All of $A_i$ are again written explicitly in the Appendix A.2).

**High energy spectrum**

Because the structure of spectral bands at high energies is an important characteristic of transport properties of a quantum graph, consider limit $k \to \infty$ at first. At the leading order, condition (3.8) reads

$$k^4 A_8 \sin kl_1 \sin kl_2 + \mathcal{O}(k^3) = 0,$$

provided that $A_8 \neq 0$. This can happen only if $-1$ is not part of the vertex matrix spectrum. Indeed, we have

$$A_8 = -2 \sin\gamma\,(\cos\vartheta + 1) + \sin\vartheta\,(\cos\gamma + \cos(\gamma - \vartheta)\,),$$

and $-1 \in \sigma(U)$ means either $s = -1$, then necessarily $\cos\vartheta = -1$ with $\sin\vartheta = 0$, and subsequently $A_8 = 0$, or $s + 4r = -1$, where we can simultaneously solve for the real and imaginary part of this expression, from there get

$$\cos\vartheta = \cos 2\gamma \quad \text{and} \quad \sin\vartheta = \sin 2\gamma, \tag{3.9}$$

then finally substituting into $A_8$

$$\begin{aligned} A_8 &= -2\sin\gamma\,(\cos 2\gamma + 1) + \sin 2\gamma\,(\cos\gamma + \cos\gamma\cos 2\gamma + \sin\gamma \sin 2\gamma) \\ &= 2\sin\gamma\,(-\sin\gamma^2 + 1 - \cos\gamma^4 - \sin\gamma^2\cos\gamma^2) \\ &= 2\sin\gamma\,[-\cos\gamma^4 + (1 - \sin\gamma^2)\cos\gamma^2] = 0. \end{aligned}$$

If $-1$ is not an eigenvalue, i.e. Dirichlet part of the matrix eigenspace is not present, the high energy spectrum is dominated by gaps, as bands can be formed only in the vicinity of points

$$k_{m,j} = \tfrac{m\pi}{l_j}, \quad j = 1{,}2 \quad \text{and} \quad m \in \mathbb{N}.$$

We consider the next-to-leading order and rewrite condition (3.8) in the asymptotic form,

$$A_8 \sin kl_1 \sin kl_2 + \frac{A_4 \sin k(l_1 + l_2) + A_2(\cos\theta_2 \sin kl_1 + \cos\theta_1 \sin kl_2)}{k} = \mathcal{O}(k^{-2}), \tag{3.10}$$

and we introduce

$$k = \frac{m\pi}{l_j} + \delta,\ m \in \mathbb{N}. \tag{3.11}$$

As a general rule for this thesis, although we shall always specify them beforehand, we use the expansions

$$\begin{aligned} \sin\ kl_i &= \sin\frac{m\pi l_i}{l_j} + \delta l_i \cos\frac{m\pi l_i}{l_j} - \frac{\delta^2 l_i^2}{2}\sin\frac{m\pi l_i}{l_j} - \frac{\delta^3 l_i^3}{6}\cos\frac{m\pi l_i}{l_j} + \mathcal{O}(\delta^4) \\ \cos\ kl_i &= \cos\frac{m\pi l_i}{l_j} - \delta l_i \sin\frac{m\pi l_i}{l_j} - \frac{\delta^2 l_i^2}{2}\cos\frac{m\pi l_i}{l_j} + \frac{\delta^3 l_i^3}{6}\sin\frac{m\pi l_i}{l_j} + \mathcal{O}(\delta^4) \end{aligned} \tag{3.12}$$

every time there is a need to get a better understanding of the said bands. In these expansions, we stick to the notation introduced in (3.11), where $l_i$ is an arbitrary length relevant to the given problem.

Because the following procedure is practically the same for both $j$, we now focus only on $j = 1$, whereas for $j = 2$ we will present only the final results. Expanding functions around $k_{m,1}$ gives us

$$\begin{aligned}
\sin kl_1 &= (-1)^m \left( \delta l_1 - \frac{\delta^3 {l_1}^3}{6} \right) \\
\sin kl_2 &= \left( 1 - \frac{\delta^2 {l_2}^2}{2} \right) \sin \frac{l_2}{l_1} m\pi + \left( \delta l_2 - \frac{\delta^3 {l_2}^3}{6} \right) \cos \frac{l_2}{l_1} m\pi \\
\sin k(l_1 + l_2) &= (-1)^m \Bigg[ \left( 1 - \frac{\delta^2 (l_1 + l_2)^2}{2} \right) \sin \frac{l_2}{l_1} m\pi \\
&\quad + \left( \delta l_2 - \frac{\delta^3 (l_1 + l_2)^3}{6} \right) \cos \frac{l_2}{l_1} m\pi \Bigg]
\end{aligned}$$

and substituting into Equation (3.10), with $k^{-1} = \frac{l_1}{m\pi} + \mathcal{O}(m^{-2})$, we get

$$\begin{aligned}
&\frac{l_1}{m\pi} [A_4 (-1)^m + A_2 \cos\theta_1] \sin \frac{l_2}{l_1} m\pi \\
&+\delta \{ A_8 (-1)^m l_1 \sin \frac{l_2}{l_1} m\pi + \frac{l_1}{m\pi} [(A_4 (-1)^m (l_1 + l_2) + A_2 l_2 \cos\theta_1) \cos \frac{l_2}{l_1} m\pi \\
&+ A_2 l_1 (-1)^m \cos\theta_2 ] \} \\
&+\delta^2 \{ A_8 (-1)^m l_1 l_2 \cos \frac{l_2}{l_1} m\pi - \frac{l_1}{m\pi} [A_4 (-1)^m \frac{(l_1 + l_2)^2}{2} + A_2 \frac{{l_2}^2}{2} \cos\theta_1 ] \sin \frac{l_2}{l_1} m\pi \} \\
&+\mathcal{O}(\delta^3) = 0.
\end{aligned}$$

Here we want to express $\delta$ as a function of the other parameters, gaining thus an insight into its behaviour. Our strategy revolves around the fact that first, we want to include some $\mathcal{O}(1)$ terms (with respect to $m$), as in the end we work in the limit $m \to \infty$, and secondly, we want to do it through the lowest order of $\delta$ as possible. Now, for example, it is sufficient to take the terms proportional to the first order in $\delta$, and including limit $m \to \infty$ we have

$$\delta(\theta_1) = \frac{-[A_4 (-1)^m + A_2 \cos\theta_1] \sin \frac{l_2}{l_1} m\pi}{A_8 (-1)^m m\pi \sin \frac{l_2}{l_1} m\pi} + \mathcal{O}(m^{-2}).$$

Here we face two possible situations:

- If $\frac{l_2}{l_1}$ is irrational, $\sin \frac{l_2}{l_1} m\pi$ for large $m \in \mathbb{N}$ is never 0, we can cancel it in both the numerator and the denominator, and
$$\delta(\theta_1) = \frac{-[A_4 + A_2 (-1)^m \cos\theta_1]}{A_8 m\pi}.$$
- If $\frac{l_2}{l_1}$ is some rational number, $\sin \frac{l_2}{l_1} m\pi$ is periodic as a function of $m$, and is in particular equal to 0 for $m = m' \frac{l_1}{l_2}$, $m' \in \mathbb{N}$. For such $m$ we must go up to the second order of $\delta$ to be able to express it, and then
$$\delta(\theta_1) = -\frac{1}{m\pi} \frac{A_4 (l_1 + l_2) + A_2 [l_2 (-1)^{m(1 + \frac{l_2}{l_1})} \cos\theta_1 + l_1 \cos\theta_2]}{A_8 l_2 (-1)^{m \frac{l_2}{l_1}}};$$
otherwise asymptotic expression of $\delta(\theta_1)$ stays the same as in the irrational case.

In the asymptotic regime we generally define the dispersion function branch $E_m(\theta)$ around $k = \frac{m\pi}{l_j}$, dependent on an arbitrary Bloch factor, as

$$E_m(\theta) := k_{m,j}^2(\theta) = \Big(\frac{m\pi}{l_j}\Big)^2 + 2\,\frac{m\pi}{l_j}\delta(\theta) + \mathcal{O}(m^0); \tag{3.13}$$

we drop the subscript $j$ because the length $l_j$ is usually not the only relevant length parameter, and we are mostly interested in dependence on $m$ (i. e. higher energies). The corresponding energy band width $\Delta E_m$ is then expressed as

$$\begin{aligned}\Delta E_m &= |k_{m,j}^2(0) - k_{m,j}^2(\pi)| \\ &\approx 2\,\frac{m\pi}{l_j}|\delta(0) - \delta(\pi)|.\end{aligned} \tag{3.14}$$

The sought energy $E_m(\theta_1)$ as a function of the Bloch parameter is now

$$E_m(\theta_1) = \Big(\frac{m\pi}{l_1}\Big)^2 - 2\frac{A_4 + A_2(-1)^m\cos\theta_1}{A_8 l_1} + \mathcal{O}(m^{-1}),$$

while the band width itself is

$$\Delta E_m = \frac{4}{l_1}\left|\frac{A_2}{A_8}\right| + \mathcal{O}(m^{-1}).$$

As for the particular case of rational $\frac{l_2}{l_1}$, the energy has the same expression with corresponding $\delta$, and the band width is

$$\Delta E_m = \frac{4(l_1+l_2)}{l_1 l_2}\left|\frac{A_2}{A_8}\right| + \mathcal{O}(m^{-1}); \tag{3.15}$$

while we do not necessarily know the value of $(-1)^{m(1+\frac{l_2}{l_1})}$, $\theta_1$ is the first component of the quasimomentum, and we can always choose a combination of $\theta_1$ and $\theta_2$ at the border of the Brillouin zone leading to a maximum difference between boundaries of said energy band(s).

The calculation for $l_i = l_2$ leads to similar results, as

- for $\frac{l_1}{l_2} \notin \mathbb{Q}$
$$\delta(\theta_2) = \frac{-[A_4 + A_2(-1)^m\cos\theta_2]}{A_8 m\pi}$$
,
- for $\frac{l_1}{l_2} \in \mathbb{Q}$
$$\delta(\theta_2) = -\frac{1}{m\pi}\,\frac{A_4(l_1+l_2) + A_2[l_2\cos\theta_1 + l_1(-1)^{m(1+\frac{l_1}{l_2})}\cos\theta_2]}{A_8 l_1(-1)^{m\frac{l_1}{l_2}}};$$
if $m = m'\frac{l_2}{l_1}$, otherwise $\delta$ stays the same as for the irrational case,

and from that

$$\Delta E_m = \frac{4}{l_2}\left|\frac{A_2}{A_8}\right| + \mathcal{O}(m^{-1})$$

for irrational and some cases of a rational fraction of lengths, or band widths given by Equation (3.15) for specific instances of a rational case where $\sin \frac{l_1}{l_2} m\pi = 0$.

However, as we have seen before, if $-1$ is part of the matrix spectrum, $A_8 = 0$ and the asymptotic band-gap structure changes. If $s = -1$, then $\vartheta = \pi$,

$$A_2 = A_4 = A_5 = A_6 = A_7 = A_8 = 0$$

and in limit $k \to \infty$ we have

$$\begin{aligned}
&A_1 \left(\cos\theta_2 \sin kl_1 + \cos\theta_1 \sin kl_2\right) + A_3 \sin k(l_1 + l_2) + \mathcal{O}(k^{-1}) \\
=&2\cos\gamma \left(\cos\theta_2 \sin kl_1 + \cos\theta_1 \sin kl_2 - \sin k(l_1 + l_2)\right) + \mathcal{O}(k^{-1}) = 0,
\end{aligned}$$

where everything except the error term is annulated by setting

$$\theta_1 = kl_1 + 2n\pi \quad \wedge \quad \theta_2 = kl_2 + 2m\pi, \quad n, m \in \mathbb{Z}.$$

If $s + 4r = -1$, for large $k$ condition (3.8) reads

$$A_2 \left(\cos\theta_2 \sin kl_1 + \cos\theta_1 \sin kl_2\right) + A_4 \sin k(l_1 + l_2) + \mathcal{O}(k^{-1}) = 0,$$

but using previously established relations (3.9) between $\vartheta$ and $\gamma$ we get

$$2\cos\gamma^3 \left(\cos\theta_2 \sin kl_1 + \cos\theta_1 \sin kl_2 + \sin k(l_1 + l_2)\right) + \mathcal{O}(k^{-1}) = 0,$$

satisfied, up to the error term, by

$$\theta_1 = kl_1 + (2n+1)\pi \quad \wedge \quad \theta_2 = kl_2 + (2m+1)\pi, \quad n, m \in \mathbb{Z},$$

so both possibilities lead to the high energy spectrum of our graph being dominated by bands, while gaps vanish in the order $\mathcal{O}(k^{-1})$, which at the energy scale means their width is asymptotically bounded.

### Low energy spectrum

Next, we consider spectral structure around the point $k = 0$. We choose $k = \delta$ as a small parameter and use Taylor expansions

$$\begin{aligned}
\sin\, kl &= \delta l - \frac{(\delta l)^3}{3!} + \frac{(\delta l)^5}{5!}, \\
\cos\, kl &= 1 - \frac{(\delta l)^2}{2!} + \frac{(\delta l)^4}{4!},
\end{aligned}$$

where $l$ denotes $l_1$, $l_2$, or $(l_1 + l_2)$, depending on the specific circumstances. Condition (3.8) transforms into

$$\begin{aligned}
&[A_6 + A_3(l_1 + l_2) + A_9 l_1 l_2 + A_1(l_1 \cos\theta_2 + l_2 \cos\theta_1) + A_5(\cos\theta_1 + \cos\theta_2)] \\
&+\delta^2[A_4(l_1 + l_2) - \frac{A_6}{2}({l_1}^2 + {l_2}^2) - \frac{A_3}{2}(\frac{{l_1}^3}{3} + {l_1}^2 l_2 + l_1 {l_2}^2 + \frac{{l_2}^3}{3}) \\
&+ A_7 l_1 l_2 - \frac{A_9}{6} l_1 l_2 ({l_1}^2 + {l_2}^2) + A_2(l_1 \cos\theta_2 + l_2 \cos\theta_1) \\
&- \frac{A_5}{2}({l_1}^2 \cos\theta_2 + {l_2}^2 \cos\theta_1) - \frac{A_1}{6}({l_1}^3 \cos\theta_2 + {l_2}^3 \cos\theta_1)] + \mathcal{O}(\delta^4) = 0.
\end{aligned}$$

The plan is to get terms with $\cos\theta_1$ and $\cos\theta_2$ to one side of the equation, and because both of these individually range from $-1$ to 1, we can rewrite our condition in the form of inequality, which will be easier to evaluate. For general expression, it means that

$$\begin{aligned}
&[A_6 + A_3(l_1+l_2) + A_9 l_1 l_2] + \delta^2[A_4(l_1+l_2) - \frac{A_6}{2}(l_1^2+l_2^2) \\
&- \frac{A_3}{2}(\frac{l_1^3}{3} + l_1^2 l_2 + l_1 l_2^2 + \frac{l_2^3}{3}) + A_7 l_1 l_2 - \frac{A_9}{6} l_1 l_2 (l_1^2+l_2^2)] + \mathcal{O}(\delta^4) \\
=& - A_1(l_1\cos\theta_2 + l_2\cos\theta_1) - A_5(\cos\theta_1 + \cos\theta_2) \\
&+ \delta^2[\frac{A_5}{2}(l_1^2\cos\theta_2 + l_2^2\cos\theta_1) + \frac{A_1}{6}(l_1^3\cos\theta_2 + l_2^3\cos\theta_1) \\
&- A_2(l_1\cos\theta_2 + l_2\cos\theta_1)] + \mathcal{O}(\delta^4) \\
=& - [(A_1 l_1 + A_5)\cos\theta_2 + (A_1 l_2 + A_5)\cos\theta_1] \\
&+ \delta^2[(\frac{A_5}{2}l_1^2 + \frac{A_1}{6}l_1^3 - A_2 l_1)\cos\theta_2 + (\frac{A_5}{2}l_2^2 + \frac{A_1}{6}l_2^3 - A_2 l_2)\cos\theta_1] + \mathcal{O}(\delta^4).
\end{aligned} \tag{3.16}$$

Because we investigate the asymptotic regime $\delta \to 0$, the terms proportional to at least $\delta^2$ in Equation (3.16) do not need to be taken into account as long as $\mathcal{O}(1)$ terms are not equal for a particular choice of $\theta_1$ and $\theta_2$. Our condition then becomes

$$A_6 + A_3(l_1+l_2) + A_9 l_1 l_2 = -[(A_1 l_1 + A_5)\cos\theta_2 + (A_1 l_2 + A_5)\cos\theta_1]. \tag{3.17}$$

Let us examine its right-hand side in more detail. It is of the form

$$t_2\cos\theta_1 + t_1\cos\theta_2,$$

and if our goal is to transform Equation (3.17) into an inequality, we need to find its maximum and minimum with respect to $\theta_1$ and $\theta_2$. After differentiation the possible stationary points are

$$(\theta_1,\theta_2) = \begin{cases} (0,0), \\ (\pi,\pi), \\ (0,\pi), \\ (\pi,0). \end{cases}$$

These points form two pairs (the first with the second and the third with the fourth), each containing maximum and minimum, depending on whether $t_1$ and $t_2$ have the same sign or not.

Explicitly written, the right-hand side of Equation (3.17) is

$$\begin{aligned}
-\cos(\gamma-\vartheta)\,\{[(\cos\vartheta - 1)l_1 + 2\sin\vartheta\,]\cos\theta_2 + [(\cos\vartheta - 1)l_2 + 2\sin\vartheta\,]\cos\theta_1\} \\
= t_2\cos\theta_1 + t_1\cos\theta_2;
\end{aligned}$$

here we, without the loss of generality, assume $l_2 > l_1 > 0$. Sign of a particular $t_i$ can be determined from inequality

$$l_i > \frac{2\sin\vartheta}{1-\cos\vartheta} = 2\cot\frac{\vartheta}{2};$$

if both $l_1$ and $l_2$ do (or do not) satisfy it, Equation (3.17) can be finally rewritten into

$$|A_6 + A_3(l_1 + l_2) + A_9 l_1 l_2| < |-A_1(l_1 + l_2) - 2A_5|, \tag{3.18}$$

then if $l_2$ does satisfy it, but $l_1$ does not, Equation (3.17) becomes

$$|A_6 + A_3(l_1 + l_2) + A_9 l_1 l_2| < |-A_1(l_2 - l_1)|. \tag{3.19}$$

If these inequalities, in their particular setting of lengths, are satisfied, then there

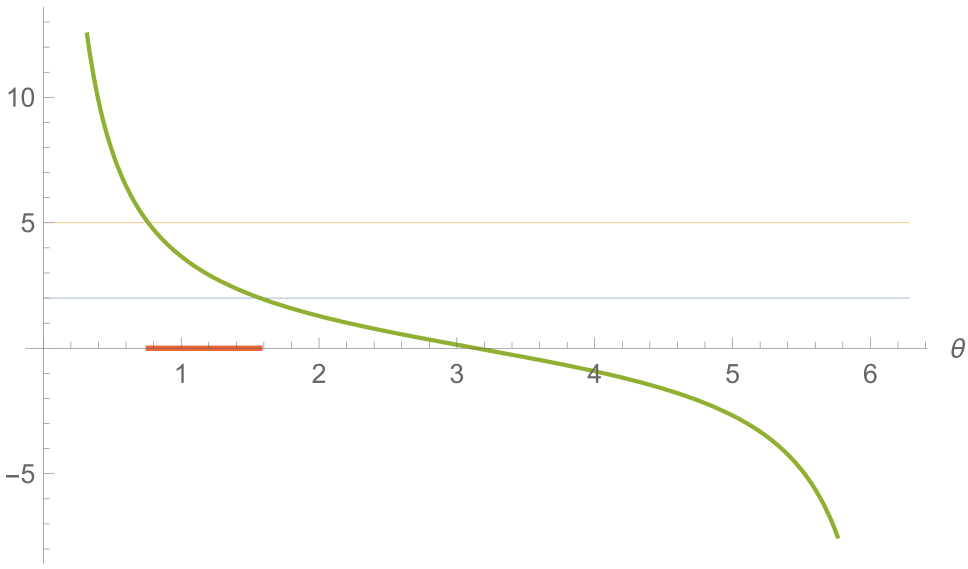


Figure 3.2: $2\cot\frac{\vartheta}{2}$ on interval $\langle 0, 2\pi\rangle$ with lines $l_2 = 5$ and $l_1 = 2$; red horizontal line on $\vartheta$ axis corresponds to interval where condition (3.19) is valid.

exists a positive band connected to the zero.

Should the left and the right side of (3.18) or (3.19) become equal, it does not mean that the positive spectrum is necessarily separated from zero, but we need to go to higher orders in the $\delta$ expansion. While we once again start from condition (3.16) generally, both of the sides are always equal specifically if 1 is a part of the vertex matrix eigenvalues. If $s = 1$,

$$A_1 = A_3 = A_5 = A_6 = A_7 = A_9 = 0,$$

and we must go up to the $\mathcal{O}(\delta^4)$ terms in condition (3.8) around 0; it then reads

$$\begin{aligned} &A_4(l_1 + l_2) + A_2(l_1 \cos\theta_2 + l_2 \cos\theta_1) \\ &+\delta^2\Big[-\frac{A_4}{2}\Big(\frac{l_1^3}{3} + l_1^2 l_2 + l_1 l_2^2 + \frac{l_2^3}{3}\Big) - \frac{A_2}{6}\big(l_1^3\cos\theta_2 + l_2^3\cos\theta_1\big) + A_8 l_1 l_2\Big] = 0. \end{aligned}$$

Similarly to the previous case, we separate terms containing $\cos\theta_1$ and $\cos\theta_2$ from the others, and we also explicitly evaluate

$$A_2 = A_4 = 2\cos\gamma \quad \text{and} \quad A_8 = -4\sin\gamma,$$

which leads to

$$
\begin{aligned}
&\delta^2[4\sin\gamma\, l_1 l_2 + \cos\gamma\,(l_1^2 l_2 + l_1 l_2^2)]\\
=&2\cos\gamma\,[l_1(1+\cos\theta_2) + l_2(1+\cos\theta_1)]\\
-&\delta^2\frac{\cos\gamma}{3}\,[{l_1}^3(1+\cos\theta_2) + {l_2}^3(1+\cos\theta_1)]\\
=&\cos\gamma\,[l_1(2-\frac{\delta^2 l_1^2}{3})(1+\cos\theta_2) + l_2(2-\frac{\delta^2 l_2^2}{3})(1+\cos\theta_1)].
\end{aligned}
\tag{3.20}
$$

On the right-hand side, the $\delta^2$ term can be omitted because $\delta$ is arbitrarily small, and not only is its sign determined by $\mathcal{O}(1)$ terms, but the right-hand side will inevitably be larger than the left-hand side. Additionally, $(1+\cos\theta_i) \in \langle 0{,}2\rangle$, and (3.20) can be rewritten as

$$0 \le \delta^2(4l_1 l_2\tan\gamma\, + {l_1}^2 l_2 + l_1 {l_2}^2) \le 4(l_1+l_2).$$

From the middle term, we can factor $l_1 l_2$ out, and because we are interested in small values of $\delta$, the final condition under which the band is connected to zero reads

$$0 \le 4\tan\gamma + l_2 + l_1. \tag{3.21}$$

The case $\tan\gamma = -\frac{l_1+l_2}{4}$ is included - when plugged into original condition (3.8), it can be rewritten as

$$(\cos\theta_1 + \cos kl_2 + \frac{kl_2}{2}\sin kl_2)\sin kl_1 + (\cos\theta_2 + \cos kl_1 + \frac{kl_1}{2}\sin kl_1)\sin kl_2 = 0,$$

which is around 0 always solvable by specific choice of $\theta_1$ and $\theta_2$ due to the fact that

$$1 \ge \cos x + \frac{x}{2}\sin x$$

near the zero. Obviously, this procedure does not apply when $\cos\gamma = 0$, but in that case $r = 0$, as $\vartheta = 0$, and that reduces original condition (3.4) to

$$\sin kl_1 \sin kl_2 = 0,$$

which means that the whole spectrum would consist only of two types of flat bands around points

$$k = \tfrac{m\pi}{l_1} \quad \text{and} \quad k = \tfrac{m\pi}{l_2}, \quad m = 0, 1, 2, \ldots$$

On the other hand, if $s + 4r = 1$, then $\sin\vartheta = -\sin 2\gamma$ and $\cos\vartheta = -\cos 2\gamma$, therefore

$$
\begin{aligned}
A_9 &= 0,\\
A_6 &= -8\sin\gamma\cos^2\gamma,\\
A_3 &= -2\cos^3\gamma,\\
A_1 &= 2\cos^3\gamma, \quad \text{and}\\
A_5 &= 4\sin\gamma\cos^2\gamma.
\end{aligned}
\tag{3.22}
$$

The condition of connection to the zero then reads

$$|-8\sin\gamma\cos^2\gamma - 2(l_1+l_2)\cos^3\gamma| < |-2(l_1+l_2)\cos^3\gamma - 8\sin\gamma\cos^2\gamma|, \tag{3.23}$$

if taken from (3.18), or

$$|4\tan\gamma + (l_1+l_2)| < (l_2 - l_1), \tag{3.24}$$

if taken from (3.19); final arrangement for this case once again excludes $\cos\gamma = 0$, but this choice would inadvertently lead to $\cos\vartheta = 1$, which we already mentioned. While it might not be immediately clear whether or when are both sides equal in (3.24) in contrast to (3.23), let us remember that, due to the relations between $\vartheta$ and $\gamma$, $\tan\gamma = -\cot\frac{\vartheta}{2}$ follows immediately, and from assumptions leading to (3.19), $\tan\gamma \in \langle -\frac{l_2}{2}, -\frac{l_1}{2}\rangle$. Furthermore, $4\tan\gamma + (l_1+l_2)$ is a linear function of $\tan\gamma$, so on the given interval it may reach maximum (or minimum) only at its endpoints, which are now $-\frac{l_2}{2}$ and $-\frac{l_1}{2}$, both leading to equality in (3.24). Otherwise it is satisfied, and in other words, if $l_2 \neq l_1$, $s + 4r = 1$, and $\vartheta \in (2\arctan\frac{2}{l_2}, 2\arctan\frac{2}{l_1})$ (illustrated for example by the red line in Figure 3.2), the positive spectrum is always connected to the point $k = 0$.

As was mentioned before, if it is appropriate to use (3.23), we need to use higher orders in $\delta$ expansion, so plugging (3.22) additionally with

$$\begin{aligned}
A_2 &= -2\sin^2\gamma\cos\gamma,\\
A_4 &= 6\sin^2\gamma\cos\gamma,\\
A_7 &= 4\sin\gamma\cos^2\gamma,
\end{aligned}$$

into (3.16) (or (3.23) respectively), we get

$$\begin{aligned}
&|-8\sin\gamma\cos^2\gamma - 2(l_1+l_2)\cos^3\gamma\\
&+\delta^2[6(l_1+l_2)\sin^2\gamma\cos\gamma + 4({l_1}^2+{l_2}^2)\sin\gamma\cos^2\gamma\\
&+(\frac{{l_1}^3}{3} + {l_1}^2 l_2 + l_1 {l_2}^2 + \frac{{l_2}^3}{3})\cos^3\gamma + 4l_1l_2\sin\gamma\cos^2\gamma]|\\
<&|-8\sin\gamma\cos^2\gamma - 2(l_1+l_2)\cos^3\gamma\\
&+\delta^2[2({l_1}^2+{l_2}^2)\sin\gamma\cos^2\gamma + ({l_1}^3+{l_2}^3)\frac{\cos^3\gamma}{3}\\
&+2(l_1+l_2)\sin^2\gamma\cos\gamma]|.
\end{aligned}$$

Effectively, we are in the situation

$$|x+y| < |x|,$$

where

$$\begin{aligned}
y &= \delta^2[4(l_1+l_2)\sin^2\gamma\cos\gamma + 2(l_1^2+l_2^2)\sin\gamma\cos^2\gamma\\
&\quad + (l_1^2 l_2 + l_1 l_2^2)\cos^3\gamma + 4l_1l_2\sin\gamma\cos^2\gamma]\\
&= \delta^2 2(l_1+l_2)\cos^3\gamma\,[2\tan^2\gamma + (l_1+l_2)\tan\gamma + \frac{l_1l_2}{2}],\\
x &= -2\cos^3\gamma\,[4\tan\gamma + (l_1+l_2)]\\
&\quad + \delta^2 2\cos^3\gamma\,[(l_1^2+l_2^2)\tan\gamma + \frac{(l_1^3+l_2^3)}{6}\\
&\quad + (l_1+l_2)\tan^2\gamma].
\end{aligned}$$

Because the expression $y$ is $\mathcal{O}(\delta^2)$ and $x$ is in the highest order $\mathcal{O}(1)$, it is only important whether $x$ and $y$ have the same sign; $\gamma$ is now taken from $(\frac{\pi}{2}, \frac{3\pi}{2})$, therefore $\cos^3\gamma < 0$ and sign of $y$ is determined by

$$2\tan^2\gamma + (l_1 + l_2)\tan\gamma + \frac{l_1 l_2}{2}, \tag{3.25}$$

while sign of $x$ is determined by

$$4\tan\gamma + (l_1 + l_2).$$

Solving quadratic equation (3.25) for $\tan\gamma$ gives us two solutions

$$\tan\gamma = -\frac{l_1}{2} \quad \text{and} \quad \tan\gamma = -\frac{l_2}{2};$$

between them is (3.25) negative, but values from this interval already correspond to (3.24), so for our current purposes is (3.25) always positive, and $y$ is always negative for $\tan\gamma$ outside of $\langle -\frac{l_2}{2}, -\frac{l_1}{2}\rangle$ (the solutions of (3.25) itself will be dealt with later). The prefactor before the relevant $\mathcal{O}(1)$ part of $x$ is always positive, therefore the final condition ensuring the existence of spectral band connected to zero is

$$0 < 4\tan\gamma + (l_1 + l_2).$$

Note that here $\tan\gamma = -\frac{l_1+l_2}{4}$ cannot occur as $-\frac{l_1+l_2}{4}$ is the average between $-\frac{l_1}{2}$ and $-\frac{l_2}{2}$, so it must definitely lie between those two values, and now we are working outside of the mentioned interval.

There are two particular cases

$$\tan\gamma = \begin{cases} -\dfrac{l_2}{2} \\ -\dfrac{l_1}{2} \end{cases}$$

solving (3.25). In both of them $y = 0$, so we must once again go to higher order terms, effectively solving the inequality

$$|x + z| < |x + z'|,$$

where

$$\begin{aligned}
z &= \delta^4\{-\frac{A_4}{6}[l_1^3 + 3(l_1^2 l_2 + l_2^2 l_1) + l_2^3] + \frac{A_6}{24}(l_1^4 + 6l_1^2 l_2^2 + l_2^4) \\
&+ \frac{A_3}{120}[l_1^5 + 5(l_1^4 l_2 + l_2^4 l_1) + 10(l_1^3 l_2^2 + l_2^3 l_1^2) + l_2^5] \\
&+ A_8 l_1 l_2 - \frac{A_7}{6}(l_1^3 l_2 + l_2^3 l_1)\} \\
&= 2\delta^4\cos^3\gamma\,\{-\frac{\tan^2\gamma}{2}[l_1^3 + 3(l_1^2 l_2 + l_2^2 l_1) + l_2^3] - \frac{\tan\gamma}{6}(l_1^4 + 6l_1^2 l_2^2 + l_2^4) \\
&- \frac{1}{120}[l_1^5 + 5(l_1^4 l_2 + l_2^4 l_1) + 10(l_1^3 l_2^2 + l_2^3 l_1^2) + l_2^5] \\
&+ 2l_1 l_2\tan^3\gamma - \frac{\tan\gamma}{3}(l_1^3 l_2 + l_2^3 l_1)\}, \\
z' &= \delta^4[-\frac{A_2}{6}(l_1^3 + l_2^3) + \frac{A_5}{24}(l_1^4 + l_2^4) + \frac{A_1}{120}(l_1^5 + l_2^5)] \\
&= 2\delta^4\cos^3\gamma\,[\frac{\tan^2\gamma}{6}(l_1^3 + l_2^3) + \frac{\tan\gamma}{12}(l_1^4 + l_2^4) + \frac{1}{120}(l_1^5 + l_2^5)]
\end{aligned}$$

.

Now if $\tan\gamma = -\frac{l_1}{2}$, then under our assumptions $x > 0$ holds, and because $\delta$ is arbitrarily small, it is sufficient to have $z' > z$. After substitution and factoring out $l_1^5$, where we denote $p = \frac{l_2}{l_1}$, we can transform it into

$$2p^5 - 10p^4 + 10p^3 - 5p^2 + 35p + 7 > 0.$$

This polynomial is on the interval $(1, \infty)$ (because $l_2 > l_1$) always positive, and therefore our condition is always satisfied and the positive spectrum is connected to zero.

On the other hand, if $\tan\gamma = -\frac{l_2}{2}$, we have $x < 0$ and $z' < z$ must be true. Again, after substitution we have

$$-7p^5 - 35p^4 + 5p^3 - 10p^2 + 10p - 2 > 0,$$

but this polynomial is on $(1, \infty)$ always negative, and as such the condition is never satisfied and the positive spectrum remains separated from zero.

### Negative spectrum

The general condition for the negative part of the spectrum is obtained by interchanging $k$ for $i\kappa$. Equation (3.7) then becomes

$$\begin{aligned}
&\kappa(A_1 - \kappa^2 A_2)(\cos\theta_2 \sinh\kappa l_1 + \cos\theta_1 \sinh\kappa l_2) \\
&+\kappa(A_3 - \kappa^2 A_4)\sinh\kappa(l_1 + l_2) \\
&+\kappa^2 A_5\,(\cos\theta_2 \cosh\kappa l_1 + \cos\theta_1 \cosh\kappa l_2) \\
&+\kappa^2 A_6 \cosh\kappa l_1 \cosh\kappa l_2 \\
&+(-\kappa^2 A_7 + \kappa^4 A_8 + A_9)\sinh\kappa l_1 \sinh\kappa l_2 = 0.
\end{aligned} \tag{3.26}$$

Both $\sinh(x)$ and $\cosh(x)$ are non-periodic functions diverging for large values of the variable $x$. This is the reason why the number of possible bands in the negative part of the spectrum is finite, in fact with a bound coming from the spectrum of $U$, as stated by the following theorem [BET22, Theorem 2.6].

**Theorem 3.1.** *Consider a periodic quantum graph and assume that its elementary cell contains $N$ vertices with the couplings described by unitary matrices $U_j$, $j = 1, \dots, N$, then the negative spectrum of the corresponding Hamiltonian consists of at most $\sum_{j=1}^{N} n_j^{(+)}$ bands (where $n_j^{(+)}$ are eigenvalues situated in the upper complex plane).*

*Remark.* This is the generalization of Proposition 2.1 for periodic graphs.

Because now our elementary cell contains one vertex, described by an unitary matrix with at most two distinct eigenvalues, the negative spectrum must also have at most two negative bands.

As far as its behaviour around zero is concerned, the calculations are the same: using Taylor expansions

$$\begin{aligned}
\sinh\,\kappa l &= \delta l + \frac{(\delta l)^3}{3!} + \frac{(\delta l)^5}{5!} + \mathcal{O}(\delta^7), \\
\cosh\,\kappa l &= 1 + \frac{(\delta l)^2}{2!} + \frac{(\delta l)^4}{4!} + \mathcal{O}(\delta^6),
\end{aligned}$$

we substitute into condition (3.26) and obtain

$$\begin{aligned}
&[A_6 + A_3(l_1+l_2) + A_9 l_1 l_2 + A_1(l_1 \cos\theta_2 + l_2\cos\theta_1) + A_5(\cos\theta_1 + \cos\theta_2)] \\
&+\delta^2[-A_4(l_1+l_2) + \frac{A_6}{2}({l_1}^2 + {l_2}^2) + \frac{A_3}{2}(\frac{{l_1}^3}{3} + {l_1}^2 l_2 + l_1 {l_2}^2 + \frac{{l_2}^3}{3}) \\
&- A_7 l_1 l_2 + \frac{A_9}{6} l_1 l_2 ({l_1}^2 + {l_2}^2) - A_2(l_1\cos\theta_2 + l_2\cos\theta_1) \\
&+ \frac{A_5}{2}({l_1}^2\cos\theta_2 + {l_2}^2\cos\theta_1) + \frac{A_1}{6}({l_1}^3\cos\theta_2 + {l_2}^3\cos\theta_1)] + \mathcal{O}(\delta^4) = 0.
\end{aligned}$$

The only difference is a change of sign in $\mathcal{O}(\delta^2)$ terms, so the same conditions as for the positive spectrum apply, but with inequality sign flipped in those cases where the relevant higher-order terms were used.

Let us summarize obtained results in the following theorem, where we recapitulate significant features of the spectrum, in particular in the limits of high and low energies, for both the positive and negative spectrum.

**Theorem 3.2.** *Let $U = rJ + sI$ be an unitary permutation invariant circulant matrix specifying vertex condition on a quantum graph with a rectangular lattice with lengths $l_2$ and $l_1$, $l_2 > l_1$, and Hamiltonian* (1.1) *on its edges. Choose parametrization*

$$\begin{aligned}
s &= \cos\vartheta + i\sin\vartheta, \\
r &= -\frac{1}{2}\cos(\gamma - \vartheta)[\cos\gamma \ + \ i\sin\gamma].
\end{aligned}$$

*Then the following is true:*

1. *If $-1$ is one of the eigenvalues of $U$, the high energy positive spectrum is dominated by spectral bands, while spectral gaps shrink as $\mathcal{O}(k^{-1})$.*

2. *If $-1$ is not an eigenvalue of $U$, the high energy positive spectrum is dominated by spectral gaps. Bands are formed only around points*

$$k_{m,i} = \tfrac{m\pi}{l_i}, \quad i = 1{,}2 \quad \text{and} \quad m \in \mathbb{N}$$

*and they have an asymptotically constant width*

$$\Delta E_m = \frac{4}{l_i}\left|\frac{\cos(\gamma-\vartheta)\,(\cos\vartheta + 1)}{-2\sin\gamma\,(\cos\vartheta+1) + \sin\vartheta\,(\cos\gamma + \cos(\gamma-\vartheta)\,)}\right| + \mathcal{O}(m^{-1}).$$

*If $\frac{l_2}{l_1}$ is irrational, this is always true; for rational $\frac{l_2}{l_1}$, there exists an additional type of band with asymptotically constant width*

$$\begin{aligned}
\Delta E_m = &\frac{4(l_1+l_2)}{l_1 l_2}\left|\frac{\cos(\gamma-\vartheta)\,(\cos\vartheta + 1)}{-2\sin\gamma\,(\cos\vartheta+1) + \sin\vartheta\,(\cos\gamma + \cos(\gamma-\vartheta)\,)}\right| \\
&+ \mathcal{O}(m^{-1}).
\end{aligned}$$

3. *If $1$ is not an eigenvalue of $U$, whether positive spectrum is connected to the point $k = 0$ is determined by inequality*

$$\begin{aligned}
&|4\sin\vartheta\cos\gamma + (-2\cos\gamma + \cos\vartheta\ \cos(\gamma-\vartheta) + \cos(\gamma+\vartheta)\,)(l_1+l_2) \\
&\quad - [2\sin\gamma\,(\cos\vartheta - 1) - \sin\vartheta\,(\cos\gamma - \cos(\gamma-\vartheta)\,)\,]\, l_1 l_2| \\
&\quad < |-\cos(\gamma-\vartheta)\,(\cos\vartheta - 1)(l_1+l_2) - 4\sin\vartheta\cos(\gamma-\vartheta)\,|
\end{aligned}$$

*in case* $\vartheta \notin (\,2\arctan(\frac{2}{l_2}), 2\arctan(\frac{2}{l_1})\,)$*, or by*

$$\begin{aligned}&|4\sin\vartheta\cos\gamma + (-2\cos\gamma + \cos\vartheta\;\cos(\gamma-\vartheta) + \cos(\gamma+\vartheta)\,)(l_1+l_2)\\ &\;-[2\sin\gamma\,(\cos\vartheta-1) - \sin\vartheta\,(\cos\gamma - \cos(\gamma-\vartheta)\,)\,]\,l_1 l_2|\\ &\;< |-\cos(\gamma-\vartheta)\,(\cos\vartheta-1)(l_2-l_1)\,|\end{aligned}$$

*in case* $\vartheta \in (\,2\arctan(\frac{2}{l_2}), 2\arctan(\frac{2}{l_1})\,)$*; if* $\vartheta = 2\arctan(\frac{2}{l_i})$*, then the relevant condition is*

$$\begin{aligned}&|4\sin\vartheta\cos\gamma + (-2\cos\gamma + \cos\vartheta\;\cos(\gamma-\vartheta) + \cos(\gamma+\vartheta)\,)(l_1+l_2)\\ &\;-[2\sin\gamma\,(\cos\vartheta-1) - \sin\vartheta\,(\cos\gamma - \cos(\gamma-\vartheta)\,)\,]\,l_1 l_2|\\ &\;< |-\cos(\gamma-\vartheta)\,(\cos\vartheta-1)l_j - 2\sin\vartheta\cos(\gamma-\vartheta)\,|,\end{aligned}$$

*where* $j$ *is the second index different from* $i$*. If any of them is satisfied, then the positive spectrum is connected to zero.*

4. *If* 1 *is an eigenvalue of* $U$*, then if* $s = 1$*, the condition for the absence of a gap around zero in the positive spectrum is*

$$0 \le 4\tan\gamma + l_2 + l_1;$$

*if it is satisfied, the positive spectrum is connected to zero, otherwise it is not.*

*Furthermore, if* $s + 4r = 1$ *and if* $\vartheta \in (\,2\arctan\frac{2}{l_2}, 2\arctan\frac{2}{l_1}\,\rangle$*, the positive spectrum is always connected to the zero; if* $\vartheta \notin (\,2\arctan\frac{2}{l_2}, 2\arctan\frac{2}{l_1}\,\rangle$*, then the condition reads*

$$0 < 4\tan\gamma + (l_1 + l_2);$$

*if satisfied, the positive spectrum is connected to the zero, otherwise it is not.*

5. *The number of negative bands is bounded from above by the number of eigenvalues of* $U$ *in the upper complex plane.*

6. *If* 1 *is not an eigenvalue of* $U$*, whether the negative spectrum is connected to the zero is determined by the exact same condition as the positive spectrum, i.e. both sides are (dis)connected if there are any negative bands.*

7. *If* 1 *is an eigenvalue of* $U$*, then if* $s = 1$*, the condition for the absence of a gap around zero in the negative spectrum is*

$$0 \ge 4\tan\gamma + l_2 + l_1;$$

*if it is satisfied, the negative spectrum is connected to zero, otherwise it is not.*

*Furthermore, if* $s + 4r = 1$ *and if* $\vartheta \in (\,2\arctan\frac{2}{l_2}, 2\arctan\frac{2}{l_1}\,\rangle$*, the negative spectrum is always connected to zero; if* $\vartheta \notin (\,2\arctan\frac{2}{l_2}, 2\arctan\frac{2}{l_1}\,\rangle$*, then the condition reads*

$$0 > 4\tan\gamma + (l_1 + l_2);$$

*if satisfied, the negative spectrum is connected to the zero, otherwise it is not.*

Square lattice $l_2 = l_1 = l$ then slightly simplifies things:

**Corollary 3.1.** *Let $U = rJ + sI$ be an unitary permutation invariant circulant matrix specifying vertex condition on a quantum graph with a square lattice with length $l$ and Hamiltonian* (1.1) *on its edges. Choose parametrization*

$$\begin{aligned} s &= \cos\vartheta + i\sin\vartheta, \\ r &= -\frac{1}{2}\cos(\gamma-\vartheta)[\cos\gamma \ + \ i\sin\gamma]. \end{aligned}$$

*Then all statements true for rectangular lattice are also valid with these additional specifications:*

1. *If $-1$ is not an eigenvalue of $U$, the high energy positive spectrum is dominated by spectral gaps. Bands are periodically formed only around points*

   $$k_m = \tfrac{m\pi}{l}, \quad m \in \mathbb{N}$$

   *and they have an asymptotically constant width*

   $$\Delta E_m = \frac{8}{l}\left|\frac{\cos(\gamma-\vartheta)\,(\cos\vartheta+1)}{-2\sin\gamma\,(\cos\vartheta+1)+\sin\vartheta\,(\cos\gamma+\cos(\gamma-\vartheta)\,)}\right| + \mathcal{O}(m^{-1}).$$

2. *If 1 is not an eigenvalue of $U$, whether the positive spectrum is connected to zero is determined by inequality*

   $$\begin{aligned} &|4\sin\vartheta\cos\gamma + 2l\,(-2\cos\gamma + \cos\vartheta\cos(\gamma-\vartheta) + \cos(\gamma+\vartheta)\,) \\ &\ - l^2\,[2\sin\gamma\,(\cos\vartheta-1) - \sin\vartheta\,(\cos\gamma - \cos(\gamma-\vartheta)\,)\,]\,| \\ &\ < |-2l\cos(\gamma-\vartheta)\,(\cos\vartheta-1) - 4\sin\vartheta\,\cos(\gamma-\vartheta)|; \end{aligned}$$

   *if it is satisfied, then the positive spectrum is connected to zero.*

3. *If 1 is one of the eigenvalues of $U$, the condition for the absence of a gap around zero in the positive spectrum is*

   $$0 \le 2\tan\gamma + l;$$

   *if it is satisfied, the positive spectrum is connected to zero, otherwise it is not.*

4. *If 1 is one of the eigenvalues of $U$, then, if $s = 1$, the condition for the absence of a gap around zero in the negative spectrum is*

   $$0 \ge 2\tan\gamma + l;$$

   *if it is satisfied, the negative spectrum is connected to zero, otherwise it is not.*

   *Furthermore, if $s + 4r = 1$, then the condition is*

   $$0 > 2\tan\gamma + l;$$

   *if satisfied, the negative spectrum is connected to zero, otherwise it is not.*

Now we present a few examples illustrating the derived results. The structure of bands and gaps in Figure 3.3 was calculated for $\vartheta = \pi/3$ and $\gamma = 2\pi/3$ with $l = 1$. It corresponds to the case of square lattice with $s + 4r = 1$, for which we have conditions

$$0 \leq 2\tan\gamma + l \approx -1.732 + 1 = -0.732$$

for small energies at the $k$ side of momentum axis and

$$0 > 2\tan\gamma + l \approx -0.732$$

for the $\kappa$ side; in this situation, we see how the (only) negative band is connected to zero, while the lowest positive one is separated. Because $-1$ is an eigenvalue of matrix $U$, we also see how positive band intervals become shorter and shorter with larger values of momentum variable $k$, and their proximity to integer multiples of $\pi$. Eigenvalue $s = \frac{1}{2} + i\frac{\sqrt{3}}{2}$ is the only one in the upper complex plane, and as such there cannot be more negative bands than the one we see in the Figure 3.3.

Figure 3.4 was calculated for $\vartheta = \pi/3$ and $\gamma = 7\pi/6$ with $l = 1$. Because here is $s + 4r = -1$, condition for both the negative and positive band is

$$\begin{aligned}
&|4\sin\vartheta\cos\gamma + 2l\,(-2\cos\gamma + \cos\vartheta\cos(\gamma-\vartheta) + \cos(\gamma+\vartheta)\,) \\
&\quad - l^2\,[2\sin\gamma\,(\cos\vartheta - 1) - \sin\vartheta\,(\cos\gamma - \cos(\gamma-\vartheta)\,)\,]\,| \\
&\quad < |-2l\cos(\gamma-\vartheta)\,(\cos\vartheta - 1) - 4\sin\vartheta\,\cos(\gamma-\vartheta)|;
\end{aligned}$$

after the substitution, it reads

$$\Big| -4\Big(\frac{\sqrt{3}}{2}\Big)^2 + 2\Big(\sqrt{3} - \frac{1}{2}\frac{\sqrt{3}}{2}\Big) - \Big(\frac{1}{2}\Big)\Big| \approx 0.902 < \Big| -\frac{\sqrt{3}}{2} + 4\Big(\frac{\sqrt{3}}{2}\Big)^2\Big| \approx 2.134,$$

so both the lowest positive and negative part of the system spectrum is connected to zero. Because $-1$ is an eigenvalue of $U$, with growing $k$ bands become larger and more prominent. There is once again only one negative band, as a larger number of them is prohibited by Theorem 3.1.

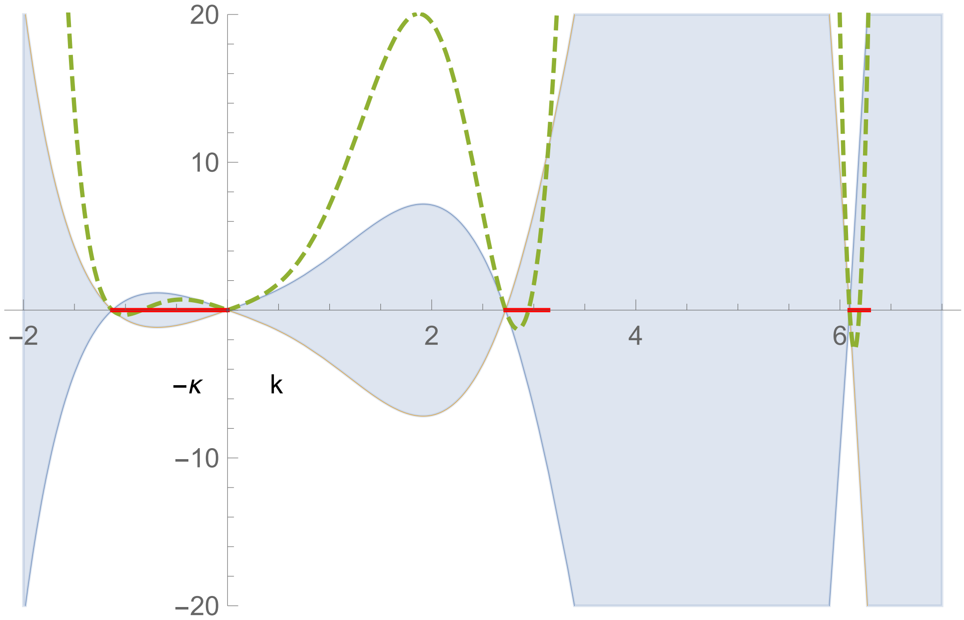


Figure 3.3: Spectral condition solution for square lattice, $l = 1$, with permutation-invariant vertex condition defined by coefficients $(r,s) = (\frac{1}{8} - i\frac{\sqrt{3}}{8}, \frac{1}{2} + i\frac{\sqrt{3}}{2})$. The green dashed line is an evaluation of the spectral condition, while the shaded region marks areas where spectral bands would occur if crossed by the dashed line. Red horizontal lines then correspond to spectral bands.

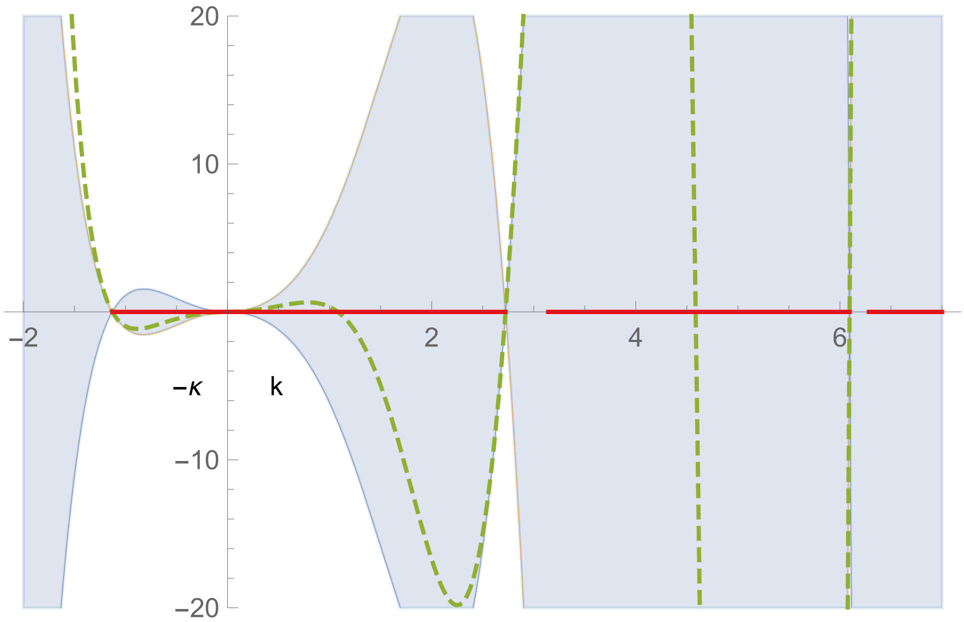


Figure 3.4: Spectral condition solution for square lattice, $l = 1$, with permutation-invariant vertex condition defined by coefficients $(r,s) = (-\frac{3}{8} - i\frac{\sqrt{3}}{8}, \frac{1}{2} + i\frac{\sqrt{3}}{2})$. The green dashed line is an evaluation of the spectral condition, while the shaded region marks areas where spectral bands would occur if crossed by the dashed line. Red horizontal lines then correspond to spectral bands.

# 4. Interpolating coupling

## 4.1 Basic properties

Another possible type of a circulant vertex condition is the one continuously interpolating between a $\delta$ condition from (3.5) and the condition generated by the matrix $R$ from (3.3). It was first introduced by authors of [ETT18] in order to analyse and distinguish behaviour of vertex couplings with different symmetries, because while both of the mentioned conditions are PT-symmetric, 'extremal' rotationally symmetric coupling, in contrast to a $\delta$ coupling, violates the time-reversal symmetry (1.5).

The interpolating coupling $\{U(t) : t \in \langle 0,1 \rangle\}$ was constructed in such a way that

$$\begin{cases} U(0) = -I + \dfrac{2}{n+i\alpha} J \text{ and } U(1) = R, \\ t \to U(t) \text{ is continuous on } \langle 0,1 \rangle, \\ U(t) \text{ is unitary circulant for all } t, \end{cases} \tag{4.1}$$

where $n$ is a vertex degree. The process itself is explained in detail in the mentioned article; in the first step the eigenvalues of corresponding vertex matrices are constructed with given properties, and through them the generating vector of the circulant matrix is expressed, as it was described in Proposition 1.3. The final eigenvalues of $U(t)$ are then

$$\lambda_l(t) = \begin{cases} e^{-i(1-t)\gamma} & \text{for } l = 0, \\ -\, e^{i\pi t(\frac{2l}{n}-1)} & \text{for } 1 \le l \le n-1, \end{cases} \tag{4.2}$$

where now

$$\gamma := \arg \frac{n+i\alpha}{n-i\alpha} \in (-\pi,\pi), \text{ thus } \frac{n-i\alpha}{n+i\alpha} = e^{-i\gamma}. \tag{4.3}$$

Writing $U(t)$ explicitly is rather lengthy and in principle not needed for further calculations; the main results of [ETT18] concerned the star graph and the periodic square lattice ($n = 4$), with the same Hamiltonian as we have used in previous chapters. They can be summarized as follows:
The star graph Hamiltonian

- has a negative eigenvalue $-\kappa^2 = -\tan^2 \frac{(1-t)\gamma}{2}$ whenever $\alpha < 0$.
- has $\lfloor \frac{n-1}{2} \rfloor$ eigenvalues for every $t \in \langle 0,1 \rangle$ if $n \ge 3$; they have the form $-\kappa^2 = -\cot^2((\frac{j}{n} - \frac{1}{2})\pi t)$, where $j = 1, \ldots, \frac{n-1}{2}$ for odd $n$ and $j = 1, \ldots, \frac{n}{2} - 1$ for even $n$.
- has all eigenvalues diverging to $-\infty$ in the limit $t \to 0_+$, except for $-\tan^2 \frac{(1-t)\gamma}{2}$, which approaches $-\tan^2 \frac{\gamma}{2} = -\frac{\alpha^2}{n^2}$.
- has all eigenvalues converging to 0 and $-\tan^2 \frac{j\pi}{n}$, if present, $j$ the same as before, in the limit $t \to 1_-$; for $t = 1$, zero is no longer an eigenvalue of the star graph, see Proposition 2.1.

The Hamiltonian of a periodic square lattice of the edge length $l_1$

- has a 'discontinuity' for $t = 0$, as there is always a spectral band, which becomes narrower for smaller values of $t$ and eventually disappears.

- has point degeneracies for $\alpha = 0$, as in that case spectral bands for particular values of $t = \frac{4}{\pi}\text{arccot}\frac{(m-\frac{1}{2})\pi}{l_1}$, $m \in \mathbb{N}$, may collapse into points, also called 'flat bands'.

- has non-monotonous gap widths with respect to $t$ for all $\alpha$.

- has some bands independent of $t$.

- has band edges curves described by analytic functions of $k$.

- has 'flat bands' for $t = 1$, which are smeared into regular bands for $t < 1$.

## 4.2 Periodic chain

Here we will consider the same interpolating vertex condition, but for a periodic chain graph presented in Figure 4.1. Our Hamiltonian is once again negative Laplacian acting on each edge, and for now, we generally assume $l_j > 0$, $j = 1, 2, 3$.

We solve this problem using a similar Ansatz as in Equation (2.1),

$$(U(t) - I)\psi(v) + il(U(t) + I)\psi^{'}(v) = 0, \tag{4.4}$$

however, now we introduce the length-type parameter $l$, which serves as a tool to scale other lengths and consequently the graph as a whole - the lengths have the form

$$l_j = \tilde{l_j}l,$$

where $\tilde{l_j} \in \mathbb{R}^+$ are some numbers. In previous chapters, we implicitly fixed the scale by requiring $l = 1$; as we will see later on, another (to a degree arbitrary) choice of scaling might be more convenient here. $\psi(v)$ denotes the value of the wave function $\psi(x)$ at the vertex, and the same equation as the (4.4) is used for $\varphi(x)$.

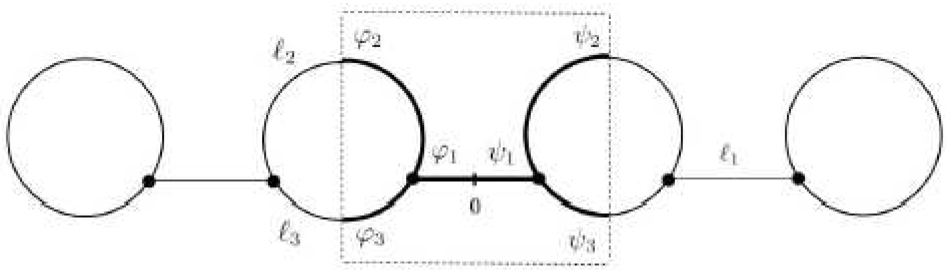


Figure 4.1: Periodic quantum chain with its elementary cell highlighted. [BET22]

We describe wave functions on the edges as

$$\begin{aligned}\psi_j(x) &= a_j^+ e^{ikx} + a_j^- e^{-ikx},\ x \in \langle 0, \frac{l_j}{2}\rangle, \\ \varphi_j(x) &= b_j^+ e^{ikx} + b_j^- e^{-ikx},\ x \in \langle -\frac{l_j}{2}, 0\rangle,\end{aligned} \tag{4.5}$$

with additional conditions

$$\begin{array}{cc} \psi_2(\frac{l_2}{2}) = e^{i\theta}\varphi_2(-\frac{l_2}{2}), & \psi_2'(\frac{l_2}{2}) = e^{i\theta}\varphi_2'(-\frac{l_2}{2}), \\ \psi_3(\frac{l_3}{2}) = e^{i\theta}\varphi_3(-\frac{l_3}{2}), & \psi_3'(\frac{l_3}{2}) = e^{i\theta}\varphi_3'(-\frac{l_3}{2}), \\ \psi_1(0) = \varphi_1(0), & \psi_1'(0) = \varphi_1'(0), \end{array}$$

which come from the Floquet conditions for the elementary cells of a periodic graph for $j = 2{,}3$, while for $j = 1$ we require the wave function and its first derivative to be continuous, as $x = 0$ was chosen in the middle of the edge connecting adjacent loops; $e^{i\theta}$ denotes Bloch phase factor. Substituting (4.5) into them gives us

$$\begin{array}{ll} b_2^+ = a_2^+ e^{ikl_2} e^{-i\theta}, & b_2^- = a_2^- e^{-ikl_2} e^{-i\theta}, \\ b_3^+ = a_3^+ e^{ikl_3} e^{-i\theta}, & b_3^- = a_3^- e^{-ikl_3} e^{-i\theta}, \\ b_1^+ = a_1^+, & b_1^- = a_1^-. \end{array} \tag{4.6}$$

To accommodate both $\psi(x)$ and $\varphi(x)$ into one equation, we now denote

$$\mathcal{U}(t) \equiv \begin{pmatrix} U(t) & 0 \\ 0 & U(t) \end{pmatrix},$$

i. e. block diagonal matrix, where each block corresponds to one vertex in the elementary cell and the vertex condition is described by 3×3 interpolating coupling matrix $U(t)$. Similarly

$$\mathcal{V} \equiv \begin{pmatrix} V & 0 \\ 0 & V \end{pmatrix},$$

where $V$ is the discrete Fourier transform matrix defined in Proposition 1.3.

We solve Equation (4.4) in the form

$$(\mathcal{U}(t) - I)\begin{pmatrix} \psi_1(\frac{l_1}{2}) \\ \psi_3(0) \\ \psi_2(0) \\ \varphi_1(-\frac{l_1}{2}) \\ \varphi_2(0) \\ \varphi_3(0) \end{pmatrix} + il(\mathcal{U}(t) + I)\begin{pmatrix} -\psi_1'(\frac{l_1}{2}) \\ \psi_3'(0) \\ \psi_2'(0) \\ \varphi_1'(-\frac{l_1}{2}) \\ -\varphi_2'(0) \\ -\varphi_3'(0) \end{pmatrix} = 0, \tag{4.7}$$

where we have chosen the direction of the chain from the left to the right, and as such inward (with respect to the vertices) derivatives must be taken with an opposite sign. The $\psi$ part of the wave function vector has an enumeration different from $\varphi$ due to the topology of our graph - vertices in the quantum chain are described by the same coupling, and each of them must have the same orientation.

Combining (4.5), (4.6) and (4.7) with Proposition 1.3 yields

$$[V^*(D(t)-I)VM - klV^*(D(t)+I)VN] \begin{pmatrix} a_1^+ \\ a_1^- \\ a_2^+ \\ a_2^- \\ a_3^+ \\ a_3^- \end{pmatrix} = 0, \tag{4.8}$$

where

$$M = \begin{pmatrix} e^{ikl_1/2} & e^{-ikl_1/2} & 0 & 0 & 0 & 0 \\ 0 & 0 & 0 & 0 & 1 & 1 \\ 0 & 0 & 1 & 1 & 0 & 0 \\ e^{-ikl_1/2} & e^{ikl_1/2} & 0 & 0 & 0 & 0 \\ 0 & 0 & e^{ikl_2}e^{-i\theta} & e^{-ikl_2}e^{-i\theta} & 0 & 0 \\ 0 & 0 & 0 & 0 & e^{ikl_3}e^{-i\theta} & e^{-ikl_3}e^{-i\theta} \end{pmatrix},$$

and

$$N = \begin{pmatrix} -e^{ikl_1/2} & e^{-ikl_1/2} & 0 & 0 & 0 & 0 \\ 0 & 0 & 0 & 0 & 1 & -1 \\ 0 & 0 & 1 & -1 & 0 & 0 \\ e^{-ikl_1/2} & -e^{ikl_1/2} & 0 & 0 & 0 & 0 \\ 0 & 0 & -e^{ikl_2}e^{-i\theta} & e^{-ikl_2}e^{-i\theta} & 0 & 0 \\ 0 & 0 & 0 & 0 & -e^{ikl_3}e^{-i\theta} & e^{-ikl_3}e^{-i\theta} \end{pmatrix}.$$

Equation (4.8) is solvable if and only if

$$\det[(D(t)-I)VM - kl(D(t)+I)VN] = 0;$$

the final spectral condition then reads, modulo numerical prefactors,

$$k^6 P_6 + k^5 P_5 + k^4 P_4 + k^3 P_3 + k^2 P_2 + k P_1 + P_0 + k^2(\sin\theta\, P_s + \cos\theta\, P_c) = 0 \tag{4.9}$$

where $P$ are products of three types of polynomials - depending on $\cos\gamma(1-t)$ or $\sin\gamma(1-t)$, and furthermore, on $\cos\frac{\pi t}{3}$ and $\sin\frac{\pi t}{3}$, and finally, on goniometric functions of $kl_j$; they are explicitly evaluated in Appendix A.3.

Let us test it on examples of previously gathered results. If we choose $t=1$, then

$$\sin\gamma(1-t) = 0,\ \cos\gamma(1-t) = 1,\ \sin\frac{\pi t}{3} = \frac{\sqrt{3}}{2},\ \cos\frac{\pi t}{3} = \frac{1}{2},$$

and using

$$\begin{aligned} \sin k(l_1+l_2+l_3) = &-\sin kl_1\, \sin kl_2\, \sin kl_3 + \cos kl_1\, \cos kl_2\, \sin kl_3 \\ &+ \cos kl_2\, \cos kl_3\, \sin kl_1 + \cos kl_3\, \cos kl_1\, \sin kl_2 \end{aligned}$$

with

$$\begin{aligned} &\sin k(l_1+l_2-l_3) + \sin k(l_1+l_2-l_3) + \sin k(l_1+l_2-l_3) = \\ &3\sin kl_1\, \sin kl_2\, \sin kl_3 + \cos kl_1\, \cos kl_2\, \sin kl_3 \\ &+ \cos kl_2\, \cos kl_3\, \sin kl_1 + \cos kl_3\, \cos kl_1\, \sin kl_2 \end{aligned}$$

we can transforms (4.9), up to a prefactor, into

$$\begin{aligned}(k^4l^4+3)&\sin kl_1\,\sin kl_2\,\sin kl_3\\ &+2(k^2l^2+1)[\sin kl_1-\sin k(l_1+l_3)\,\cos kl_2-\cos kl_3\,\cos kl_1\,\sin kl_2]\\ &+2\cos\theta\,(k^2l^2+1)[\sin kl_2+\sin kl_3]+4kl\sin\theta\,[\cos kl_3-\cos kl_2]=0,\end{aligned}\tag{4.10}$$

which is nothing but the spectral condition (2.8) of [BET22].

One of the possible ways to fix the scaling, which will be particularly useful for the periodic chain, is requiring $l_2+l_3=2\pi$ to be always satisfied. Keeping that in mind, we inspect the case $t=0$ in the symmetric example $l_2=l_3=\pi$ in the limit $l_1\to 0$, in which

$$\sin\gamma(1-t)=\sin\gamma,\ \cos\gamma(1-t)=\cos\gamma,\ \sin\frac{\pi t}{3}=0,\ \cos\frac{\pi t}{3}=1,$$

and (4.9) reads

$$\cos k\pi+\cos\theta+\frac{\sin\gamma}{\cos\gamma+1}\frac{\sin k\pi}{k}\frac{3}{2}=0;$$

its spectral *band* condition is then

$$\left|\cos k\pi+\frac{3}{2}\tan\frac{\gamma}{2}\frac{\sin k\pi}{k}\right|\le 1.\tag{4.11}$$

This is the same result as in [DET08][Proposition 2.1], except for one thing: from (4.3) we can see that

$$\cos\gamma=\frac{n^2-\alpha^2}{n^2+\alpha^2}\ \text{and}\ \sin\gamma=\frac{2n\alpha}{n^2+\alpha^2}.$$

From there then

$$\tan\gamma=\frac{2n\alpha}{n^2-\alpha^2}=\frac{2\frac{\alpha}{n}}{1-(\frac{\alpha}{n})^2},$$

and it is not difficult to realize how

$$\tan\frac{\gamma}{2}=\frac{\alpha}{n}\tag{4.12}$$

must be fulfilled; but when we compare (4.11) with the aforementioned result

$$\left|\cos k\pi+\frac{\alpha}{4}\frac{\sin k\pi}{k}\right|\le 1,\tag{4.13}$$

it gives us

$$\tan\frac{\gamma}{2}=\frac{\alpha}{6}=\frac{1}{2}\frac{\alpha}{3},$$

which is one half of the value we would have expected from the periodic quantum chain with vertices of degree three, $n=3$. It can be understood with a physical insight into the problem, as well as by a careful look into the definition of $\delta$ condition (1.2). Function(s) living on the edges adjacent to the given vertex acquire the same value $f(v)$ in it. As $l_1\to 0_+$, the difference between values $f(v)$ of the two neighbouring vertices becomes smaller, until it must be the same when the vertices join. The sum of the derivatives along adjacent edges must be always equal to $\alpha f(v)$, but for $l_1 = 0$, there cannot possibly be a derivative along its edge and the equality must be satisfied by functions on the other two edges. In the end, there are four edges adjacent to one vertex, with two pairs of edges, where derivatives of their respective functions both sum to $\alpha f(v)$. In other words, we combined two vertices into one with doubled strength constant. This means that $\alpha$ present in (4.13) is two times larger than the one in (4.11), and, if $\alpha$ now labels our original constant from a general periodic chain, (4.12) is again satisfied.

Alternatively, we can explain this by symmetries - noting that the quantum chain is symmetric along the horizontal axis passing through vertices, which allows us to decompose our Hamiltonian into a direct sum of its symmetric and antisymmetric part, the latter of which contains functions vanishing at the axis of the chain which can contribute only to the point spectrum, in other words, to the flat bands [DET08].

If we make use of the fixed scaling $l_2 + l_3 = 2\pi$ also in (4.10), it can be solved independently of $\theta$ due to the fact that

$$\begin{aligned}
\sin kl_3 + \sin kl_2 &= \sin kl_3 + \sin 2k\pi\, \cos kl_3 - \sin kl_3\, \cos 2k\pi \\
&= \sin kl_3 + 2\sin k\pi\, \cos k\pi\, \cos kl_3 - \sin kl_3\, [1 - 2\sin^2 k\pi] \\
&= 2\sin k\pi\, \cos k(\pi - l_3), \\
\cos kl_3 - \cos kl_2 &= \cos kl_3 - \cos kl_3\, \cos 2k\pi - \sin kl_3\, \sin 2k\pi \\
&= \cos kl_3 - \cos kl_3\, [1 - 2\sin^2 k\pi] - 2\sin k\pi\, \cos k\pi\, \sin kl_3 \\
&= 2\sin k\pi\, \sin k(\pi - l_3),
\end{aligned}$$

which vanishes provided that $\sin k\pi = 0$. In principle, we can use the same procedure for any scale fixing constant $\beta > 0$, $l_2 + l_3 = \beta$, but $2\pi$ gives conveniently expressible results, detailed in the article [BET22].

We would like to present something similar for our interpolating spectral condition (4.9), as both $P_s$ and $P_c$ contain terms proportional to $\sin kl_3 + \sin kl_2$, but while the former also includes part multiplied by $\cos kl_3 - \cos kl_2$, the latter has $\cos kl_3 + \cos kl_2$ instead; that is why

- spectral condition (4.9) cannot be, outside of $t = 1$ [BET22] and $t = 0$ (as will be seen later on), generally solved without the dependence on parameter $\theta$, i. e. our system generally does not contain flat bands in its spectrum.

Spectrum given by our condition (4.9) thus has only continuous band-gap structure. Similarly to the (4.10), it can be rewritten into the form

$$v_c \cos\theta + v_s \sin\theta = v_z, \tag{4.14}$$

where we now introduce angle $\vartheta$ as

$$\sin\vartheta = \frac{v_c}{\sqrt{v_c^2 + v_s^2}}, \;\cos\vartheta = \frac{v_s}{\sqrt{v_c^2 + v_s^2}};$$

the denominator of these two quantities cannot be equal to 0, as it is directly constructed from polynomials $P_c$ and $P_s$, and we already established these cannot vanish simultaneously. From there (4.14) transforms into

$$\sin(\theta + \vartheta) = \frac{v_z}{\sqrt{v_c^2 + v_s^2}}$$

and because

$$0 \leq \sin^2(\theta + \vartheta) \leq 1,$$

particular $k^2$ is part of a spectral *band* if

$$v_c^2 + v_s^2 - v_z^2 \geq 0, \tag{4.15}$$

while spectral *gap* condition reads

$$v_c^2 + v_s^2 - v_z^2 < 0. \tag{4.16}$$

This solution is completely general and valid for the whole range of every parameter present - we might specify it further only if interesting properties emerge for some values of $l_j$, $t$ or $\gamma$.

Because $t \in \langle 0,1 \rangle$, $\cos \frac{\pi t}{3} \in \langle \frac{1}{2},1 \rangle$ and, looking at the structure of polynomials in (4.9), only $t = 0$ significantly alters spectral condition as a whole due to the fact that for it $P_6 = P_5 = P_4 = P_3 = P_s = 0$. Similarly $\gamma \in (-\pi,\pi)$, and therefore $\cos\gamma(1-t) \in (-1,1\rangle$. Keeping these two observations in mind, we can handle particular cases separately, which will enable us later to make some algebraic operations without complications.

## 4.3 Spectral properties

### 4.3.1 Case of $t = 0$

Let us start with the limit case of a $\delta$-type condition. As was mentioned above, for $t = 0$ is $P_s = 0$. Consequently is $v_s = 0$, and from (4.15) with (4.16) spectral band and gap condition become, respectively,

$$\left|\frac{v_z}{v_c}\right| \leq 1, \ \left|\frac{v_z}{v_c}\right| > 1, \tag{4.17}$$

with

$$v_c = -32k^2 l^2 (\cos\gamma + 1)(\sin kl_2 + \sin kl_3) \tag{4.18}$$

and

$$\begin{aligned} v_z = &- 16k^2 l^2 (\cos\gamma + 1)\{2 \sin kl_1 + 3 \sin kl_1 \sin kl_2 \sin kl_3 \\ &- 2[\cos kl_1 \cos kl_2 \sin kl_3 + \cos kl_2 \cos kl_3 \sin kl_1 + \cos kl_3 \cos kl_1 \sin kl_2]\} \\ &+ 96kl \sin\gamma[\cos kl_1 \sin kl_2 \sin kl_3 + \cos kl_2 \sin kl_3 \sin kl_1 + \cos kl_3 \sin kl_1 \sin kl_2] \\ &- 144(\cos\gamma - 1) \sin kl_1 \sin kl_2 \sin kl_3. \end{aligned} \tag{4.19}$$

#### Flat bands

We will return to the form (4.14) of the spectral condition for a moment. Using our preferred scaling $l_2 + l_3 = 2\pi$, (4.18) becomes

$$v_c = -64k^2 l^2 (\cos\gamma + 1) \ \sin k\pi \ \cos k(\pi - l_3), \tag{4.20}$$

and we are now able to find the *flat* bands, i. e. $k$, for which is the solution of a given spectral condition independent of $\theta$. In our case, this happens for

$$k = m, \text{ or } k = \frac{m\pi}{2(\pi - l_3)}, \ m \in \mathbb{N}.$$

We may without loss of generality assume $l_3 < \pi$, because $k$ must be from $\mathbb{R}_0^+$ by its definition. If $l_3 > \pi$, we will use the fact that $\cos x$ in an even function, or symmetry of solutions with corresponding $l_2$; symmetric case $l_2 = l_3 = \pi$ will be treated separately. For the former choice of $k = m$, (4.19) becomes, with some additional algebraic manipulations,

$$\begin{aligned}
v_z =& -16m^2l^2(\cos\gamma+1)\{2\sin ml_1 + 3\sin ml_1\, \sin ml_2\, \sin ml_3\\
&- 2[\cos ml_1\, \sin m(l_2+l_3) + \cos ml_2\, \cos ml_3\, \sin ml_1]\}\\
&+ 96ml\sin\gamma[\cos ml_1\, \sin ml_2\, \sin ml_3 + \sin ml_1\, \sin m(l_2+l_3)]\\
&- 144(\cos\gamma-1)\, \sin ml_1\, \sin ml_2\, \sin ml_3\\
=& -16m^2l^2(\cos\gamma+1)\sin ml_1\{2 + \sin ml_2\, \sin ml_3 - 2\cos m(l_2+l_3)\}\\
&+ 96ml\sin\gamma\, \cos ml_1\, \sin ml_2\, \sin ml_3\\
&- 144(\cos\gamma-1)\, \sin ml_1\, \sin ml_2\, \sin ml_3\\
=& -16m^2l^2(\cos\gamma+1)\sin ml_1\, \sin ml_2\, \sin ml_3\\
&+ 96ml\sin\gamma\, \cos ml_1\, \sin ml_2\, \sin ml_3\\
&- 144(\cos\gamma-1)\, \sin ml_1\, \sin ml_2\, \sin ml_3.
\end{aligned}$$

Therefore (4.14) reduces to

$$\begin{aligned}
&\sin ml_2\, \sin ml_3\, [m^2l^2\, \sin ml_1 - 6ml\, \cos ml_1\, \tan(\frac{\gamma}{2}) - 9\, \sin ml_1 \tan^2(\frac{\gamma}{2})] =\\
&\sin ml_1\, \sin ml_2\, \sin ml_3\, [ml - \frac{3(\cos ml_1 - 1)\tan(\frac{\gamma}{2})}{\sin ml_1}][ml - \frac{3(\cos ml_1 + 1)\tan(\frac{\gamma}{2})}{\sin ml_1}] =\\
&\sin ml_1\, \sin ml_2\, \sin ml_3\, [ml + \alpha\tan(\frac{ml_1}{2})][ml - \alpha\cot(\frac{ml_1}{2})] = 0,
\end{aligned}$$

and we can infer that

- if $l_3$, and consequently $l_2$, is a rational multiple of $\pi$, i. e. $l_3 = \frac{p}{q}\pi$ with coprime $p, q \in \mathbb{N}$, then $k^2 = q^2m^2$, $m \in \mathbb{N}$, is part of the spectrum for all $p$ regardless of the other parameters.
- if $\gamma = 0$, or equivalently $\alpha = 0$, then the first statement is also valid for $l_j = l_1$.
- if $\gamma \neq 0$ and $l_1$ is an integer multiple of $\pi$, there are no flat bands except those mentioned in the first statement, if present.
- for other values of $l_1$, both rational and irrational, with $\gamma \neq 0$, there might be another flat band $k^2 = m^2$, as long as there exist integer solution $m$ for either $ml + \alpha\tan(\frac{ml_1}{2}) = 0$ or $ml - \alpha\cot(\frac{ml_1}{2}) = 0$.

For case $k = \frac{m\pi}{2(\pi - l_3)} \equiv \tilde{k}$ Equation (4.19) becomes

$$\begin{aligned}
v_z =& -16\tilde{k}^2l^2(\cos\gamma+1)\{2\sin\tilde{k}l_1 + \sin\tilde{k}l_1\, \sin\tilde{k}l_2\, \sin\tilde{k}l_3\\
&- 2\cos\tilde{k}l_1\, \sin 2\tilde{k}\pi - 2\sin\tilde{k}l_1\, \cos 2\tilde{k}\pi\}\\
&+ 96\tilde{k}l\sin\gamma[\cos\tilde{k}l_1\, \sin\tilde{k}l_2\, \sin\tilde{k}l_3 + \sin\tilde{k}l_1\, \sin 2\tilde{k}\pi]\\
&- 144(\cos\gamma-1)\, \sin\tilde{k}l_1\, \sin\tilde{k}l_2\, \sin\tilde{k}l_3 = 0.
\end{aligned} \tag{4.21}$$

A procedure similar to the previous case might be performed only if

$$\frac{m\pi^2}{2(\pi - l_3)} = m'\pi,\ m, m' \in \mathbb{N}.$$

Now we come to three different possibilities:

- $l_3$ being an irrational multiple of $\pi$, for which this simplification is not possible and solutions of (4.21) must be obtained numerically, if there are any;
- $l_3 = 0$, which will be treated separately later on;
- and $l_3$ being a rational multiple of $\pi$, which is doable with some restrictions imposed on numbers $m, m'$ or $q$, using previous notation, but in the end it would lead to similar conclusions as the case $k = m$ (looking at the structure of (4.21), it would mainly require finding a $\tilde{k}$ for which $\sin \tilde{k} l_1$, $\sin \tilde{k} l_3$ and $\sin 2\tilde{k}\pi$ vanish simultaneously).

*Example* 4.1. Let us consider quantum chain with parameters $t = 0$, $\gamma = 0$, $l = 1$, $l_1 = \frac{2\pi}{3}$ and $l_3 = \frac{4\pi}{5}$. According to our results, flat bands should occur at every integer multiple of 5 (stemming from $l_3$) and 3 (stemming from $l_1$ and $\gamma$ being 0). Furthermore, because $\frac{m\pi}{2(\pi - l_3)} = m\frac{5}{2}$, we should see flat bands at multiples of $\frac{5}{2}$ for which is $m$ an odd multiple of 3. Figure 4.2 shows spectral structure of described quantum chain for $k \in \langle 20, 27\rangle$. Because flat bands are eigenvalues of infinite multiplicity but of zero Lebesgue measure, they are not visible directly in the colour-coded spectral decomposition, but they can be identified by peaks that are touching, but not (necessarily) crossing, zero of the vertical axis. We can see them in all suspected points on a given interval, specifically $k = \{20, 21, 22.5, 24, 25, 27\}$.

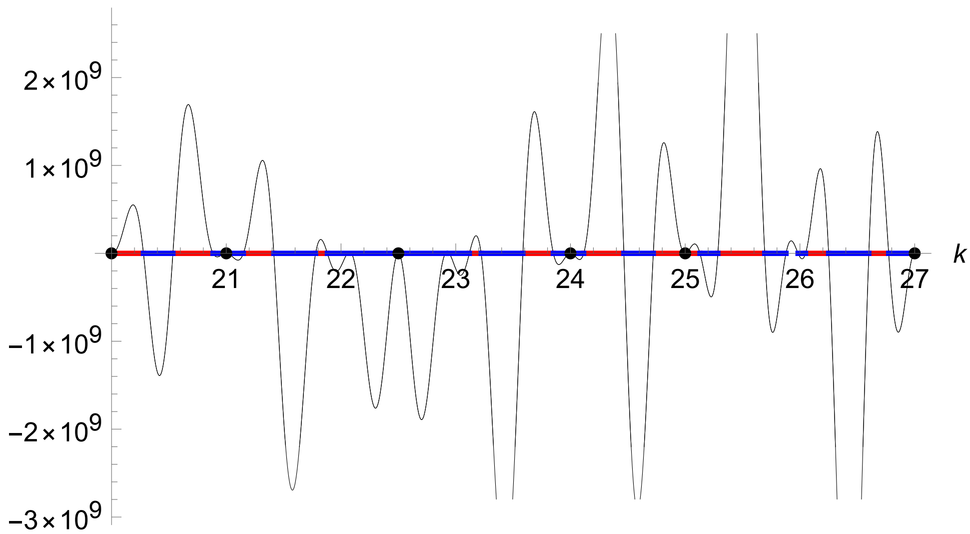


Figure 4.2: Evaluation of spectral condition with parameters set in Example 4.1. Spectral bands are coloured red, while spectral gaps are blue. Flat bands are denoted by black points.

### High energy limit

Let us move to the asymptotic region. Restricting ourselves to the leading power of $k$ appearing in the fractions in (4.17),

$$\begin{aligned}&\frac{4\sin kl_1 \sin^2 k\pi - 4\cos kl_1 \cos k\pi \sin k\pi + \sin kl_1 \sin kl_2 \sin kl_3}{2(\sin kl_2 + \sin kl_3)} = \\ &\frac{\sin kl_1 \sin kl_2 \sin kl_3 - 4\sin k\pi \cos k(\pi + l_1)}{4\sin k\pi \cos k(\pi - l_3)}.\end{aligned} \tag{4.22}$$

The only time when its denominator would be equal to zero are the instances of flat bands, so we now consider only $k$ away from these points, where the spectrum has a band-gap structure. Any further simplifications are unfortunately not possible, except for particular values of the lengths $l_1$, $l_2$ and $l_3$. Nevertheless, it is true that

- in the high energy limit, the spectrum of (4.17) in momentum variable $k$ is independent of strength parameter $\gamma$ up to an $\mathcal{O}(k^{-1})$ error and its structure can be changed only through differences to the length parameters of a chain graph. $\delta$ condition is an energy potential type interaction, and therefore becomes less relevant for system behaviour in the high energy regime.

*Example* 4.2. Consider quantum chain graph with $t = 0$, $l = 1$, $l_1 = 2$ and $l_3 = \frac{1\pi}{3}$. Figure 4.3 shows its spectral condition for $\gamma = 1$ and $k \in \langle 40, 42\rangle$, while Figure 4.4 was made with $\gamma = -2$. There are subtle differences with regard to the width of the bands, but overall is the structure of the spectrum in momentum scale nearly identical, even for these relatively small values of $k$.

### Low energy limit

To gain an insight into the behaviour around 0, we now set $k = \delta$ and Taylor expand relevant functions, specifically

$$\begin{aligned}\sin\, kl_j &= \delta l_j - \frac{\delta^3 l_j^3}{6} + \mathcal{O}(\delta^4),\\ \cos\, kl_j &= 1 - \frac{\delta^2 l_j^2}{2} + \mathcal{O}(\delta^4).\end{aligned}$$

Looking at the (4.18), $v_c$ is proportional at least to the $\delta^3$. While not as obvious, the same is true for $v_z$ as a whole. It is then sufficient to include only the leading terms from expansions above and ratio $\frac{v_z}{v_c}$ now reads

$$\begin{aligned}&\frac{32\, l^2\,(l_2 + l_3) + 96\, l\,(l_2 l_3 + l_1 l_3 + l_1 l_2)\, \tan\frac{\gamma}{2} + 144\, l_1 l_2 l_3\, \tan^2\frac{\gamma}{2}}{-32\, l^2\,(l_2 + l_3)} = \\ &-1 - 3\frac{(l_2 l_3 + l_1 l_3 + l_1 l_2)\, \tan\frac{\gamma}{2}}{l\,(l_2 + l_3)} - \frac{9}{2}\frac{l_1 l_2 l_3\, \tan^2\frac{\gamma}{2}}{l^2\,(l_2 + l_3)}.\end{aligned} \tag{4.23}$$

Here we choose to evaluate the band part of spectral condition (4.17). The gap condition would be done analogically, but it will follow automatically as a negation of the obtained result. Substitution of given $\frac{v_z}{v_c}$ means that

$$0 \le -3\frac{(l_2 l_3 + l_1 l_3 + l_1 l_2)\, \tan\frac{\gamma}{2}}{l\,(l_2 + l_3)} - \frac{9}{2}\frac{l_1 l_2 l_3\, \tan^2\frac{\gamma}{2}}{l^2\,(l_2 + l_3)} \le 2.$$

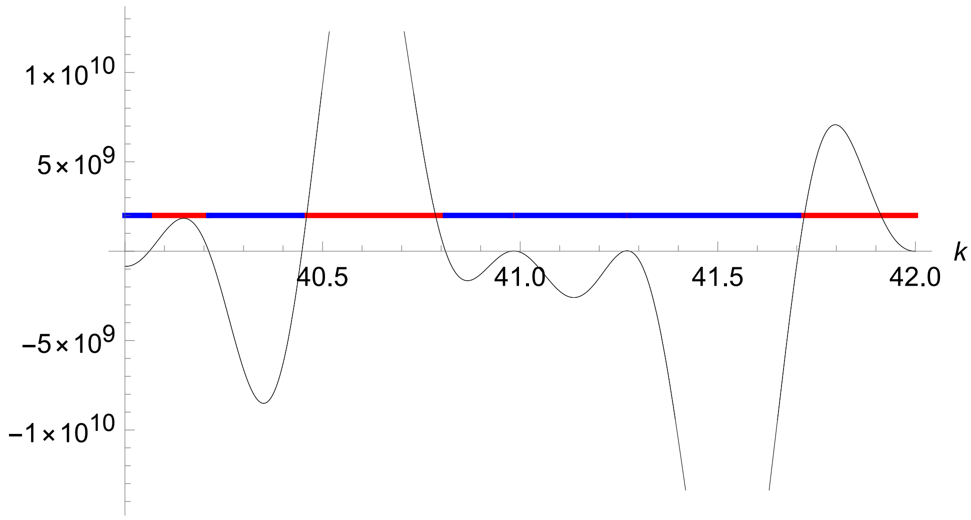


Figure 4.3: Evaluation of spectral condition with parameters set in Example 4.2 and $\gamma = 1$. Spectral bands are coloured red, while spectral gaps are blue.

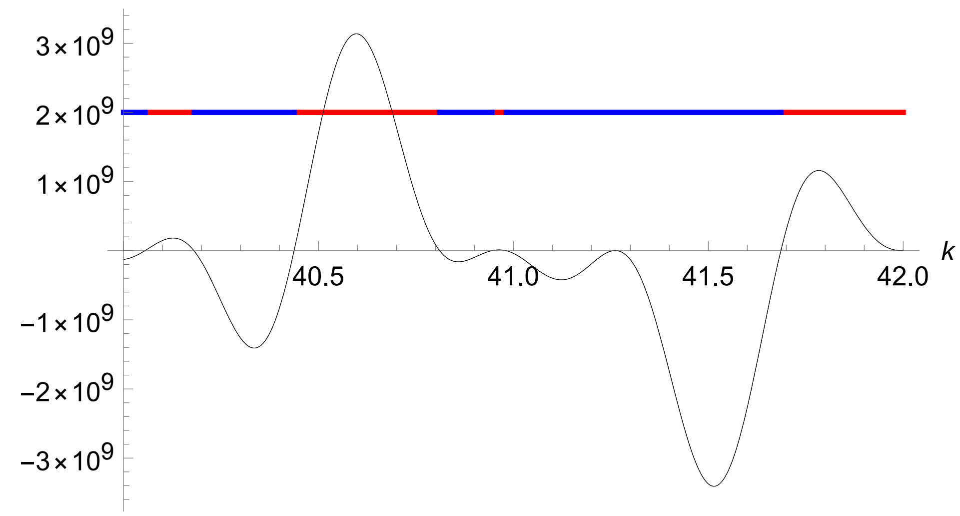


Figure 4.4: Evaluation of spectral condition with parameters set in Example 4.2 and $\gamma = -2$. Spectral bands are coloured red, while spectral gaps are blue.

Dividing by $-1$ and keeping $\tan\frac{\gamma}{2}$ as an independent variable, we complete the square as

$$0 \geq \frac{9}{2}\frac{l_1 l_2 l_3}{l^2\,(l_2+l_3)}\Big[\Big(\tan\frac{\gamma}{2}+\frac{1}{3}\frac{l\,(l_2l_3+l_1l_3+l_1l_2)}{l_1l_2l_3}\Big)^2-\frac{1}{9}\frac{l^2\,(l_2l_3+l_1l_3+l_1l_2)^2}{l_1^2l_2^2l_3^2}\Big] \geq -2,$$

leading to

$$\begin{aligned}\frac{1}{9}\frac{l^2\,(l_2l_3+l_1l_3+l_1l_2)^2}{l_1^2l_2^2l_3^2} &\geq \Big(\tan\frac{\gamma}{2}+\frac{1}{3}\frac{l\,(l_2l_3+l_1l_3+l_1l_2)}{l_1l_2l_3}\Big)^2\\ \geq -\frac{4}{9}\frac{(l_2+l_3)l^2}{l_1l_2l_3}+\frac{1}{9}\frac{l^2\,(l_2l_3+l_1l_3+l_1l_2)^2}{l_1^2l_2^2l_3^2} &= \frac{1}{9}\frac{l^2\,(l_2l_3-l_1l_3-l_1l_2)^2}{l_1^2l_2^2l_3^2}.\end{aligned}$$

The upper bound is always positive, so we can take its square root without any additional thought, but the same cannot be said for the lower bound. First, assume that

$$l_2l_3-l_1l_3-l_1l_2 \geq 0 \Rightarrow l_1 \leq \frac{l_2l_3}{l_2+l_3}.$$

Then after taking the square root of the whole inequality we have

$$\frac{1}{3}\frac{l\,(l_2l_3+l_1l_3+l_1l_2)}{l_1l_2l_3} \geq \left|\tan\frac{\gamma}{2}+\frac{1}{3}\frac{l\,(l_2l_3+l_1l_3+l_1l_2)}{l_1l_2l_3}\right| \geq \frac{1}{3}\frac{l\,(l_2l_3-l_1l_3-l_1l_2)}{l_1l_2l_3},$$

and we can assume the inside of the resulting absolute value to be either positive, leading to

$$0 \geq \tan\frac{\gamma}{2} \geq -\frac{2}{3}\frac{l\,(l_2+l_3)}{l_2l_3} = -\frac{4\pi}{3}\frac{l}{(2\pi-l_3)l_3} \tag{4.24}$$

or negative, in which case

$$-\frac{2}{3}\frac{l\,(l_2l_3+l_1l_3+l_1l_2)}{l_1l_2l_3} = -\frac{2}{3}\frac{l}{l_1}-\frac{2}{3}\frac{l\,(l_2+l_3)}{l_2l_3} \leq \tan\frac{\gamma}{2} \leq -\frac{2}{3}\frac{l}{l_1}. \tag{4.25}$$

On the other hand, if

$$l_2l_3-l_1l_3-l_1l_2 \leq 0 \Rightarrow l_1 \geq \frac{l_2l_3}{l_2+l_3},$$

we get

$$\frac{1}{3}\frac{l\,(l_2l_3+l_1l_3+l_1l_2)}{l_1l_2l_3} \geq \left|\tan\frac{\gamma}{2}+\frac{1}{3}\frac{l\,(l_2l_3+l_1l_3+l_1l_2)}{l_1l_2l_3}\right| \geq \frac{1}{3}\frac{l\,(-l_2l_3+l_1l_3+l_1l_2)}{l_1l_2l_3},$$

and through the same procedure, we have

$$0 \geq \tan\frac{\gamma}{2} \geq -\frac{2}{3}\frac{l}{l_1} \tag{4.26}$$

together with

$$-\frac{2}{3}\frac{l}{l_1}-\frac{4\pi}{3}\frac{l}{(2\pi-l_3)l_3} \leq \tan\frac{\gamma}{2} \leq -\frac{4\pi}{3}\frac{l}{(2\pi-l_3)l_3}. \tag{4.27}$$

If any of those inequalities, chosen accordingly to match given length ratios, is satisfied, the positive spectrum is connected to the 0, otherwise it is not. Additionally, because $\tan(x)$ is an odd function, the positive spectrum cannot be connected to zero for $\gamma > 0$.

**Negative spectrum**

The negative spectral condition is again obtained by substitution $k = i\kappa$, $\kappa > 0$, meaning that

$$v_c = i32\kappa^2 l^2(\cos\gamma + 1)(\sinh\kappa l_2 + \sinh\kappa l_3)$$

and

$$\begin{aligned} v_z = i16\kappa^2 l^2(\cos\gamma+1)\{&2\sinh\kappa l_1 - 3\sinh\kappa l_1\sinh\kappa l_2\sinh\kappa l_3 \\ &- 2[\cosh\kappa l_1\cosh\kappa l_2\sinh\kappa l_3 + \cosh\kappa l_2\cosh\kappa l_3\sinh\kappa l_1 \\ &+ \cosh\kappa l_3\cosh\kappa l_1\sinh\kappa l_2]\} \\ &- i96\kappa l\sin\gamma[\cosh\kappa l_1\sinh\kappa l_2\sinh\kappa l_3 + \cosh\kappa l_2\sinh\kappa l_3\sinh\kappa l_1 \\ &+ \cosh\kappa l_3\sinh\kappa l_1\sinh\kappa l_2] \\ &+ i144(\cos\gamma-1)\sinh\kappa l_1\sinh\kappa l_2\sinh\kappa l_3. \end{aligned}$$

The number of possible negative spectral bands still satisfies the bound of Theorem 3.1. Our elementary cell has two vertices, each of them described by the same coupling matrix, in which all of the eigenvalues, except one, are equal to -1, therefore

- there are at most two negative spectral bands, whose appearance is conditioned by $\gamma < 0$ (equivalently $\tan\frac{\gamma}{2}$ or $\alpha$ less than zero); for $\gamma \geq 0$, the negative spectrum is empty.

This can be understood from the fact that $v_z$ grows as $\kappa^2 e^{\kappa(l_1+l_2+l_3)}$, while the $v_c$ grows at most as $\kappa^2 e^{\kappa(l_j)}$, $j = 2, 3$, whichever $l_j$ is higher; their ratio then must be larger than 1, satisfying the gap condition of (4.17).

In a similar way, one finds the behaviour in the low energy limit - in the leading term

$$\begin{aligned} \sin xl_j &\approx \delta l_j \approx \sinh xl_j, \\ \cos xl_j &\approx 1 \approx \cosh xl_j. \end{aligned}$$

$x$ now denotes both $k$ and $\kappa$; here it is only important that both quantities are positive and approaching zero. But because all relevant parts retain their relative sign in the ratio $\frac{v_z}{v_c}$, we arrive at the exact same conditions as for the positive part of the spectrum, only with $\tan\frac{\gamma}{2}$ separated from 0, and conclude that

- if there is any negative spectral band, it and the lowest positive band are either both connected to $k^2 = 0$, or they both remain separated.

*Example* 4.3. Consider quantum chain with $t = 0$, $l = 1$, $l_1 = 2$ and $l_3 = \frac{\pi}{3}$. Because

$$l_1 = 2 \geq \frac{\frac{\pi}{3}\frac{5\pi}{3}}{2\pi} = \frac{5\pi}{18} = \frac{l_2 l_3}{l_2 + l_3},$$

we make use of conditions (4.26) and (4.27). From there the boundaries read

$$\tan\frac{\gamma}{2} = \begin{cases} 0 \text{ and} \\ -\dfrac{1}{3}, \end{cases}$$

$$\tan\frac{\gamma}{2} = \begin{cases} -\dfrac{12}{5\pi} \text{ and} \\ -\dfrac{12}{5\pi} - \dfrac{1}{3}, \end{cases}$$

respectively. Figures 4.5 and 4.6 show spectral bands with non-negative $\gamma$ - not only is continuous negative spectrum empty, but for the former are positive bands separated from $k = 0$. Figures 4.8, 4.10 and 4.12 were made with $\gamma$ corresponding to respective boundary values of $\tan\frac{\gamma}{2}$, demonstrating how spectral bands in positive and negative spectrum shift between being simultaneously (dis)connected from zero, while Figures 4.7, 4.9 and 4.11 were chosen as examples of particular conditions (not) being satisfied.

**Limit** $l_1 \to 0$

There are two possible ways how we can pass into a quantum chain connected with vertices of degree four - one of them is when $l_1$ shrinks to zero. We will not treat the symmetric quantum chain (and vice versa later on) as some exceptional case, because spectrum of this quantum graph topology with $\delta$ coupling was already described in more detail in [DET08].

Because $v_c$ from (4.18), or rather (4.20), is not a function of $l_1$, it remains unchanged, while $v_z$ takes on the form

$$\begin{aligned} v_z =& 32k^2l^2(\cos\gamma + 1)\sin k(l_2 + l_3) \\ &+ 96kl\sin\gamma\sin kl_2 \sin kl_3. \end{aligned}$$

Apart from being a considerably more compact expression, there is no difference in evaluating (4.17), so we pass directly to the individual characteristics.

Considering flat bands, those coming from $l_1$ are naturally absent, the others are present once again if $l_3$ is a rational multiple of $\pi$.

Evaluation of the high energy limit will be in the end easier if done through spectral condition (4.15). In the leading order, it gives

$$\begin{aligned} (\sin kl_2 + \sin kl_3)^2 - \sin^2 k(l_2 + l_3) &= \\ 2\sin^2 kl_2\,\sin^2 kl_3 + 2\sin kl_2\,\sin kl_3(1 - \cos kl_2\,\cos kl_3) &= \\ 2\sin kl_2\,\sin kl_3(1 - \cos k(l_2 + l_3)) &\geq 0, \end{aligned}$$

up to an $\mathcal{O}(k^{-1})$ error. It is also the exact form of the spectral band condition if we choose $\gamma = 0$ in this setting. Because

$$2(1 - \cos k(l_2 + l_3)) = 2(1 - \cos 2\pi k) = 4\sin^2 k\pi > 0$$

is always satisfied (here we operate outside of flat bands), we can divide by this term and the effective condition becomes

$$\sin kl_2\,\sin kl_3 \geq 0. \tag{4.28}$$

Note that exactly the same condition was obtained in [BET22, Equation (3.33)]. This indicates a shared property, which we will briefly describe below.

To this aim, we introduce the *probability of belonging to the (positive) spectrum*, by which we can compare features of individual spectra. Defined in [BB13] as

$$P_\sigma(H) := \lim_{K\to\infty} \frac{1}{K}\left|\sigma(H) \cap \langle 0,K\rangle\right|, \tag{4.29}$$

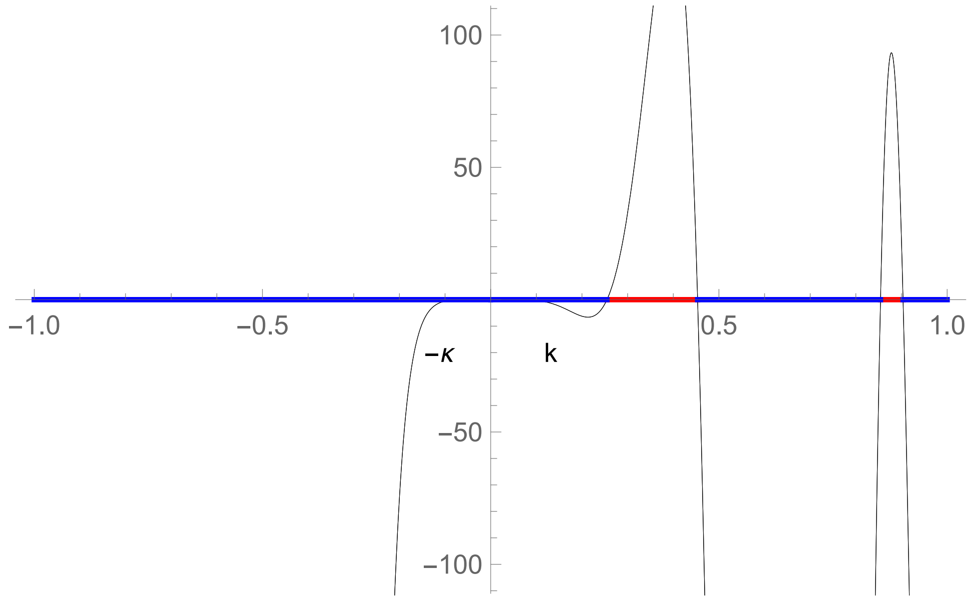


Figure 4.5: Evaluation of spectral condition with parameters set in Example 4.3 and $\gamma = 0.2$. Spectral bands are coloured red, while spectral gaps are blue.

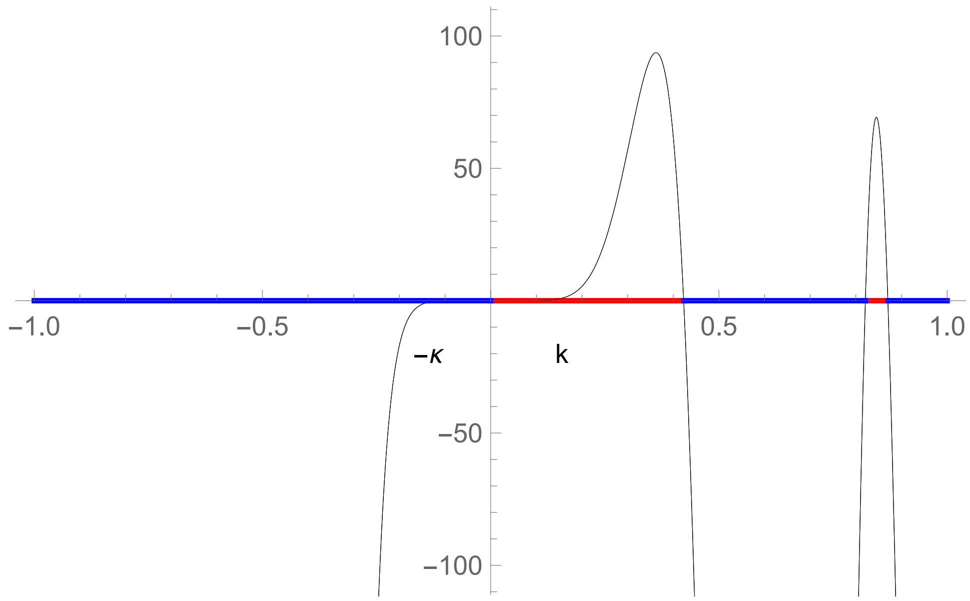


Figure 4.6: Evaluation of spectral condition with parameters set in Example 4.3 and $\gamma = 0$. Spectral bands are coloured red, while spectral gaps are blue.

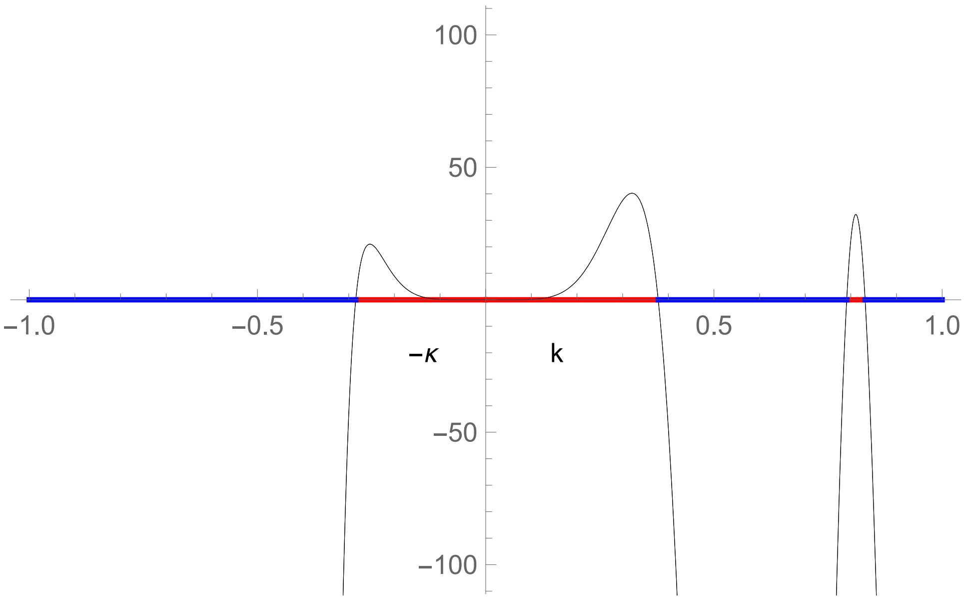


Figure 4.7: Evaluation of spectral condition with parameters set in Example 4.3 and $\gamma = -0.2$. Spectral bands are coloured red, while spectral gaps are blue.

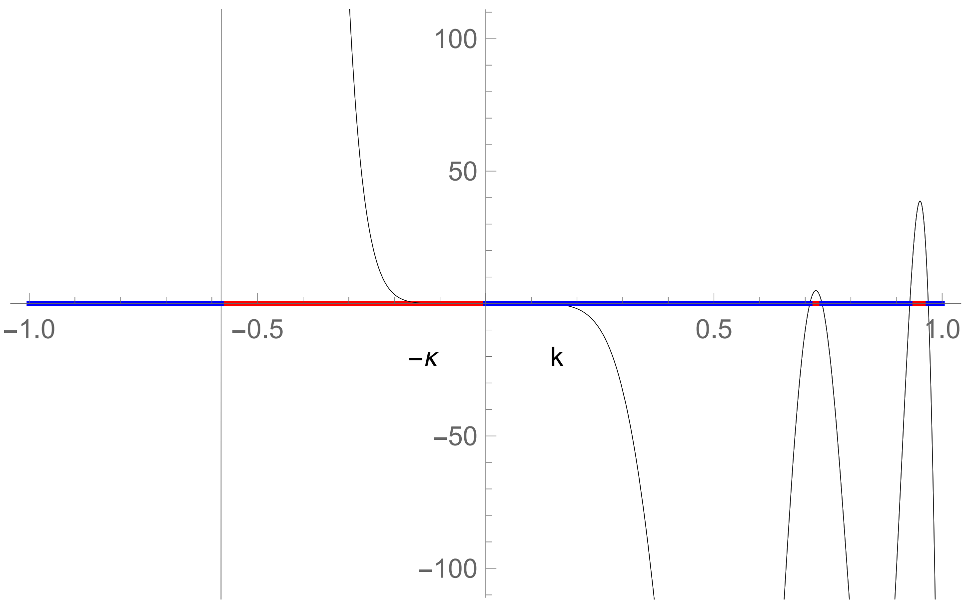


Figure 4.8: Evaluation of spectral condition with parameters set in Example 4.3 and $\gamma = -2\arctan\frac{1}{3} \approx -0.64$. Spectral bands are coloured red, while spectral gaps are blue.

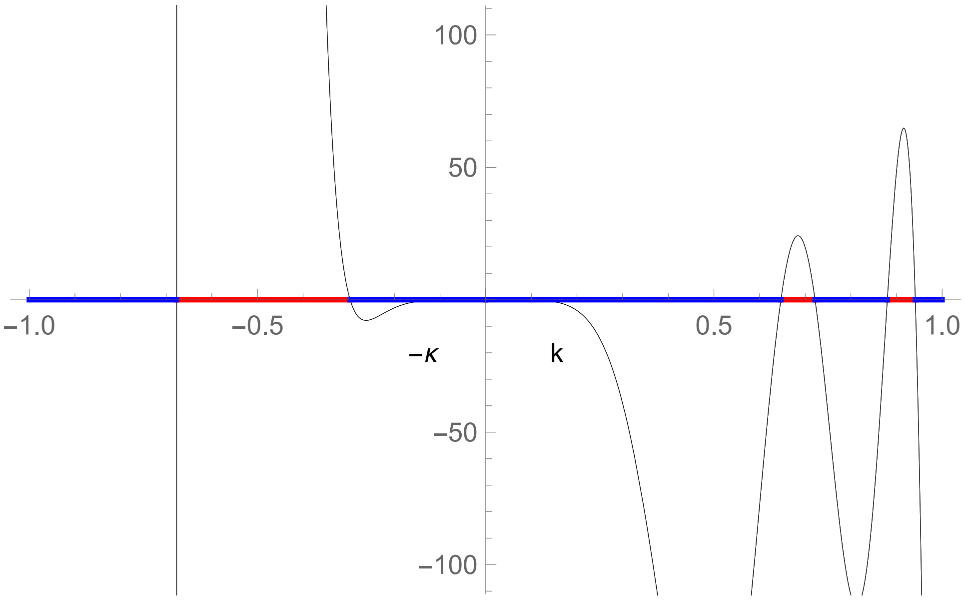


Figure 4.9: Evaluation of spectral condition with parameters set in Example 4.3 and $\gamma = -0.8$. Spectral bands are coloured red, while spectral gaps are blue.

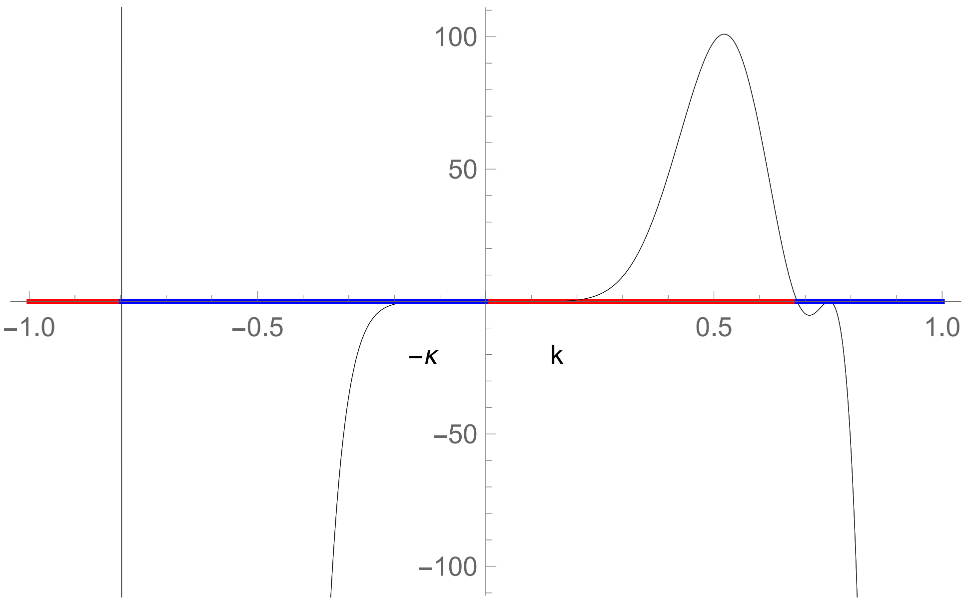


Figure 4.10: Evaluation of spectral condition with parameters set in Example 4.3 and $\gamma = -2\arctan\frac{12}{5\pi} \approx -1.30$. Spectral bands are coloured red, while spectral gaps are blue.

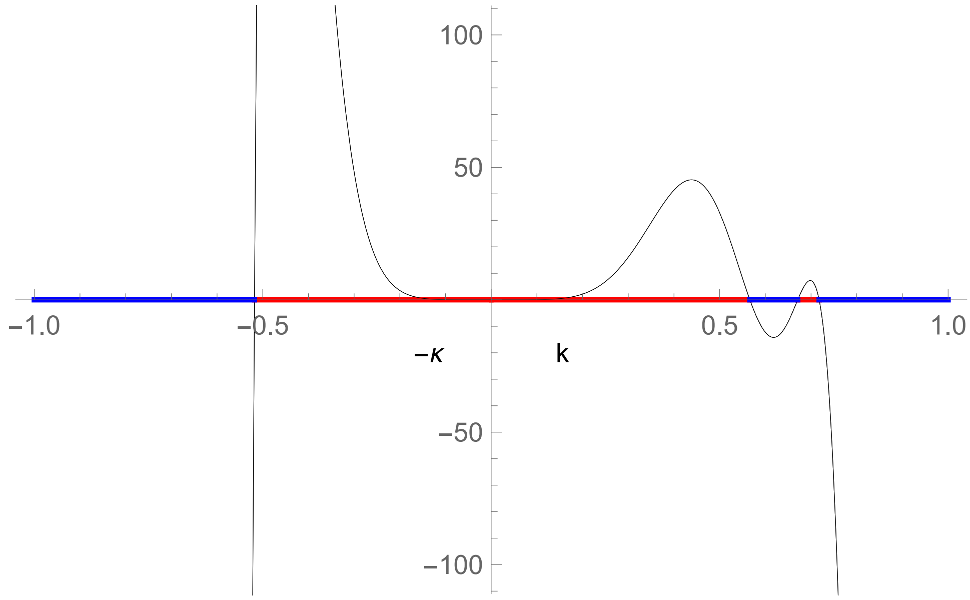


Figure 4.11: Evaluation of spectral condition with parameters set in Example 4.3 and $\gamma = -1.5$. Spectral bands are coloured red, while spectral gaps are blue.

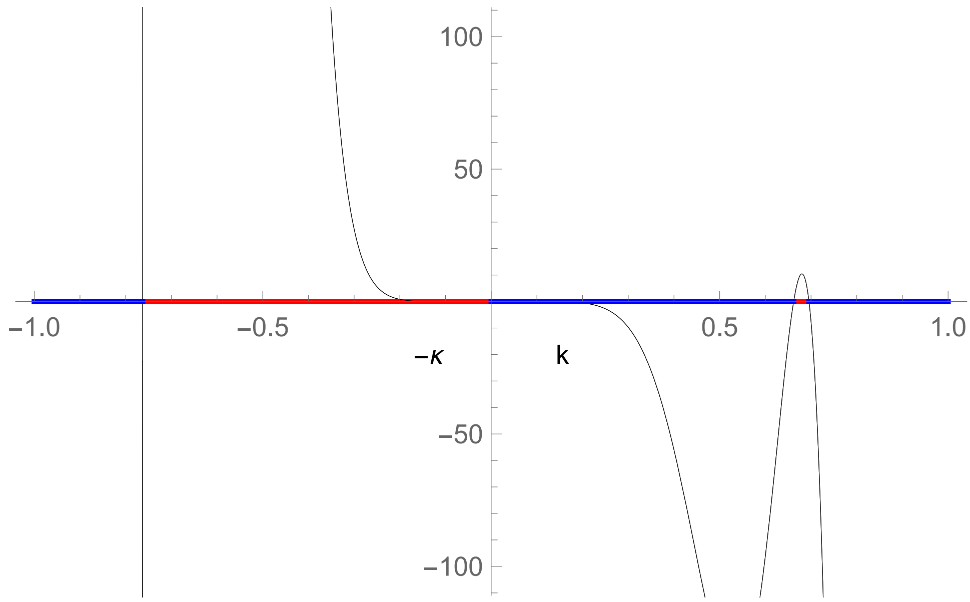


Figure 4.12: Evaluation of spectral condition with parameters set in Example 4.3 and $\gamma = -2\arctan\left(\frac{12}{5\pi} + \frac{1}{3}\right) \approx -1.66$. Spectral bands are coloured red, while spectral gaps are blue.

for (4.28) we have

$$\begin{aligned} P_\sigma(H) &= 1 \ \dots \ l_3 = \pi \\ P_\sigma(H) &= \frac{1}{2} \ \dots \ l_3 \neq \pi \end{aligned} \tag{4.30}$$

Zero in the definition of (4.29) can be in the asymptotic regime replaced by any positive number, therefore we can use it on the spectral condition determined by (4.28). For each of the sine factors from the said condition, the probability that it will be positive, or negative, for a random value of $k$ is equal to $\frac{1}{2}$. When $l_2 = l_3 = \pi$, these probabilities are correlated (or rather $\sin^2 x$ is always non-negative). For any other possible combination of lengths, the positive spectrum has an infinite number of open gaps, and while the concrete shape of the spectrum depends on ratio $\frac{l_3}{l_2}$ - periodic for rational and aperiodic for irrational, both in the momentum scale - the $P_\sigma(H)$ is always $\frac{1}{2}$, because for uncorrelated probabilities we have

$$\left(\frac{1}{2}\right)^2 + \left(\frac{1}{2}\right)^2 = \frac{1}{2}$$

In their article, [BB13] have proven the universality of $P_\sigma(H)$ for quantum graphs equipped with Kirchhoff (or more generally $\delta$) coupling - its value remains the same regardless of the specific lengths characterizing the graph, as long as they remain incommensurate. This applies to our graph as well, but here is the set of length values leading to universal $P_\sigma(H)$ (which is, in particular, obtainable analytically) larger, containing $\forall l_3 \neq \pi$, due to the simple form of the (asymptotic) spectral condition.

The procedure in the low energy limit could be repeated exactly the same as before, and we can directly substitute into (4.23) to gain

$$-1 - 3\frac{l_2 l_3 \tan\frac{\gamma}{2}}{l\,(l_2 + l_3)},$$

meaning that

$$0 \leq -3\frac{l_2 l_3 \tan\frac{\gamma}{2}}{l\,(l_2 + l_3)} = -3\frac{l_2 l_3 \tan\frac{\gamma}{2}}{l\,2\pi} \leq 2.$$

Therefore there is just one condition for the spectrum connected to $k^2 = 0$,

$$0 \geq \tan\frac{\gamma}{2} \geq -\frac{4\pi}{3}\frac{l}{(2\pi - l_3) l_3}, \tag{4.31}$$

which in the language of $\alpha$, assuming it was specified earlier before limit $l_1 \to 0$, can be rewritten as

$$0 \geq \alpha \geq -2\pi\frac{l}{(2\pi - l_3) l_3}.$$

While we have confirmed it by explicit calculation, it could have been shown directly from conditions (4.24) and (4.25) - because $l_1$ is equal to 0, it is necessarily smaller than $\frac{l_2 l_3}{2\pi}$, making use of both conditions valid, but in our case both the upper and lower bound from (4.25) go to $-\infty$, so the condition cannot be fulfilled for a fixed $\gamma$.

Whether the negative spectrum is connected to 0 is determined by the same condition (4.31), excluding $\tan\frac{\gamma}{2} = 0$, and the only remarkable difference is that our elementary cell now contains only one vertex, which is the reason why the upper limit for the number of negative bands decreases to one; it can exist only for $\gamma < 0$.

*Example* 4.4. Consider quantum chain with $t = 0$, $l = 1$, $l_1 = 0$ and $\gamma = 2$. If we choose $l_3 \neq \pi$, for example $\frac{\pi}{2}$, we get picture similar to Figure 4.13. Behaviour at low energies depends on a specific value of $\gamma$, but as $k$ grows, the band-gap structure saturates into the pattern we see starting around $k = 10$, which is periodic and equally populated by bands and gaps with respect to their widths in momentum scale. On the other hand, if we choose $l_3 = \pi$, an example of which is Figure 4.14, from a certain moment, depending on $\gamma$, spectral bands quickly start to dominate and eventually dominate the whole momentum axis $k$ in the asymptotic regime.

**Limit** $l_3 \to 0$

The second way how we can obtain vertices of degree four is by shrinking $l_3$ to zero, or doing the same with $l_2$. The other length is in our scale automatically fixed to $2\pi$, changing (4.18) to

$$v_c = -64k^2 l^2 (\cos\gamma + 1)\ \sin k\pi\ \cos k\pi$$

and

$$\begin{aligned} v_z = &-64k^2 l^2 (\cos\gamma + 1) \sin k\pi [\sin kl_1 \sin k\pi - \cos kl_1 \cos k\pi] \\ &+ 192kl \sin\gamma \sin kl_1 \sin k\pi \cos k\pi \\ = &\, 64k^2 l^2 (\cos\gamma + 1) \sin k\pi \cos k(\pi + l_1) \\ &+ 192kl \sin\gamma \sin kl_1 \sin k\pi \cos k\pi \end{aligned}$$

Firstly, all $k^2 = m^2$, $m \in \mathbb{N}$ are in the positive spectrum, in accordance with the previous result, but now we have flat bands also possible for $k = \frac{2m-1}{2}$. Substitution into (4.14) yields

$$64\left(\frac{2m-1}{2}\right)^2 l^2 (\cos\gamma + 1) \sin\frac{(2m-1)\pi}{2}\ \cos\frac{(2m-1)(\pi + l_1)}{2} = 0.$$

Thus in addition there are flat bands present if $l_1$ is a $\pi$-multiple of an even integer (for all $m \in \mathbb{N}$), or if $l_1$ is a rational multiple of $\pi$, $l_1 = \frac{p}{q}$, and

$$(2m-1)(1 + \frac{p}{q}) \mod 2 = 1$$

(for some $m \in \mathbb{N}$).

For the high energies, we have from (4.15)

$$4 \sin^2 \frac{kl_2}{2}\ \sin kl_1\ \sin k(l_2 + l_1) \geq 0,$$

which corresponds to

$$\sin kl_1\ \sin k(2\pi + l_1) \geq 0,$$

up to $\mathcal{O}(k^{-1})$. This is once again the same condition as was found in [BET22, Section 4.1] for $t = 1$ in the limit $l_3 \to 0$. Even though there is a periodicity if $l_1$

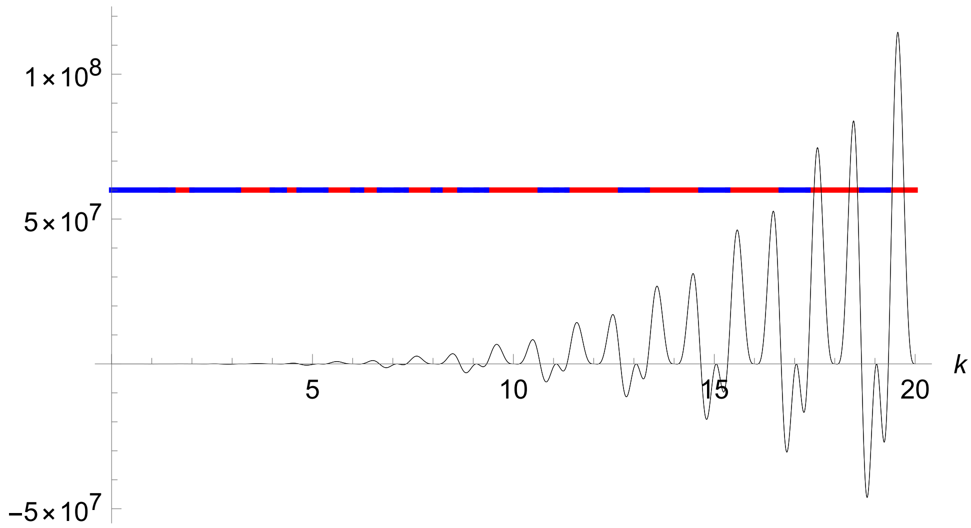


Figure 4.13: Evaluation of spectral condition with parameters set in Example 4.4 and $l_3 = \frac{\pi}{2}$. Spectral bands are coloured red, while spectral gaps are blue.

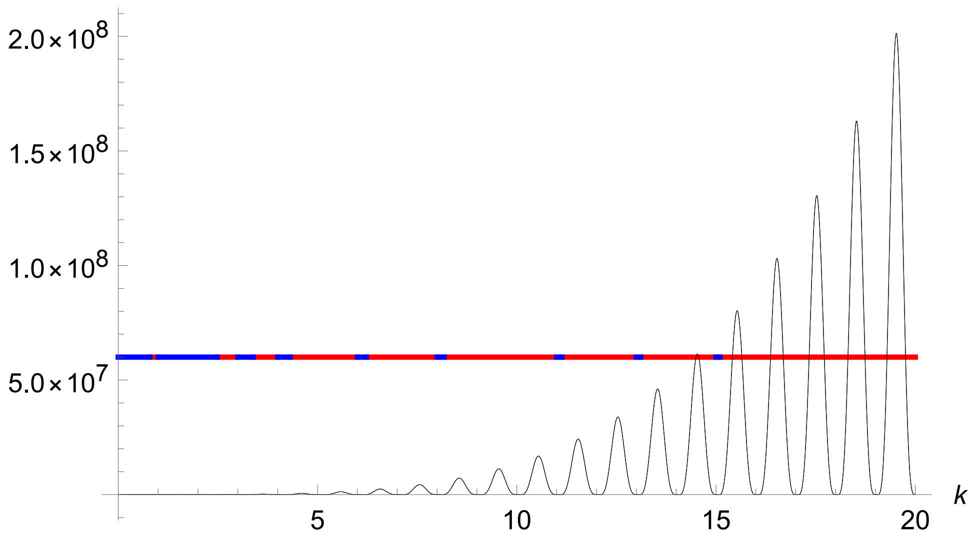


Figure 4.14: Evaluation of spectral condition with parameters set in Example 4.4 and $l_3 = \pi$. Spectral bands are coloured red, while spectral gaps are blue.

is a rational multiple of $\pi$, using argument similar to when $l_1$ was approaching 0, we arrive to

$$P_\sigma(H) = \frac{1}{2}.$$

When $l_1 \to \infty$, the positive spectrum becomes 'denser' if we talk about the number of spectral bands (or gaps) per fixed interval, but the share of the momentum scale covered remains the same.

Low energy behaviour can be again simply described by (4.23), leading to

$$-1 - 3\frac{l_1}{l}\tan\frac{\gamma}{2}$$

and consequently

$$0 \geq \tan\frac{\gamma}{2} \geq -\frac{2}{3}\frac{l}{l_1}. \tag{4.32}$$

Whether is the positive and negative spectrum connected to zero is determined (up to exclusion of 0 from the latter) by this condition, and the negative spectrum still has at most one spectral band. Again, this fact could have been read directly from (4.26) and (4.27) using argumentation similar to limit $l_1 \to 0$.

### Symmetric quantum chain

Let us finish this section with a case of the symmetric chain graph, $l_2 = l_3 = \pi$. Substituting into (4.20) we have

$$v_c = -64k^2l^2(\cos\gamma + 1)\,\sin k\pi,$$

and there are once again flat bands for all $k = m$, $m \in \mathbb{N}$, as $l_3$ is now rational multiple of $\pi$ with $p = q = 1$.

In the high energy region, (4.22) simplifies to

$$\frac{\sin kl_1 \sin k\pi}{4} - \cos k(\pi + l_1). \tag{4.33}$$

In comparison to the general case, we can clearly see that points

$$k = \frac{m\pi}{l_1},\, m \in \mathbb{N},$$

belong to spectral bands, because

$$\left| -\cos\frac{m\pi(\pi + l_1)}{l_1} \right| \leq 1,$$

up to an $\mathcal{O}(k^{-1})$ error, but there are no further simplifications giving additional insight into the behaviour of the spectrum.

While the length values of the symmetric chain were in some sense special for the high energy limit, behaviour in the negative part of the spectrum and around zero remains unchanged, and the formulae derived do not undergo substantial simplification after these lengths are plugged in, and for that reason we do not present them explicitly.

Overall, let us recapitulate obtained results in the following theorem.

**Theorem 4.1.** *Let $\Gamma$ be a quantum chain graph with the topology illustrated by Figure 4.1, described by lengths $l_j \geq 0$, $j = 1, 2, 3$, length scaling parameter $l > 0$, and a circulant vertex matrix $U(0)$ (describing $\delta$ coupling), with strength parameter $\gamma \in (-\pi,\pi)$. Assuming we fix the scaling by requiring $l_2 + l_3 = 2\pi$, we can draw these conclusions about its spectrum:*

1. *For all possible length and coupling strength configurations, flat bands $k^2 = m^2q^2$, $m \in \mathbb{N}$ are present if $l_3$ a rational multiple of $\pi$, $l_3 = \frac{p}{q}\pi$.*
   - *There might be additional flat bands of the same type if $\gamma = 0$ (Kirchhoff coupling) and $l_1$ is a rational multiple of $\pi$.*
   - *With an arbitrary $\gamma$ and $l_1$, except for $l_1$ being an integer multiple of $\pi$, there might be extra flat band $k^2 = m^2$ if $ml + \alpha \tan(\frac{ml_1}{2}) = 0$ or $ml - \alpha \cot(\frac{ml_1}{2}) = 0$ is satisfied.*
   - *For $l_1 = 0$, there are no other flat bands present.*
   - *For $l_3 = 0$, there are additional flat bands only if $l_1$ is an integer multiple of $2\pi$ ($\forall m$), or a rational multiple of $\pi$ (some $m$).*
2. *The high energy spectrum is generally independent of $\gamma$, up to an $\mathcal{O}(k^{-1})$ error.*
   - *Probability of a random point $k$ belonging to the positive spectrum is constant in the limits $l_1$ or $l_3$ going to zero. If the value of the length $l_3$ is $\pi$ in the former case, this probability is equal to 1, otherwise it is always equal to $\frac{1}{2}$, regardless of other parameters.*
3. *Whether the positive spectrum is connected to energy $k^2 = 0$ is dependent on all parameters of a quantum chain.*
   - *It might be connected only if $\gamma \leq 0$.*
   - *If $l_1 \leq \frac{l_2 l_3}{2\pi}$, whether the positive or negative spectrum is connected is determined by conditions (4.24) and (4.25), respectively.*
   - *If $l_1 \geq \frac{l_2 l_3}{2\pi}$, whether the positive or negative spectrum is connected is determined by conditions (4.26) and (4.27), respectively.*
   - *When either $l_1$ or $l_3$ shrinks to zero, positive spectrum is possibly connected if similar conditions are satisfied, see (4.31) or (4.32) respectively.*
4. *There are always at most two negative spectral bands, possibly appearing only for $\gamma < 0$. This maximal number decreases to one in limits $l_1 \to 0$ and $l_3 \to 0$. The negative spectrum, if present, is connected to $k^2 = \kappa^2 = 0$ only if the positive spectrum is also connected.*

### 4.3.2 Case of $t \neq 0$

While the concrete spectral structure is obviously dependent on a specific value of $t$, cases of $t = 0$ and $t = 1$ are the only ones radically changing equation (4.9), because some polynomials $P$ vanish. Outside of them, the behaviour of the spectral condition is similar across all of the remaining $t$.

#### High energy limit

We explained why the flat bands are absent except at the two extremal values of the interpolation parameter $t$. As such, we can now continue straight to the limit $k \to \infty$ of our quantum chain. Looking at (4.16) in the highest order of $k$, where we already factored out $(\cos\frac{\pi t}{3} - 1)^2$, gives us

$$-1296\, k^{12}\, l^{12}\, (\cos\gamma(1-t)+1)^2 \sin^2 kl_1 \sin^2 kl_2 \sin^2 kl_3 + \mathcal{O}(k^{11}) < 0;$$

therefore the high energies are dominated by spectral gaps, as could have been expected from the absence of eigenvalue $-1$ for vertices of degree three, see (4.2). Bands are formed only around the points

$$k_{m,j} = \frac{m\pi}{l_j},\ m \in \mathbb{N},\ j = 1{,}2{,}3,$$

and to gain a deeper insight, we rewrite (4.9) into the asymptotic form

$$\frac{P_6}{l^6} + \frac{P_5}{kl^6} + \frac{P_4}{k^2 l^6} + \frac{P_c\cos\theta + P_s\sin\theta}{k^4 l^6} = \mathcal{O}(k^{-3}). \tag{4.34}$$

Each of the three cases follows the analysis in the same way, and we will write it explicitly only for $l_1$ and $l_3$ - (4.34) is symmetric in the $l_2$ and $l_3$, and the final result can be obtained by simply switching these two quantities.

Starting with $l_1$, we substitute it in (3.11) and make use of (3.12). This specifically means

$$\begin{aligned}
\sin\, kl_1 &= (-1)^m \delta l_1 - (-1)^m \frac{\delta^3 l_1^3}{6} + \mathcal{O}(\delta^4),\\
\cos\, kl_1 &= (-1)^m - (-1)^m \frac{\delta^2 l_1^2}{2} + \mathcal{O}(\delta^4),\\
\sin\, kl_2 &= \sin\,\frac{m\pi l_2}{l_1}(1 - \frac{\delta^2 l_2^2}{2}) + \cos\,\frac{m\pi l_2}{l_1}(\delta l_2 - \frac{\delta^3 l_2^3}{6}) + \mathcal{O}(\delta^4),\\
\cos\, kl_2 &= \cos\,\frac{m\pi l_2}{l_1}(1 - \frac{\delta^2 l_2^2}{2}) - \sin\,\frac{m\pi l_2}{l_1}(\delta l_2 - \frac{\delta^3 l_2^3}{6}) + \mathcal{O}(\delta^4),\\
\sin\, kl_3 &= \sin\,\frac{m\pi l_3}{l_1}(1 - \frac{\delta^2 l_3^2}{2}) + \cos\,\frac{m\pi l_3}{l_1}(\delta l_3 - \frac{\delta^3 l_3^3}{6}) + \mathcal{O}(\delta^4),\\
\cos\, kl_3 &= \cos\,\frac{m\pi l_3}{l_1}(1 - \frac{\delta^2 l_3^2}{2}) - \sin\,\frac{m\pi l_3}{l_1}(\delta l_3 - \frac{\delta^3 l_3^3}{6}) + \mathcal{O}(\delta^4).
\end{aligned} \tag{4.35}$$

Plugging these into (4.34), with

$$\begin{aligned}
k^{-1} &= \frac{l_1}{m\pi} + \mathcal{O}(m^{-1}),\\
k^{-2} &= (\frac{l_1}{m\pi})^2 + \mathcal{O}(m^{-2}),
\end{aligned}$$

leads to

$$
\begin{aligned}
&\{-(-1)^m\frac{24\beta_b l_1}{m\pi l}\sin\frac{m\pi l_2}{l_1}\sin\frac{m\pi l_3}{l_1}\\
&\quad+\frac{(-1)^m l_1^2}{m^2\pi^2 l^2}[\cos\frac{m\pi l_2}{l_1}\sin\frac{m\pi l_3}{l_1}+\sin\frac{m\pi l_2}{l_1}\cos\frac{m\pi l_3}{l_1}][9\beta_d+\beta_e]\\
&\quad+\frac{16 l_1^2}{m^2\pi^2 l^2}[\sin\frac{m\pi l_2}{l_1}+\sin\frac{m\pi l_3}{l_1}][-\beta_c\cos\theta+\beta_f\sin\theta]\}\\
&+\delta\{(-1)^m l_1\sin\frac{m\pi l_2}{l_1}\sin\frac{m\pi l_3}{l_1}[36\beta_a+\frac{3l_1^2}{m^2\pi^2 l^2}(-3\beta_d+\beta_e)]\\
&\quad-(-1)^m\frac{24\beta_b l_1}{m\pi l}[(l_1+l_3)\sin\frac{m\pi l_2}{l_1}\cos\frac{m\pi l_3}{l_1}+(l_1+l_2)\cos\frac{m\pi l_2}{l_1}\sin\frac{m\pi l_3}{l_1}]\\
&\quad+\frac{(-1)^m l_1^2}{m^2\pi^2 l^2}[(l_1+l_2+l_3)\cos\frac{m\pi l_2}{l_1}\cos\frac{m\pi l_3}{l_1}-(l_2+l_3)\sin\frac{m\pi l_2}{l_1}\sin\frac{m\pi l_3}{l_1}]\\
&\quad(9\beta_d+\beta_e)\\
&\quad-\frac{(-1)^m 16 l_1^2}{m^2\pi^2 l^2}l_1\beta_c\\
&\quad+\frac{16 l_1^2}{m^2\pi^2 l^2}[l_2\cos\frac{m\pi l_2}{l_1}+l_3\cos\frac{m\pi l_3}{l_1}][-\beta_c\cos\theta+\beta_f\sin\theta]\}\\
&+\delta^2\{(-1)^m 36\beta_a(l_1 l_3\sin\frac{m\pi l_2}{l_1}\cos\frac{m\pi l_3}{l_1}+l_1 l_2\sin\frac{m\pi l_3}{l_1}\cos\frac{m\pi l_2}{l_1})\\
&\quad-(-1)^m\frac{24\beta_b l_1}{m\pi l}[(l_1 l_2+l_2 l_3+l_1 l_3)\cos\frac{m\pi l_2}{l_1}\cos\frac{m\pi l_3}{l_1}\\
&\quad-(\frac{l_1^2}{2}+l_1 l_2+\frac{l_2^2}{2}+l_1 l_3+\frac{l_3^2}{2})\sin\frac{m\pi l_2}{l_1}\sin\frac{m\pi l_3}{l_1}]+\mathcal{O}(m^{-2})\}\\
&+\delta^3\{(-1)^m 36\beta_a[l_1 l_2 l_3\cos\frac{m\pi l_2}{l_1}\cos\frac{m\pi l_3}{l_1}\\
&\quad-(\frac{l_1^3}{6}+\frac{l_1 l_2^2}{2}+\frac{l_1 l_3^2}{2})\sin\frac{m\pi l_2}{l_1}\sin\frac{m\pi l_3}{l_1}]+\mathcal{O}(m^{-1})\}+\mathcal{O}(\delta^4)=0,
\end{aligned}
\tag{4.36}
$$

where

$$
\begin{aligned}
\beta_a &= \cos\gamma(1-t)+1,\\
\beta_b &= \sin\gamma(1-t),\\
\beta_c &= \cos\gamma(1-t)\ \frac{\cos\frac{\pi t}{3}+2}{\cos\frac{\pi t}{3}-1}+2\ \frac{\cos\frac{\pi t}{3}+\frac{1}{2}}{\cos\frac{\pi t}{3}-1},\\
\beta_d &= \cos\gamma(1-t)\ \frac{\cos\frac{\pi t}{3}+3}{\cos\frac{\pi t}{3}-1}+3\ \frac{\cos\frac{\pi t}{3}+\frac{1}{3}}{\cos\frac{\pi t}{3}-1},\\
\beta_e &= 7\ \cos\gamma(1-t)\ \frac{\cos\frac{\pi t}{3}+\frac{5}{7}}{\cos\frac{\pi t}{3}-1}+5\ \frac{\cos\frac{\pi t}{3}+\frac{7}{5}}{\cos\frac{\pi t}{3}-1},\\
\beta_f &= \sqrt{3}\ \sin\gamma(1-t)\ \frac{\sin\frac{\pi t}{3}\ (\cos\frac{\pi t}{3}+1)}{(\cos\frac{\pi t}{3}-1)^2}.
\end{aligned}
\tag{4.37}
$$

In the leading order of the asymptotic regime, if we assume that both $\frac{l_3}{l_1}$ and $\frac{l_2}{l_1}$

are irrational, $\delta$ can be easily obtained from (4.36):

$$\begin{aligned}&\{-(-1)^m\frac{24\beta_b l_1}{m\pi l}\sin\frac{m\pi l_2}{l_1}\sin\frac{m\pi l_3}{l_1}\\&\quad+\frac{(-1)^m l_1^2}{m^2\pi^2 l^2}[\cos\frac{m\pi l_2}{l_1}\sin\frac{m\pi l_3}{l_1}+\sin\frac{m\pi l_2}{l_1}\cos\frac{m\pi l_3}{l_1}][9\beta_d+\beta_e]\\&\quad+\frac{16l_1^2}{m^2\pi^2 l^2}[\sin\frac{m\pi l_2}{l_1}+\sin\frac{m\pi l_3}{l_1}][-\beta_c\cos\theta+\beta_f\sin\theta]\}\\&+\delta\{(-1)^m 36\beta_a l_1\sin\frac{m\pi l_2}{l_1}\sin\frac{m\pi l_3}{l_1}\}=0;\end{aligned}$$

here we have retained only the leading term in $m$ from the part linear in $\delta$. Expression for energy is still given by (3.13), but what is more interesting is the width of the bands. The relevant part of $\delta$ - terms which do not vanish in (3.14), i.e. proportional to $\theta$ - is now given by

$$\delta(\theta)\propto\frac{\frac{16l_1^2}{m^2\pi^2l^2}[\sin\frac{m\pi l_2}{l_1}+\sin\frac{m\pi l_3}{l_1}][\beta_c\cos\theta-\beta_f\sin\theta]}{(-1)^m 36\beta_a l_1\sin\frac{m\pi l_2}{l_1}\sin\frac{m\pi l_3}{l_1}}.$$

When dealing with the case $t=0$, we had spectral condition containing $\cos\theta$ only, so it was easy to determine the points in the Brillouin zone $\langle-\pi,\pi\rangle$ corresponding to the maxima and minima of dispersion curves. This is related to the fact that, in graphs we are considering here, they correspond to the antisymmetric and symmetric solutions, respectively, provided the coupling is time-reversal invariant [EKW10]. For $t\neq 0$ it is not the case, as now there is also $\sin\theta$ term; therefore we must find extrema of $\delta(\theta)$. Differentiating with respect to $\theta$, we have

$$\beta_c\sin\theta+\beta_f\cos\theta=0,$$

and from there

$$-\frac{\beta_f}{\beta_c}=\tan\theta. \tag{4.38}$$

On $\langle-\pi,\pi\rangle$, this equation has indeed two solutions, whose difference is always $\pi$. Further on, we can make use of the property

$$\sin(\theta+\pi)=-\sin\theta,\ \cos(\theta+\pi)=-\cos\theta,$$

meaning that substitution of one of the roots can be simply replaced by a change of sign. Equation (3.14), now with proper values of $\theta$, now gives

$$\Delta E_m=\frac{16}{9m\pi l^2}\left|\frac{(\beta_c\cos\theta_1-\beta_f\sin\theta_1)(\sin\frac{m\pi l_2}{l_1}+\sin\frac{m\pi l_3}{l_1})}{\beta_a\sin\frac{m\pi l_2}{l_1}\sin\frac{m\pi l_3}{l_1}}\right|+\mathcal{O}(m^{-2}), \tag{4.39}$$

where $\theta_1=\arctan(-\frac{\beta_f}{\beta_c})$, and will be denoted as such for the rest of this chapter.

If at least one of the fractions $\frac{l_3}{l_1}$ or $\frac{l_2}{l_1}$ is rational, then there exist some values of $m$, for which either $\sin\frac{m\pi l_2}{l_1}$ or $\sin\frac{m\pi l_3}{l_1}$, and consequently the denominator of (4.39), would be zero. Because all the remaining terms proportional to $\delta$ from (4.36) are at least $\mathcal{O}(m^{-1})$, they would also go to zero with $m\to\infty$, and in contrast to the previous calculation, we must go up to $\delta^2$ terms. When $l_2 \neq l_3$, let us without loss of generality assume that for given $m$ it holds

$$\sin\frac{m\pi l_2}{l_1} = 0,\ \cos\frac{m\pi l_2}{l_1} = (-1)^{m\frac{l_2}{l_1}}$$

and that $\sin\frac{m\pi l_3}{l_1}$ is different from 0; hence

$$\begin{aligned}
&\{\frac{(-1)^m l_1^2}{m^2\pi^2 l^2}[(-1)^{m\frac{l_2}{l_1}}\sin\frac{m\pi l_3}{l_1}][9\beta_d + \beta_e] \\
&\quad + \frac{16 l_1^2}{m^2\pi^2 l^2}\sin\frac{m\pi l_3}{l_1}[-\beta_c\cos\theta + \beta_f\sin\theta]\} \\
&+\delta\{-(-1)^m\frac{24\beta_b l_1}{m\pi l}(l_1+l_2)(-1)^{m\frac{l_2}{l_1}}\sin\frac{m\pi l_3}{l_1} + \mathcal{O}(m^{-2})\} \\
&+\delta^2\{(-1)^m 36\beta_a l_1 l_2 \sin\frac{m\pi l_3}{l_1}(-1)^{m\frac{l_2}{l_1}} + \mathcal{O}(m^{-1})\} = 0.
\end{aligned} \tag{4.40}$$

Two solutions of this quadratic equation eventually result in the same energy band width, so we again display only the relevant part for one of them:

$$\delta(\theta) \propto \sqrt{\left(\frac{\beta_b l_1}{3m\pi\beta_a l}\right)^2\frac{(l_1+l_2)^2}{l_1^2 l_2^2} - \frac{l_1^2[9\beta_d + \beta_e + (-1)^{m(1+\frac{l_2}{l_1})}16(-\beta_c\cos\theta + \beta_f\sin\theta)]}{36 m^2\pi^2 l^2\beta_a l_1 l_2}}. \tag{4.41}$$

Determining sought points in the Brillouin zone is now even harder - not only are we limited by the extrema of the dispersion functions, but in order to get a valid solution, inside of the square root in (4.41) must be non-negative. Let us take a closer look. In the first term, every number present is real and squared, thus it is positive as a whole. The denominator of the second term is also positive. We do not necessarily have information about the sign of

$$(-1)^{m(1+\frac{l_2}{l_1})}(-\beta_c\cos\theta + \beta_f\sin\theta),$$

but because the values in the extremal points of the dispersion function differ only by sign, we have freedom of choice depending on the situation. The sign of the numerator must then be governed by $9\beta_d + \beta_e$. But this quantity is always negative. Looking for its extrema, we have

$$\frac{\partial}{\partial\gamma}(9\beta_d + \beta_e) = \frac{(1-t)\sin\gamma(1-t)}{1-\cos\frac{\pi t}{3}}16(2+\cos\frac{\pi t}{3}) = 0,$$

and, on intervals we now consider, $t = 1$ or $\gamma = 0$ must be true. For $t = 1$,

$$9\beta_d + \beta_e = -144$$

regardless of $\gamma$. The other partial derivative, on the line $\gamma = 0$, reads

$$\frac{\partial}{\partial t}(9\beta_d + \beta_e) = 32\frac{\pi\sin\frac{\pi t}{3}}{(1-\cos\frac{\pi t}{3})^2} = 0,$$

which for $t \neq 0$ does not have a solution. As such there are no local extrema, and quick check in the endpoints of $t$ and $\gamma$ (possibly in limit) confirms that $-144$ is in fact the maximal value.

Due to this reasoning, (4.41) has always at least one real solution. If there are two, band width is determined from their difference; if there is only one, band width is proportional to it (the inside of (4.41) is an analytic function of Bloch parameter $\theta$, and there must exist a $\theta$ for which it is equal to 0, marking the second edge of this spectral band). Nevertheless, both options have from (4.41)

$$\delta(\theta) \propto \frac{1}{m}$$

ergo, according to (3.14),

$$\Delta E_m = \text{const.} + \mathcal{O}(m^{-1})$$

in the leading order, proportional specifically to $l_1$, $l_2$, and functions $\beta$. Under the other set of assumptions, $l_2$ would be switched for $l_3$.

There are possible combination of lengths where for certain $m$ both $\sin\frac{m\pi l_2}{l_1}$ and $\sin\frac{m\pi l_3}{l_1}$ are equal to 0. If for example

$$\begin{aligned} &\frac{m\pi l_3}{l_1} = m^{'}\pi,\ m, m^{'} \in \mathbb{N} \\ \Longrightarrow &\frac{m\pi l_2}{l_1} = \frac{m\pi(2\pi - l_3)}{l_1} = \frac{2m\pi^2}{l_1} - m^{'}\pi, \end{aligned}$$

and this can happen if $l_1$ is a rational multiple of $\pi$ (note that, parity-wise, both numbers are the same). It is also trivially true for the symmetric quantum chain. In those cases we consider terms up to $\delta^3$ from Equation (4.36), solving

$$\begin{aligned} &\delta\{\frac{(-1)^m l_1^2}{m^2\pi^2 l^2}(l_1 + l_2 + l_3)(9\beta_d + \beta_e) \\ &\quad - \frac{(-1)^m 16 l_1^2}{m^2\pi^2 l^2} l_1\beta_c \\ &\quad + \frac{(-1)^{m\frac{l_2}{l_1}} 16 l_1^2}{m^2\pi^2 l^2}(l_2 + l_3)(-\beta_c \cos\theta + \beta_f \sin\theta)\} \\ &-\delta^2\{(-1)^m \frac{24\beta_b l_1}{m\pi l}(l_1 l_2 + l_2 l_3 + l_1 l_3)\} \\ &+\delta^3\{(-1)^m 36\beta_a l_1 l_2 l_3\} = 0. \end{aligned}$$

In the next step, we make use of

$$-16\beta_c + 9\beta_d + \beta_e = 0,$$

and after that

$$\begin{aligned} \delta(\theta) \propto &\left\{\left(\frac{\beta_b l_1}{3m\pi\beta_a l}\right)^2 \frac{(l_1 l_2 + l_2 l_3 + l_1 l_3)^2}{l_1^2 l_2^2 l_3^2}\right. \\ &\left. - \frac{l_1^2(l_2 + l_3)[9\beta_d + \beta_e + (-1)^{m(1+\frac{l_2}{l_1})} 16(-\beta_c \cos\theta + \beta_f \sin\theta)]}{36 m^2\pi^2 l^2 \beta_a l_1 l_2 l_3}\right\}^{\frac{1}{2}}. \end{aligned} \tag{4.42}$$

Using the same arguments as earlier, we arrive at the conclusion that

$$\Delta E_m = \text{const.} + \mathcal{O}(m^{-1})$$

in the leading order, now proportional to $l_1$, $l_2$, $l_3$ and $\beta$.

If $k$ is close to the point $\frac{m\pi}{l_1}$, then:

- If both ratios $\frac{l_3}{l_1}$ and $\frac{l_2}{l_1}$ are irrational, width of the spectral band has asymptotic behaviour $\mathcal{O}(m^{-1})$, or rather $\mathcal{O}(k^{-1})$, as $k \to \infty$.
- If $\frac{l_2}{l_1}$ or $\frac{l_3}{l_1}$ is rational, there are periodically distributed bands with asymptotically constant widths, their specific limits depending on concrete values of $t$, $\gamma$, $l$, $l_1$ and $l_2$ or $l_3$, respectively. Otherwise the $\mathcal{O}(k^{-1})$ asymptotic above applies to them as well.

When we choose $l_j = l_3$, special cases of the expansion around $\frac{m\pi}{l_3}$ are the same as (4.35), only with roles of $l_3$ and $l_1$ interchanged. Substitution into (4.34) gives

$$\begin{aligned}
&\{-(-1)^m\frac{24\beta_b l_3}{m\pi l}\sin\frac{m\pi l_1}{l_3}\sin\frac{m\pi l_2}{l_3}\\
&-\frac{(-1)^m 16 l_3^2}{m^2\pi^2 l^2}\beta_c\sin\frac{m\pi l_1}{l_3}\\
&+\frac{(-1)^m l_3^2}{m^2\pi^2 l^2}[\cos\frac{m\pi l_2}{l_3}\sin\frac{m\pi l_1}{l_3}+\sin\frac{m\pi l_2}{l_3}\cos\frac{m\pi l_1}{l_3}][9\beta_d+\beta_e]\\
&+\frac{16 l_3^2}{m^2\pi^2 l^2}\sin\frac{m\pi l_2}{l_3}[-\beta_c\cos\theta+\beta_f\sin\theta]\}\\
+\delta&\{(-1)^m l_3\sin\frac{m\pi l_2}{l_3}\sin\frac{m\pi l_1}{l_3}[36\beta_a+\frac{3l_3^2}{m^2\pi^2 l^2}(-3\beta_d+\beta_e)]\\
&-(-1)^m\frac{24\beta_b l_3}{m\pi l}[(l_1+l_3)\sin\frac{m\pi l_2}{l_3}\cos\frac{m\pi l_1}{l_3}+(l_2+l_3)\cos\frac{m\pi l_2}{l_3}\sin\frac{m\pi l_1}{l_3}]\\
&+\frac{(-1)^m l_3^2}{m^2\pi^2 l^2}[(l_1+l_2+l_3)\cos\frac{m\pi l_2}{l_3}\cos\frac{m\pi l_1}{l_3}-(l_1+l_2)\sin\frac{m\pi l_2}{l_3}\sin\frac{m\pi l_1}{l_3}]\\
&(9\beta_d+\beta_e)\\
&-\frac{16 l_3^2}{m^2\pi^2 l^2}l_1\beta_c\cos\frac{m\pi l_1}{l_3}\\
&+\frac{16 l_3^2}{m^2\pi^2 l^2}[l_2\cos\frac{m\pi l_2}{l_3}+(-1)^m l_3][-\beta_c\cos\theta+\beta_f\sin\theta]\}\\
+\delta^2&\{(-1)^m 36\beta_a(l_1 l_3\sin\frac{m\pi l_2}{l_3}\cos\frac{m\pi l_1}{l_3}+l_2 l_3\sin\frac{m\pi l_1}{l_3}\cos\frac{m\pi l_2}{l_3})\\
&-(-1)^m\frac{24\beta_b l_3}{m\pi l}[(l_1 l_2+l_2 l_3+l_1 l_3)\cos\frac{m\pi l_2}{l_3}\cos\frac{m\pi l_1}{l_3}\\
&-(\frac{l_1^2}{2}+l_1 l_3+\frac{l_2^2}{2}+l_2 l_3+\frac{l_3^2}{2})\sin\frac{m\pi l_2}{l_3}\sin\frac{m\pi l_1}{l_3}]+\mathcal{O}(m^{-2})\}\\
+\delta^3&\{(-1)^m 36\beta_a[l_1 l_2 l_3\cos\frac{m\pi l_2}{l_3}\cos\frac{m\pi l_1}{l_3}\\
&-(\frac{l_3^3}{6}+\frac{l_3 l_2^2}{2}+\frac{l_3 l_1^2}{2})\sin\frac{m\pi l_2}{l_3}\sin\frac{m\pi l_1}{l_3}]+\mathcal{O}(m^{-1})\}+\mathcal{O}(\delta^4)=0,
\end{aligned} \tag{4.43}$$

we similarly express $\delta$ in the first approximation and get

$$\Delta E_m = \frac{16}{9m\pi l^2}\left|\frac{(\beta_c\cos\theta_1-\beta_f\sin\theta_1)}{\beta_a\sin\frac{m\pi l_1}{l_3}}\right| + \mathcal{O}(m^{-2}), \tag{4.44}$$

for both $\frac{l_1}{l_3}$ and $\frac{l_2}{l_3}$ irrational.

Because the leading term (with respect to $m$) proportional to $\delta^2$ is exactly the same as in (4.40), except for $l_1$ and $l_3$ interchanged, $\delta(\theta)$ proportionality is nearly identical to (4.41) and we get

$$\Delta E_m = \text{const.} + \mathcal{O}(m^{-1})$$

in the leading order for some $m$ when $\frac{l_1}{l_3}$ is rational and we assume $\sin\frac{m\pi l_2}{l_3}$ different from 0. As we would expect, our results remain unchanged.

If $\frac{l_2}{l_3}$ is rational, there exist some $m$ for which functions of Bloch parameter $\theta$ necessarily vanish in term constant in $\delta$ from (4.43). Assuming $\sin\frac{m\pi l_1}{l_3}$ different from 0, solutions for $\delta$ now depend on parity - because

$$m\frac{l_2}{l_3} = m\frac{2\pi - l_3}{l_3} = 2\frac{m\pi}{l_3} - m = m^{'} \in \mathbb{N},$$

for even $m$ we have $m\frac{l_2}{l_3}$ also even and vice versa.

Therefore for odd $m$

$$\begin{aligned}
&\{\frac{l_3^2}{m^2\pi^2 l^2}\sin\frac{m\pi l_1}{l_3}(16\beta_c + 9\beta_d + \beta_e)\} \\
+\delta\{&-\frac{24\beta_b l_3}{m\pi l}(l_2+l_3)\sin\frac{m\pi l_1}{l_3} \\
&+\frac{l_3^2}{m^2\pi^2 l^2}(l_2+l_3)\cos\frac{m\pi l_1}{l_3}(9\beta_d+\beta_e) \\
&+\frac{16 l_3^2}{m^2\pi^2 l^2}(l_2+l_3)(\beta_c\cos\theta - \beta_f\sin\theta)\} \\
+\delta^2\{&36\beta_a l_2 l_3\sin\frac{m\pi l_1}{l_3}\} = 0.
\end{aligned}$$

When solving a given quadratic equation for $\delta$, $\theta$ functions inside the discriminant are at least, depending on the values of $\beta$, of the order $\mathcal{O}(m^{-3})$, while outside of it they have an $\mathcal{O}(m^{-2})$ behaviour. For $m$ large enough, we could modify the discriminant through

$$\frac{l_3}{m\pi l}\sqrt{1 - \frac{l_3\,x(\theta)}{m\pi l}} \approx \frac{l_3}{m\pi l}\left(1 - \frac{1}{2}\frac{l_3\,x(\theta)}{m\pi l}\right),$$

but the relevant part of $\delta(\theta)$ will always be $\mathcal{O}(m^{-2})$ at the minimum. That is why

$$\Delta E_m = \mathcal{O}(m^{-1})$$

in the leading order, considering that we work in the limit $m \to \infty$ and parts of $\delta$ not proportional to $\theta$ will cancel out when computing band width.

For even $m$, we solve

$$\begin{aligned}
+\delta\{&-\frac{24\beta_b l_3}{m\pi l}(l_2+l_3)\sin\frac{m\pi l_1}{l_3} \\
&+\frac{l_3^2}{m^2\pi^2 l^2}(l_2+l_3)(9\beta_d+\beta_e)\cos\frac{m\pi l_1}{l_3} \\
&+\frac{16 l_3^2}{m^2\pi^2 l^2}(l_2+l_3)(-\beta_c\cos\theta + \beta_f\sin\theta)\} \\
+\delta^2\{&36\beta_a l_2 l_3\sin\frac{m\pi l_1}{l_3}\} = 0,
\end{aligned}$$

and using the same method we eventually arrive at

$$\Delta E_m = \frac{16}{9m\pi l^2}\left|\frac{(\beta_c \cos\theta_1 - \beta_f \sin\theta_1)(l_2+l_3)}{\beta_a l_2 \sin\frac{m\pi l_1}{l_3}}\right| + \mathcal{O}(m^{-2}),$$
$$= \frac{32}{9ml^2 l_2}\left|\frac{(\beta_c \cos\theta_1 - \beta_f \sin\theta_1)}{\beta_a \sin\frac{m\pi l_1}{l_3}}\right| + \mathcal{O}(m^{-2}).$$

Finally if both $\frac{l_1}{l_3}$ and $\frac{l_2}{l_3}$ are rational, there are some $m$ for which

$$\sin\frac{m\pi l_1}{l_3} = \sin\frac{m\pi l_2}{l_3} = 0.$$

We solve

$$\begin{aligned}
&\delta\{(-1)^{m\frac{l_1}{l_3}}\frac{l_3^2}{m^2\pi^2 l^2}(l_2+l_3)(9\beta_d+\beta_e) \\
&\quad + (-1)^m \frac{16 l_3^2}{m^2\pi^2 l^2}(l_2+l_3)(-\beta_c \mathrm{cos}\theta + \beta_f \mathrm{sin}\theta)\} \\
&+\delta^2\{-(-1)^{m\frac{l_1}{l_3}}\frac{24\beta_b l_3}{m\pi l}(l_1 l_2 + l_2 l_3 + l_1 l_3)\} \\
&+\delta^3\{(-1)^{m\frac{l_1}{l_3}} 36\beta_a l_1 l_2 l_3\} = 0,
\end{aligned}$$

and from there, having $\delta(\theta)$ with very similar structure to (4.42),

$$\Delta E_m = \text{const.} + \mathcal{O}(m^{-1})$$

in the leading order.

- The asymptotic remains the same as before near the points $k = \frac{m\pi}{l_3}$ - always $\mathcal{O}(m^{-1})$ for $\frac{l_2}{l_3}$ and $\frac{l_1}{l_3}$ irrational, sometimes constant when $\frac{l_2}{l_3}$ or $\frac{l_1}{l_3}$ is rational.

- Analogous statement is true even if we are near points $k = \frac{m\pi}{l_2}$.

Spectral band widths are then maximally of the order $\mathcal{O}(m^0) = \mathcal{O}(1)$ with respect to the power of $m$, otherwise they shrink. From its definition (3.14),

$$\begin{aligned}
\Delta E_m &= |{k_{m,j}}^2(0) - {k_{m,j}}^2(\pi)|, \\
&= |[k_{m,j}(0) + k_{m,j}(\pi)][k_{m,j}(0) - k_{m,j}(\pi)]|, \\
&\approx 2\frac{m\pi}{l_j}|k_{m,j}(0) - k_{m,j}(\pi)|,
\end{aligned}$$

or with the extremum points in the Brillouin zone. In order to stay asymptotically constant at the energy scale, $|k_{m,j}(0) - k_{m,j}(\pi)|$ must behave (at least) as $\mathcal{O}(m^{-1})$. Intervals belonging to the spectrum in momentum scale $k$ are then smaller and smaller, and because our high energy asymptotic is a combination of three periodic functions, the number of those intervals is surely countable. In the language of probability (4.29),

$$P_\sigma(H) = 0.$$

*Example* 4.5. Consider quantum chain with $t = 0.5$, $\gamma = 1$, $l = 1$, $l_1 = 2$ and $l_3 = \frac{\pi}{2}$. Spectral bands can appear only around points $k = \frac{m\pi}{l_j}$, $j = 1, 2, 3$. This on displayed interval $k \in \langle 10, 13\rangle$ in Figure 4.15 matches to points {10,12} (from $l_3$), $\{10, \frac{32}{3} \approx 10.67, \frac{34}{3} \approx 11.33, 12, \frac{38}{3} \approx 12.67\}$ (from $l_2$) and $\{\frac{7\pi}{2} \approx 11, 4\pi \approx 12.57\}$ (from $l_1$). Each of those points is accompanied by a peak in spectral condition function, and by spectral band, groups of which may merge if their respective points are sufficiently close. For higher energies, these bands become smaller and overshadowed by spectral gaps.

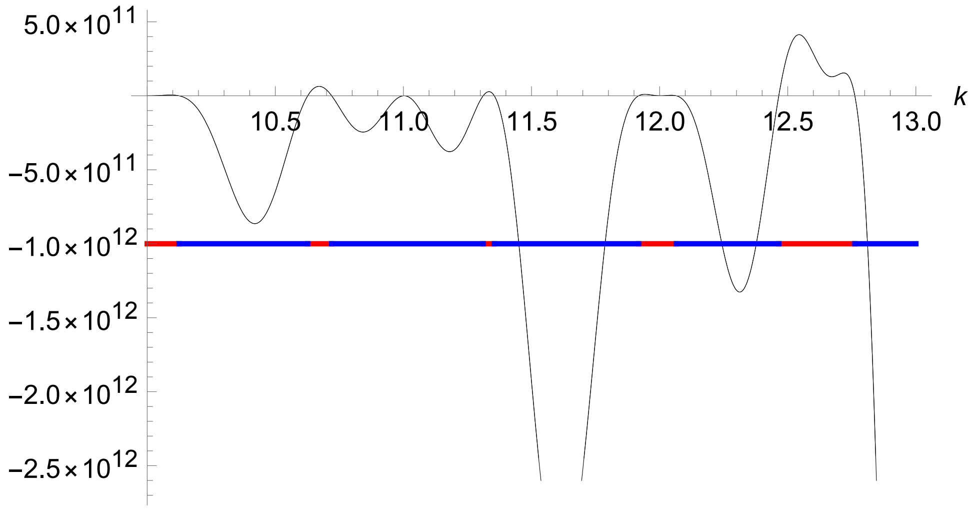


Figure 4.15: Evaluation of spectral condition with parameters set in Example 4.5. Spectral bands are coloured red, while spectral gaps are blue.

### Low energy limit

Analogously to the $t = 0$ case, when we expand trigonometric functions of $k$ around $k = 0$, there is at least $\delta^3$ proportionality in the equation (4.9) for some small $\delta$. While here we must operate with condition (4.15), individual $v$ are just functions of $P$, and when squared, their leading terms will be squares of leading terms from polynomials $P$.

We are effectively solving the equation

$$\delta^3 P_3 + \delta^2 P_2 + \delta P_1 + P_0 + \delta^2 (P_s \sin\theta + P_c \cos\theta) = \mathcal{O}(\delta^4)$$

where now

$$\begin{aligned}
&P_3 \approx -64l^3\beta_g,\\
&P_2 \approx \delta l^2[-16l_1\beta_h + (l_1+l_2+l_3)(9\beta_k+\beta_l)] = \delta l^2(l_2+l_3)(9\beta_k+\beta_l),\\
&P_1 \approx -24\delta^2 l(l_2l_3 + l_1l_2 + l_1l_3)\beta_b,\\
&P_0 \approx 36\delta^3 l_1l_2l_3\beta_o,\\
&P_s \approx 16\delta l^2(l_2+l_3)\beta_p,\\
&P_c \approx 16\delta l^2[(l_2+l_3)\beta_h + 4l\beta_g],
\end{aligned} \tag{4.45}$$

with

$$
\begin{aligned}
\beta_g &= \sin\gamma(1-t)\,\frac{\cos\frac{\pi t}{3}-1}{\cos\frac{\pi t}{3}+1},\\
\beta_h &= \cos\gamma(1-t)\,\frac{\cos\frac{\pi t}{3}-2}{\cos\frac{\pi t}{3}+1}-2\,\frac{\cos\frac{\pi t}{3}-\frac{1}{2}}{\cos\frac{\pi t}{3}+1},\\
\beta_k &= \cos\gamma(1-t)\,\frac{\cos\frac{\pi t}{3}-3}{\cos\frac{\pi t}{3}+1}-3\,\frac{\cos\frac{\pi t}{3}-\frac{1}{3}}{\cos\frac{\pi t}{3}+1},\\
\beta_l &= 7\,\cos\gamma(1-t)\,\frac{\cos\frac{\pi t}{3}-\frac{5}{7}}{\cos\frac{\pi t}{3}+1}-5\,\frac{\cos\frac{\pi t}{3}-\frac{7}{5}}{\cos\frac{\pi t}{3}+1},\\
\beta_o &= \cos\gamma(1-t)-1,\\
\beta_p &= \sqrt{3}\,\sin\gamma(1-t)\,\frac{\sin\frac{\pi t}{3}\,(\cos\frac{\pi t}{3}-1)}{(\cos\frac{\pi t}{3}+1)^2}.
\end{aligned}
\tag{4.46}
$$

Substituting (4.45) into (4.15), while other polynomials are in our approximation nearly 0, gives us the final condition

$$
\begin{aligned}
&\{64l^3\beta_g - l^2(l_2+l_3)(9\beta_k+\beta_l)\\
&+24l(l_2l_3+l_1l_2+l_1l_3)\beta_b - 36l_1l_2l_3\beta_o\}^2\\
&\le 256l^4\{(l_2+l_3)^2\beta_p^2 + [(l_2+l_3)\beta_h + 4l\beta_g]^2\}.
\end{aligned}
\tag{4.47}
$$

Several of the $\beta$'s contain $\cos\gamma(1-t)$ term non-trivially intertwined with functions of $t$. This does not allow simplifications we have seen earlier with $t = 0$, and for this reason, we will not discuss it further.

**Negative spectrum**

Once again we are interested in two particular characteristics concerning the negative spectrum: the number of spectral bands, and whether the lowest one, if present, is connected to $k^2 = 0$. The work for the second answer was done in the previous section - in the used approximation $\cos x$ gives the same expression as $\cosh x$, similarly with $\sin x$ and $\sinh x$; while individual terms in $v_z$ change sign, it changes for each of them, and $v_z^2$ is unaffected; similarly for $v_c$ and $v_s$. Hence for all $t < 1$ the negative spectrum is connected only if the same is true for the positive one.

Regarding the number of negative spectral bands, our elementary cell has two vertices of degree three with eigenvalues (4.2). Their imaginary parts are, in order,

$$
\begin{aligned}
&-\sin\gamma(1-t),\\
&-\sin\pi t(\frac{2}{3}-1) = \sin\frac{\pi t}{3},\\
&-\sin\pi t(\frac{4}{3}-1) = -\sin\frac{\pi t}{3}.
\end{aligned}
$$

Sign of $\gamma(1-t)$ is determined by $\gamma$, $\pi t$ is always positive. According to Theorem 3.1, for negative $\gamma$ there might be at most four distinct negative spectral bands, one for the first and one for the second eigenvalue, per vertex, while non-negative $\gamma$ allows maximally two of them, each stemming from the second eigenvalue.

In the limit $t \to 0_+$, the maximal number of bands must necessarily decrease (to two for negative $\gamma$ or zero if $\gamma \ge 0$). Therefore, if for $t > 0$ the number of bands exceeds the indicated limit, they could either become thinner until they eventually vanish, or they might merge.

**Limit** $l_1 \to 0$

The presence of flat bands or behaviour around $k^2 = 0$ is undisturbed when we move to the quantum chain with vertices of degree four. On the other hand, the high energy spectrum is different in both possible limits $l_1 \to 0$ and $l_3 \to 0$, if only because $P_6 = 0$ in each of them.

Starting with $l_1 = 0$, (4.34) now reads

$$\frac{P_5}{l^5} + \frac{P_4}{kl^5} + \frac{P_c \cos\theta + P_s \sin\theta}{k^3 l^5} = \mathcal{O}(k^{-2}), \tag{4.48}$$

$$\begin{aligned} P_5 &= -24 l^5 \beta_b \sin kl_2 \, \sin kl_3, \\ P_4 &= 2l^4 (9\beta_d + \beta_e) \sin k\pi \, \cos k\pi, \\ P_c &\approx -16 k^2 l^4 \beta_c (\sin kl_2 + \sin kl_3), \\ P_s &\approx 16 k^2 l^4 \beta_f (\sin kl_2 + \sin kl_3). \end{aligned}$$

Bands are formed only around $k = \frac{m\pi}{l_2}$ or $k = \frac{m\pi}{l_3}$. Again, without loss of generality, we choose $\frac{m\pi}{l_3}$ and express trigonometric functions in $\delta$ neighbourhoods of those points as

$$\begin{aligned} \sin\, kl_2 &= (1 - \frac{\delta^2 l_2^2}{2}) \sin\frac{m\pi l_2}{l_3} + \delta l_2 \, \cos\frac{m\pi l_2}{l_3} + \mathcal{O}(\delta^{-3}), \\ \sin\, kl_3 &= (-1)^m \delta l_3 + \mathcal{O}(\delta^{-3}), \\ \sin\, k\pi &= (1 - \frac{\delta^2 \pi^2}{2}) \sin\frac{m\pi^2}{l_3} + \delta\pi \, \cos\frac{m\pi^2}{l_3} + \mathcal{O}(\delta^{-3}), \\ \cos\, k\pi &= (1 - \frac{\delta^2 \pi^2}{2}) \cos\frac{m\pi^2}{l_3} - \delta\pi \, \sin\frac{m\pi^2}{l_3} + \mathcal{O}(\delta^{-3}), \end{aligned}$$

Equation (4.48) is explicitly written as

$$\begin{aligned} &\{2\frac{l_3}{m\pi l}(9\beta_d + \beta_e)\cos\frac{m\pi^2}{l_3}\sin\frac{m\pi^2}{l_3} + 16\frac{l_3}{m\pi l}(-\beta_c\cos\theta + \beta_f \sin\theta)\sin\frac{m\pi l_2}{l_3}\} \\ &\delta\{-(-1)^m 24\beta_b l_3 \sin\frac{m\pi l_2}{l_3} + 2\frac{l_3}{m\pi l}\pi(9\beta_d + \beta_e)(\cos^2\frac{m\pi^2}{l_3} - \sin^2\frac{m\pi^2}{l_3}) \\ &\quad + 16\frac{l_3}{m\pi l}(l_2 \cos\frac{m\pi l_2}{l_3} + (-1)^m l_3)(-\beta_c \cos\theta + \beta_f \sin\theta)\} \\ &\delta^2\{-(-1)^m 24\beta_b l_2 l_3 \cos\frac{m\pi l_2}{l_3} + \mathcal{O}(m^{-1})\} = 0. \end{aligned}$$

If $\frac{l_2}{l_3}$ is irrational, we can express

$$\delta(\theta) = \frac{2\frac{l_3}{m\pi l}(9\beta_d + \beta_e)\cos\frac{m\pi^2}{l_3}\sin\frac{m\pi^2}{l_3} + 16\frac{l_3}{m\pi l}(-\beta_c\cos\theta + \beta_f\sin\theta)\sin\frac{m\pi l_2}{l_3}}{(-1)^m 24\beta_b l_3 \sin\frac{m\pi l_2}{l_3}}$$

and from (3.14)

$$\Delta E_m = \frac{8}{3ll_3}\left|\frac{-\beta_c\cos\theta_1 + \beta_f \sin\theta_1}{\beta_b}\right| + \mathcal{O}(m^{-1}).$$

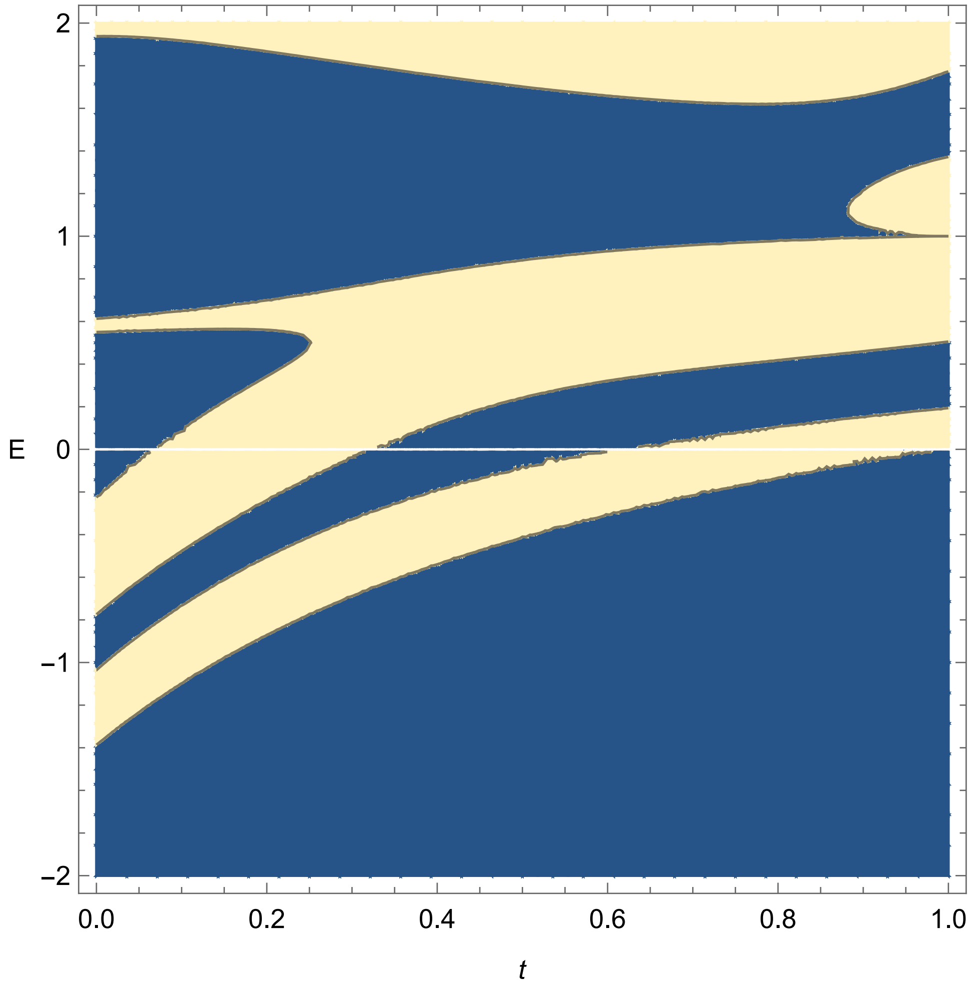


Figure 4.16: Evaluation of spectral condition around small values of $E = k^2$ and its dependence on $t$ with $l = 1$, $l_1 = 2$, $l_3 = \frac{\pi}{2}$ and $\gamma = -\frac{\pi}{2}$. Spectral bands are indicated by light colour, while spectral gaps are dark.

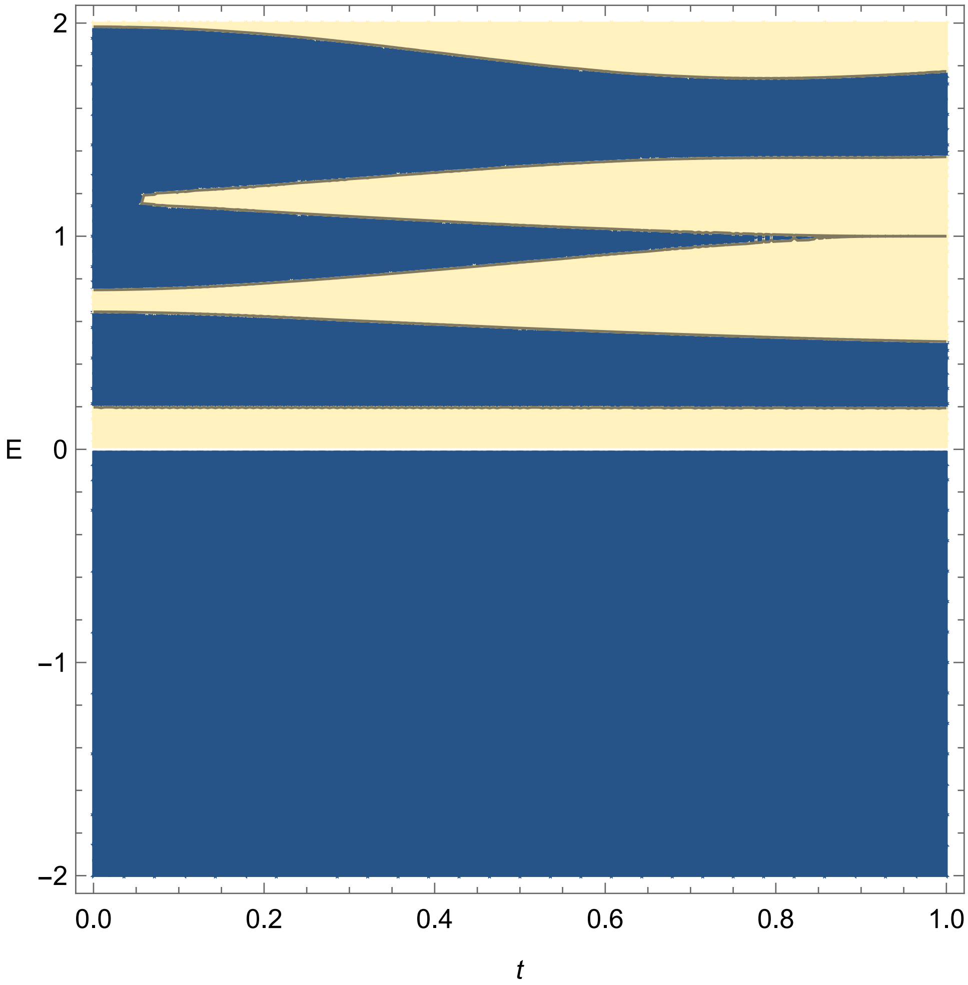


Figure 4.17: Evaluation of spectral condition around small values of $E = k^2$ and its dependence on $t$ with $l = 1$, $l_1 = 2$, $l_3 = \frac{\pi}{2}$ and $\gamma = 0$. Spectral bands are indicated by light colour, while spectral gaps are dark.

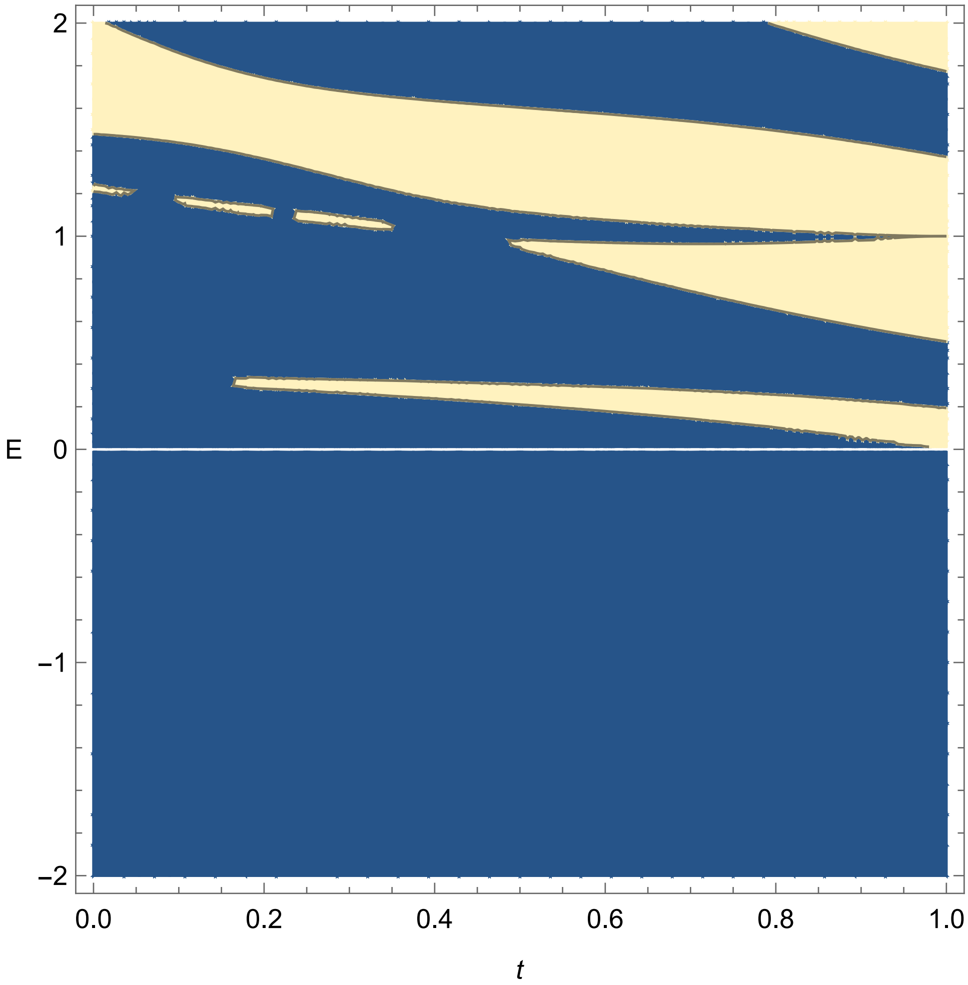


Figure 4.18: Evaluation of spectral condition around small values of $E = k^2$ and its dependence on $t$ with $l = 1$, $l_1 = 2$, $l_3 = \frac{\pi}{2}$ and $\gamma = \frac{\pi}{2}$. Spectral bands are indicated by light colour, while spectral gaps are dark.

If $\frac{l_2}{l_3}$ is rational, then if for some $m$ is $\sin\frac{m\pi l_2}{l_3} = 0$, we recall that

$$\begin{aligned}\frac{ml_2}{l_3} &= m\frac{2\pi - l_3}{l_3} = \frac{2m\pi}{l_3} - m = m^{'} \in \mathbb{N} \\ \implies \frac{m\pi}{l_3} &= \frac{m + m^{'}}{2} \in \mathbb{N},\end{aligned}$$

where we utilized the fact that $m$ and $m^{'}$ have the same parity. Because of that, we solve

$$\begin{aligned}&\delta\{2\frac{l_3}{m\pi l}\pi(9\beta_d + \beta_e) + (-1)^m 16\frac{l_3}{m\pi l}(l_2 + l_3)(-\beta_c\cos\theta + \beta_f\sin\theta)\} \\ &\delta^2\{-24\beta_b l_2 l_3 + \mathcal{O}(m^{-1})\} = 0.\end{aligned}$$

$\delta$ is easily obtained:

$$\delta(\theta) = \frac{2\frac{l_3}{m\pi l}\pi(9\beta_d + \beta_e) + (-1)^m 16\frac{l_3}{m\pi l}(l_2 + l_3)(-\beta_c\cos\theta + \beta_f\sin\theta)}{24\beta_b l_2 l_3}$$

and finally

$$\Delta E_m = \frac{8(l_2 + l_3)}{3ll_2l_3}\left|\frac{-\beta_c\cos\theta_1 + \beta_f\sin\theta_1}{\beta_b}\right| + \mathcal{O}(m^{-1}).$$

- In the limit $l_1 \to 0$, the positive spectrum has only asymptotically constant bands at the energy scale.

In the momentum scale, these spectral bands must behave as $\mathcal{O}(k^{-1})$. Therefore

$$P_\sigma(H) = 0.$$

The last remaining question for this part is the number of negative spectral bands. Imaginary parts of $U(t)$ eigenvalues are now

$$\begin{aligned}&-\sin\gamma(1-t), \\ &-\sin\pi t(\frac{2}{4} - 1) = \sin\frac{\pi t}{2}, \\ &-\sin\pi t(\frac{4}{4} - 1) = 0, \\ &-\sin\pi t(\frac{6}{4} - 1) = -\sin\frac{\pi t}{2}.\end{aligned}$$

Through Theorem 3.1, for negative $\gamma$ there are at most two negative spectral bands, while for non-negative, this number decreases to one.

**Limit** $l_3 \to 0$

For $l_3 \to 0$, the structure of the given asymptotic equation remains the same as (4.48), but now with

$$\begin{aligned}P_5 &= -24l^5\beta_b\sin kl_1\, 2\,\sin k\pi\,\cos k\pi, \\ P_4 &= -16l^4\beta_c\sin kl_1 + l^4(9\beta_d + \beta_e)\sin k(l_1 + 2\pi) \\ &= l^4\sin kl_1(-16\beta_c + 9\beta_d + \beta_e) + 2l^4(9\beta_d + \beta_e)\,\sin k\pi\,\cos k(l_1 + \pi) \\ &= 2l^4(9\beta_d + \beta_e)\,\sin k\pi\,(\cos kl_1\,\cos k\pi - \sin kl_1\,\sin k\pi), \\ P_c &\approx -16k^2l^4\beta_c 2\,\sin k\pi\,\cos k\pi, \\ P_s &\approx 16k^2l^4\beta_f 2\,\sin k\pi\,\cos k\pi.\end{aligned}$$

As always, the appearance of the spectral bands is determined by the polynomial next to the highest order of $k$ (now $P_5$), which gives us three options - $k = \frac{m\pi}{l_1}$, $k = m$ and $k = \frac{(2m-1)}{2}$. In all of them, we can factor out $2\sin k\pi$ and focus only on the remaining trigonometric functions.

Around $\frac{m\pi}{l_1}$, spectral condition (4.48) reads

$$
\begin{aligned}
&\{(-1)^m \frac{l_1}{m\pi l}(9\beta_d+\beta_e)\cos\frac{m\pi^2}{l_1} + 16\frac{l_1}{m\pi l}(-\beta_c\cos\theta+\beta_f\sin\theta)\cos\frac{m\pi^2}{l_1}\}\\
&\delta\{-(-1)^m 24\beta_b l_1 \cos\frac{m\pi^2}{l_1} - (-1)^m\frac{l_1}{m\pi l}(l_1+\pi)(9\beta_d+\beta_e)\sin\frac{m\pi^2}{l_1}\\
&\quad - 16\frac{l_1}{m\pi l}\pi\sin\frac{m\pi^2}{l_1}(-\beta_c\cos\theta+\beta_f\sin\theta)\}\\
&\delta^2\{(-1)^m 24\beta_b l_1\pi \sin\frac{m\pi^2}{l_1} + \mathcal{O}(m^{-1})\} = 0.
\end{aligned}
$$

Therefore for $l_1$ incommensurable with $l_2$,

$$
\delta(\theta) \propto \frac{2}{3}\frac{1}{m\pi l}\frac{(-1)^m(-\beta_c\cos\theta+\beta_f\sin\theta)}{\beta_b}
$$

and

$$
\Delta E_m = \frac{8}{3}\frac{1}{l\,l_1}\left|\frac{-\beta_c\cos\theta_1+\beta_f\sin\theta_1}{\beta_b}\right| + \mathcal{O}(m^{-1}),
$$

while if $l_1$ is a rational multiple of $\pi$,

$$
\cos\frac{m\pi^2}{l_1} = 0,\ \sin\frac{m\pi^2}{l_1} = \pm 1,
$$

and we get exactly the same result, only obtained from higher orders of $\gamma$.

If $k = m$, the spectral condition is

$$
\begin{aligned}
&\{-(-1)^m 24\beta_b\sin ml_1 + (-1)^m\frac{1}{ml}(9\beta_d+\beta_e)\cos ml_1\\
&\quad + (-1)^m 16\frac{1}{ml}(-\beta_c\cos\theta+\beta_f\sin\theta)\}\\
&\delta\{-(-1)^m 24\beta_b l_1\cos ml_1 - (-1)^m\frac{1}{ml}(l_1+\pi)(9\beta_d+\beta_e)\sin ml_1\}\\
&\delta^2\{(-1)^m 24\beta_b(\frac{l_1^2}{2}+\frac{\pi^2}{2})\sin ml_1 + \mathcal{O}(m^{-1})\} = 0,
\end{aligned}
$$

then, generally,

$$
\delta(\theta) \propto \frac{2}{3}\frac{1}{m\,l_1\,l\cos ml_1}\frac{(-1)^m(-\beta_c\cos\theta+\beta_f\sin\theta)}{\beta_b},
$$

$$
\Delta E_m = \frac{8}{3}\frac{1}{l\,l_1}\left|\frac{-\beta_c\cos\theta_1+\beta_f\sin\theta_1}{\beta_b\cos ml_1}\right| + \mathcal{O}(m^{-1}).
$$

On the other hand, if $\cos ml_1 = 0$, we must solve the quadratic equation for $\delta$. Functions of Bloch parameter $\theta$ are again inside the discriminant, which reads

$$
\left(\frac{\frac{1}{ml}(l_1+\pi)(9\beta_d+\beta_e)}{48\beta_b(\frac{l_1^2}{2}+\frac{\pi^2}{2})}\right)^2 + \frac{24\beta_b - 16\frac{1}{ml\sin ml_1}(-\beta_c\cos\theta+\beta_f\sin\theta)}{24\beta_b(\frac{l_1^2}{2}+\frac{\pi^2}{2})}.
$$

The first term is of the order $\mathcal{O}(m^{-2})$, and is small in comparison with the second term in the high energy limit. Ergo,

$$\begin{aligned}\delta(\theta) &\propto \frac{1}{(\frac{l_1^2}{2}+\frac{\pi^2}{2})^{\frac{1}{2}}}\sqrt{1-\frac{2}{3}\frac{1}{ml\sin ml_1}\frac{-\beta_c\cos\theta+\beta_f\sin\theta}{\beta_b}} \\ &\approx \frac{1}{(\frac{l_1^2}{2}+\frac{\pi^2}{2})^{\frac{1}{2}}}\left(1-\frac{1}{3}\frac{1}{ml\sin ml_1}\frac{-\beta_c\cos\theta+\beta_f\sin\theta}{\beta_b}\right),\end{aligned}$$

and from there ($\sin\, ml_1$ must be equal to $\pm 1$)

$$\Delta E_m = \frac{4}{3\,l}\frac{1}{(\frac{l_1^2}{2}+\frac{\pi^2}{2})^{\frac{1}{2}}}\left|\frac{-\beta_c\cos\theta_1+\beta_f\sin\theta_1}{\beta_b}\right| + \mathcal{O}(m^{-1}).$$

Finally, if $k = \frac{(2m-1)}{2}$, we start from

$$\begin{aligned}&\{-(-1)^m\frac{1}{kl}(9\beta_d+\beta_e)\sin kl_1\} \\ &\delta\{(-1)^m 24\beta_b\pi\sin kl_1-(-1)^m\frac{1}{kl}(l_1+\pi)(9\beta_d+\beta_e)\cos kl_1 \\ &\quad+(-1)^m\frac{16}{kl}\pi(-\beta_c\cos\theta+\beta_f\sin\theta)\} \\ &\delta^2\{(-1)^m 24\beta_b l_1\pi\cos kl_1+\mathcal{O}(m^{-1})\}=0.\end{aligned}$$

In the first approximation, we express

$$\delta \approx \frac{\frac{1}{kl}(9\beta_d+\beta_e)\sin kl_1}{24\beta_b\pi\sin kl_1-\frac{1}{kl}(l_1+\pi)(9\beta_d+\beta_e)\cos kl_1+\frac{16}{kl}\pi(-\beta_c\cos\theta+\beta_f\sin\theta)}.$$

Isolating the denominator of this quantity, we can recast it in the limit $m\to\infty$ as

$$\begin{aligned}&\frac{1}{24\beta_b\pi\sin kl_1}\frac{1}{1-\frac{1}{kl}\frac{l_1+\pi}{\pi}\frac{9\beta_d+\beta_e}{24\beta_b}\cot kl_1+\frac{2}{3kl\,\sin kl_1}\frac{-\beta_c\cos\theta+\beta_f\sin\theta}{\beta_b}} \\ \approx&\frac{1}{24\beta_b\pi\sin kl_1}(1+\frac{1}{kl}\frac{l_1+\pi}{\pi}\frac{9\beta_d+\beta_e}{24\beta_b}\cot kl_1-\frac{2}{3kl\,\sin kl_1}\frac{-\beta_c\cos\theta+\beta_f\sin\theta}{\beta_b});\end{aligned}$$

therefore

$$\delta(\theta) \propto -\frac{1}{kl}\frac{9\beta_d+\beta_e}{24\beta_b\pi}\frac{2}{3kl\,\sin kl_1}\frac{-\beta_c\cos\theta+\beta_f\sin\theta}{\beta_b},$$

$$\Delta E_m = \frac{2}{9(2m-1)\pi l^2}\left|\frac{(9\beta_d+\beta_e)(-\beta_c\cos\theta_1+\beta_f\sin\theta_1)}{\beta_b^2\sin kl_1}\right| + \mathcal{O}(m^{-2}),$$

assuming $l_1$ attains value for which $\sin kl_1 \neq 0$. Should it not be the case, we simply go to the second order of $\delta$ and get

$$\delta(\theta) \propto -\frac{2}{3kl}\frac{1}{l_1\cos kl_1}\frac{-\beta_c\cos\theta+\beta_f\sin\theta}{\beta_b},$$

$$\Delta E_m = \frac{8}{3}\frac{1}{l\,l_1}\left|\frac{-\beta_c\cos\theta_1+\beta_f\sin\theta_1}{\beta_b}\right| + \mathcal{O}(m^{-1}).$$

Overall,

$$P_\sigma(H) = 0;$$

the reasoning behind this argument stays the same, because the majority of possible band widths at the energy scale stays asymptotically constant, and the rest decreases as $\mathcal{O}(m^{-1})$.

**Case of $\gamma = 0$**

We finish this section by considering $\gamma = 0$. This case has common behaviour with the $t = 1$ case in some sense -

$$P_5 = P_3 = P_1 = P_0 = 0,$$

all other polynomials are much simpler, and the structure of spectral condition is analogous to Equation (4.10). Results obtained earlier for $t \neq 0$, particularly the high energy limit and whether is the spectrum connected to energy $k^2 = 0$, still hold, but our choice of $\gamma$ gives rise to some peculiarities not seen before.

First of all, according to Appendix A.3,

$$\begin{aligned}
&P_6 = 72l^6(\cos\frac{\pi t}{3} - 1)^2 \sin kl_1 \sin kl_2 \sin kl_3,\\
&P_4 = 12l^4(\cos\frac{\pi t}{3} - 1)(\cos\frac{\pi t}{3} + 1)[-4\sin kl_1 + 3\sin k(l_1 + l_2 + l_3)\\
&\ + \sin k(l_1 + l_2 - l_3) + \sin k(l_2 + l_3 - l_1) + \sin k(l_3 + l_1 - l_2)],\\
&P_2 = 2l^2(\cos\frac{\pi t}{3} + 1)^2[8\sin kl_1 - 9\sin k(l_1 + l_2 + l_3)\\
&\ + \sin k(l_1 + l_2 - l_3) + \sin k(l_2 + l_3 - l_1) + \sin k(l_3 + l_1 - l_2)],\\
&P_c = -48l^2(k^2l^2 - 1)\,(\cos\frac{\pi t}{3} - 1)\,(\cos\frac{\pi t}{3} + 1)(\sin kl_2 + \sin kl_3),\\
&P_s = 32kl^3\sqrt{3}\,\sin\frac{\pi t}{3}\,(\cos\frac{\pi t}{3} + 1)\,(\cos kl_3 - \cos kl_2).
\end{aligned}$$

Recalling (4.2), we can find flat bands by enforcing $k = m$, $m \in \mathbb{N}$. Additionally, $P_4$ and $P_2$ can be rewritten as

$$\begin{aligned}
P_4 &\propto -4\sin kl_1 + 3\sin k(l_1 + l_2 + l_3)\\
&\quad + \sin k(l_1 + l_2 - l_3) + \sin k(l_2 + l_3 - l_1) + \sin k(l_3 + l_1 - l_2)\\
&\quad = 4[\sin kl_1\,(-1 + \cos k(2\pi - l_3)\,\cos kl_3) + \cos kl_1\,\sin 2k\pi],
\end{aligned}$$

$$\begin{aligned}
P_2 &\propto 8\sin kl_1 - 9\sin k(l_1 + l_2 + l_3)\\
&\quad + \sin k(l_1 + l_2 - l_3) + \sin k(l_2 + l_3 - l_1) + \sin k(l_3 + l_1 - l_2)\\
&\quad = 4[2\sin kl_1\,(1 - \cos k(2\pi - l_3)\,\cos kl_3) + 2\cos kl_1\,\sin 2k\pi\\
&\quad + 3\sin kl_1\,\sin k(2\pi - l_3)\,\sin kl_3],
\end{aligned}$$

which for $k = m$ simplify to

$$\begin{aligned}
&P_4 \propto -4\sin ml_1\,\sin^2 ml_3,\\
&P_2 \propto 12\sin kl_1\,\sin k(2\pi - l_3)\,\sin kl_3 + 8\sin ml_1\,\sin^2 ml_3.
\end{aligned}$$

Therefore, similarly to previous examples,

- if $l_j = \frac{p}{q}\pi$, $j = 1, 3$, comprime $p, q \in \mathbb{N}$, then $k^2 = q^2m^2$, $m \in \mathbb{N}$ are energies of the flat bands in the spectrum.

Finally, in the limits of a quantum chain with vertices of degree four, $P_6$ is always 0. The highest order of $k$ present is now $k^4$, and the whole spectral condition now reads either

$$\sin k(l_2 + l_3) - (\sin kl_2 + \sin kl_3)\,\cos\theta + \mathcal{O}(k^{-1}) = 0$$

for $l_1 \to 0$, or

$$\begin{gathered} -\sin kl_1 + \sin k(l_1 + 2\pi) - \cos\theta \, \sin 2k\pi + \mathcal{O}(k^{-1}) = \\ 2 \, \sin k\pi \, \cos k(\pi + l_1) - 2 \, \cos\theta \, \sin k\pi \, \cos k\pi + \mathcal{O}(k^{-1}) = 0 \end{gathered}$$

with $l_3 \to 0$. We have seen the exact same conditions in the asymptotic regime for $t = 0$; this automatically means that for $l_1 = 0$

$$\begin{aligned} P_\sigma(H) &= 1 \ \ldots \ l_3 = \pi \\ P_\sigma(H) &= \frac{1}{2} \ \ldots \ l_3 \neq \pi, \end{aligned}$$

while if $l_3 = 0$,

$$P_\sigma(H) = \frac{1}{2}.$$

**Theorem 4.2.** *Let $\Gamma$ be a quantum chain graph with the topology illustrated by Figure 4.1, described by lengths $l_j \geq 0$, $j = 1,2,3$, length scaling parameter $l > 0$, and a circulant vertex matrix $U(t)$, $t \neq 0$, $t \neq 1$, with strength parameter $\gamma \in (-\pi,\pi)$. Assuming we fix the scaling by requiring $l_2 + l_3 = 2\pi$, we can draw these conclusions about its spectrum:*

1. *In this setting, flat bands are generally not present in the spectrum.*
   - *For $\gamma = 0$ (Kirchhoff coupling), we are able to find flat bands in the spectrum if lengths $l_1$ or $l_3$ (consequently $l_2$) are rational multiples of $\pi$.*
2. *The high energy spectrum is generally dominated by spectral gaps, and the probability of belonging to the positive spectrum is 0, unless $\gamma = 0$.*
   - *For $\gamma = 0$, the probability is non-zero only for a quantum chain with vertices of degree four. It is equal to 1 if $l_1 = 0$ and $l_3 = \pi$, otherwise it is equal to $\frac{1}{2}$.*
3. *The positive spectrum is connected to energy $k^2 = 0$ only if condition* (4.47) *is satisfied; this is a general condition for all possible configurations.*
4. *The maximum number of negative spectral bands is four, which might happen only for $\gamma < 0$. When $\gamma \geq 0$, there might be at most two negative spectral bands.*
   - *For a quantum chain with vertices of degree four, these numbers change to two and one, respectively.*

   *Both numbers are independent of other quantum graph parameters. Once again, the negative spectrum is connected to $k^2 = \kappa^2 = 0$ only if the positive spectrum is connected.*

# Conclusion

We have equipped quantum star graph 2.1 with $n$ adjacent edges with a general unitary circulant vertex condition from Definition 1.11, represented by matrix $U$, and found out

- number of its eigenstates, which is the same as the number of eigenvalues of matrix $U$ in the upper complex plane;
- their individual energies (in atomic units), given by

$$-\kappa_l^2 = -\frac{1 - \Re(\sum_{a=1}^n c_a e^{\frac{2\pi i l(a-1)}{n}})}{1 + \Re(\sum_{a=1}^n c_a e^{\frac{2\pi i l(a-1)}{n}})},$$

  where $l+1$ is a row and column index of a given eigenvalue in the diagonal representation of $U$;
- the general form of scattering vertex matrix $S(k)$ and its dependence on coefficients $c$ and momentum variable $k$, given by Equation (2.8);
- and its high and low energy limit in dependence on spectral decomposition of vertex matrix $U$, see Equation (2.12) for high energy and (2.14) for low energy. These results are in accordance with results obtainable from general considerations of functional calculus. Additionally, we have successfully tested them on specific examples of vertex conditions.

We continued with general circulant vertex condition on rectangular lattice 3.1 described by lengths $l_1$, $l_2$ and

- calculated its spectral condition (3.2). Again, the substitution of concrete coefficients $c$, specifically for 'extremal' rotationally symmetric, $\delta$ and $\delta'$ coupling, leads to correct spectral conditions derived by earlier authors.

While usable for any imaginable circulant matrix $U$, this spectral condition is in itself too complex for detailed analysis. Therefore we chose permutation-invariant vertex condition (1.4) and

- found structure of its spectrum, summarized in Theorem 3.2. Case-to-case differences are to be present as in any parametric system, but there is no deviation from the behaviour we would expect from vertex couplings with Dirichlet, Neumann or Robin eigenspaces respectively (see for example [ET21]);
- illustrated some of the properties and accuracy of our conclusions on a square lattice.

Then we combined a quantum chain graph 4.1 with interpolating vertex condition (4.1), getting

- general spectral condition (4.9) and tested its viability on boundary value $U(1)$ as well as special symmetric case of $U(0)$ with $l_1 = 0$;

- overall view of the spectrum in the special case $U(0)$, summed up in Theorem 4.1. Several features were graphically demonstrated, showing the correctness of our results. Additionally, we have shown that high energy behaviour, in particular the probability of belonging to the positive spectrum, is tightly linked with graph geometry rather than the equipped vertex condition.

- overall view of the spectrum $\forall t \neq \{0, 1\}$, explained in Theorem 4.2. We have described its parametric dependence in full detail while highlighting phenomena not present previously, for example similarities between cases with $\gamma = 0$ and $U(1)$.

# Bibliography


[BB13] Ram Band and Gregory Berkolaiko. Universality of the momentum band density of periodic networks. *Physical Review Letters*, 111(13):130404, 2013.

[BET21] Marzieh Baradaran, Pavel Exner, and Miloš Tater. Ring chains with vertex coupling of a preferred orientation. *Reviews in Mathematical Physics*, 33(01):2060005, 2021.

[BET22] Marzieh Baradaran, Pavel Exner, and Miloš Tater. Spectrum of periodic chain graphs with time-reversal non-invariant vertex coupling. *Annals of Physics*, 443:168992, 2022.

[BK13] Gregory Berkolaiko and Peter Kuchment. *Introduction to quantum graphs*. Number 186. American Mathematical Soc., 2013.

[DET08] Pierre Duclos, Pavel Exner, and Ondřej Turek. On the spectrum of a bent chain graph. *Journal of Physics A: Mathematical and Theoretical*, 41(41):415206, 2008.

[EG96] Pavel Exner and Ralf Gawlista. Band spectra of rectangular graph superlattices. *Physical Review B*, 53(11):7275, 1996.

[EKMN18] Pavel Exner, Aleksey Kostenko, Mark Malamud, and Hagen Neidhardt. Spectral theory of infinite quantum graphs. In *Annales Henri Poincaré*, volume 19, pages 3457–3510. Springer, 2018.

[EKW10] Pavel Exner, Peter Kuchment, and Brian Winn. On the location of spectral edges in Z-periodic media. *Journal of Physics A: Mathematical and Theoretical*, 43(47):474022, 2010.

[ET18] Pavel Exner and Miloš Tater. Quantum graphs with vertices of a preferred orientation. *Physics Letters A*, 382(5):283–287, 2018.

[ET21] Pavel Exner and Miloš Tater. Quantum graphs: Self-adjoint, and yet exhibiting a nontrivial PT-symmetry. *Physics Letters A*, 416:127669, 2021.

[ETT18] Pavel Exner, Ondřej Turek, and Miloš Tater. A family of quantum graph vertex couplings interpolating between different symmetries. *Journal of Physics A: Mathematical and Theoretical*, 51(28):285301, 2018.

[Exn96] Pavel Exner. Contact interactions on graph superlattices. *Journal of Physics A: Mathematical and General*, 29(1):87, 1996.

[SK15] Pavel Středa and Jan Kučera. Orbital momentum and topological phase transformation. *Physical Review B*, 92(23):235152, 2015.

[SV23] Pavel Středa and Karel Výborný. Anomalous Hall conductivity and quantum friction. *Physical Review B*, 107(1):014425, 2023.

[Wei12] Joachim Weidmann. *Linear operators in Hilbert spaces*, volume 68. Springer Science & Business Media, 2012.

# Appendices

## A Full expressions of spectral conditions

### A.1 Rectangular lattice - general vertex condition

| | |
|---|---|
| $K_1$ | $-(c_1-c_2+c_3-c_4)(c_1+c_2+c_3+c_4)[(c_1-c_3)^2+(c_2-c_4)^2]$ |
| $F_1$ | $[2k\cos kl_1+i(k^2+1)\sin kl_1][2k\cos kl_2+i(k^2+1)\sin kl_2]$ |
| $K_2$ | $-1$ |
| $F_2$ | $[-2k\cos kl_1+i(k^2+1)\sin kl_1][-2k\cos kl_2+i(k^2+1)\sin kl_2]$ |
| $K_3$ | $2c_1$ |
| $F_3$ | $(k^2-1)\{(k^2+1)[\cos k(l_1-l_2)-\cos k(l_1+l_2)]+2ik\sin k(l_1+l_2)\}$ |
| $K_4$ | $-4c_3$ |
| $F_4$ | $k\{\cos\theta_2\,[-2k\cos kl_1+i(k^2+1)\sin kl_1]+\cos\theta_1\,[-2k\cos kl_2+i(k^2+1)\sin kl_2]\}$ |
| $K_5$ | $16(c_2c_4-c_3^2)$ |
| $F_5$ | $k^2\cos\theta_1\cos\theta_2$ |
| $K_6$ | $-4(c_2c_4-c_1^2)$ |
| $F_6$ | $(k^2-1)^2\sin kl_1\sin kl_2$ |
| $K_7$ | $(c_1^2-c_3^2)$ |
| $F_7$ | $(k^4+6k^2+1)\cos k(l_1-l_2)-(k^2-1)^2\cos k(l_1+l_2)$ |
| $K_8$ | $4i(c_2^2+c_4^2-2c_1c_3)$ |
| $F_8$ | $k(k^2-1)[\cos\theta_1\sin kl_2+\cos\theta_2\sin kl_1]$ |
| $K_9$ | $4[c_1(c_2^2+c_4^2)+c_3(c_3^2-c_1^2-2c_2c_4)]$ |
| $F_9$ | $k\{\cos\theta_2\,[2k\cos kl_1+i(k^2+1)\sin kl_1]+\cos\theta_1\,[2k\cos kl_2+i(k^2+1)\sin kl_2]\}$ |
| $K_{10}$ | $2[c_3(c_2^2+c_4^2)+c_1(c_1^2-c_3^2-2c_2c_4)]$ |
| $F_{10}$ | $(k^2-1)\{(k^2+1)[\cos k(l_1-l_2)-\cos k(l_1+l_2)]-2ik\sin k(l_1+l_2)\}$ |

## A.2 Permutation-invariant vertex condition for rectangular and square lattice

| | |
|---|---|
| $A_1$ | $\cos(\gamma - \vartheta)\,(\cos\vartheta - 1)$ |
| $A_2$ | $\cos(\gamma - \vartheta)\,(\cos\vartheta + 1)$ |
| $A_3$ | $-2\cos\gamma + \cos\vartheta\ \cos(\gamma - \vartheta) + \cos(\gamma + \vartheta)$ |
| $A_4$ | $2\cos\gamma - \cos\vartheta\ \cos(\gamma - \vartheta) + \cos(\gamma + \vartheta)$ |
| $A_5$ | $2\sin\vartheta\ \cos(\gamma - \vartheta)$ |
| $A_6$ | $4\sin\vartheta\ \cos\gamma$ |
| $A_7$ | $-2\sin\vartheta\ \cos\gamma$ |
| $A_8$ | $-2\sin\gamma\,(\cos\vartheta + 1) + \sin\vartheta\,[\cos\gamma + \cos(\gamma - \vartheta)]$ |
| $A_9$ | $-2\sin\gamma\,(\cos\vartheta - 1) + \sin\vartheta\,[\cos\gamma - \cos(\gamma - \vartheta)]$ |

## A.3 Interpolating vertex condition for periodic chain

In order to display all polynomials properly, some of them have been separated into smaller parts - these are denoted by an additional subindex.

| | |
|---|---|
| $P_6$ | $36l^6(\cos\gamma(1-t)+1)(\cos\frac{\pi t}{3}-1)^2\sin kl_1\sin kl_2\sin kl_3$ |
| $P_5$ | $-24l^5\ \sin\gamma(1-t)\ (\cos\frac{\pi t}{3}-1)^2$ $[\cos kl_1\sin kl_2\sin kl_3+\sin kl_1\sin k(l_2+l_3)]$ |
| $P_{4,1}$ | $-16l^4\sin kl_1$ $[\cos\gamma(1-t)\,(\cos\frac{\pi t}{3}-1)(\cos\frac{\pi t}{3}+2)+2\,(\cos\frac{\pi t}{3}-1)(\cos\frac{\pi t}{3}+\frac{1}{2})]$ |
| $P_{4,2}$ | $9l^4\sin k(l_1+l_2+l_3)$ $[\cos\gamma(1-t)\,(\cos\frac{\pi t}{3}-1)(\cos\frac{\pi t}{3}+3)+3\,(\cos\frac{\pi t}{3}-1)(\cos\frac{\pi t}{3}+\frac{1}{3})]$ |
| $P_{4,3}$ | $l^4[\sin k(l_1+l_2-l_3)+\sin k(l_2+l_3-l_1)+\sin k(l_3+l_1-l_2)]$ $[7\ \cos\gamma(1-t)\,(\cos\frac{\pi t}{3}-1)(\cos\frac{\pi t}{3}+\frac{5}{7})+5\,(\cos\frac{\pi t}{3}-1)(\cos\frac{\pi t}{3}+\frac{7}{5})]$ |
| $P_3$ | $4l^3\sin\gamma(1-t)\,(\cos\frac{\pi t}{3}-1)(\cos\frac{\pi t}{3}+1)$ $\{8\cos kl_1-9\cos k(l_1+l_2+l_3)$ $-5\,[\cos k(l_1+l_2-l_3)+\cos k(l_2+l_3-l_1)+\cos k(l_3+l_1-l_2)]\}$ |
| $P_{2,1}$ | $-16l^2\sin kl_1$ $[\cos\gamma(1-t)\,(\cos\frac{\pi t}{3}+1)(\cos\frac{\pi t}{3}-2)-2\,(\cos\frac{\pi t}{3}+1)(\cos\frac{\pi t}{3}-\frac{1}{2})]$ |
| $P_{2,2}$ | $9l^2\sin k(l_1+l_2+l_3)$ $[\cos\gamma(1-t)\,(\cos\frac{\pi t}{3}+1)(\cos\frac{\pi t}{3}-3)-3\,(\cos\frac{\pi t}{3}+1)(\cos\frac{\pi t}{3}-\frac{1}{3})]$ |
| $P_{2,3}$ | $l^2[\sin k(l_1+l_2-l_3)+\sin k(l_2+l_3-l_1)+\sin k(l_3+l_1-l_2)]$ $[7\ \cos\gamma(1-t)\,(\cos\frac{\pi t}{3}+1)(\cos\frac{\pi t}{3}-\frac{5}{7})-5\,(\cos\frac{\pi t}{3}+1)(\cos\frac{\pi t}{3}-\frac{7}{5})]$ |
| $P_1$ | $-24l\sin\gamma(1-t)\,(\cos\frac{\pi t}{3}+1)^2$ $[\cos kl_1\sin kl_2\sin kl_3+\sin kl_1\sin k(l_2+l_3)]$ |
| $P_0$ | $36(\cos\gamma(1-t)-1)(\cos\frac{\pi t}{3}+1)^2\ \sin\ kl_1\ \sin\ kl_2\ \sin\ kl_3$ |
| $P_s$ | $16l^2\sqrt{3}\ \sin\frac{\pi t}{3}$ $\{[\sin kl_2+\sin kl_3]\ \sin\gamma(1-t)\,[k^2l^2(\cos\frac{\pi t}{3}+1)+(\cos\frac{\pi t}{3}-1)]$ $+2kl[\cos kl_3-\cos kl_2][\cos\frac{\pi t}{3}\ \cos\gamma(1-t)+1]\}$ |
| $P_c$ | $-16l^2\{[\sin kl_2+\sin kl_3]$ $[k^2l^2\,(\cos\gamma(1-t)\,(\cos\frac{\pi t}{3}-1)(\cos\frac{\pi t}{3}+2)+2\,(\cos\frac{\pi t}{3}-1)(\cos\frac{\pi t}{3}+\frac{1}{2}))$ $-\cos\gamma(1-t)\,(\cos\frac{\pi t}{3}+1)(\cos\frac{\pi t}{3}-2)+2\,(\cos\frac{\pi t}{3}+1)(\cos\frac{\pi t}{3}-\frac{1}{2})]$ $-2kl\,[\cos kl_3+\cos kl_2]\ \sin\gamma(1-t)\,(\cos\frac{\pi t}{3}-1)(\cos\frac{\pi t}{3}+1)\}$ |